Asymmetric segregation of lysosomes during hematopoietic stem and progenitor cell divisions

Dissertation

der Fakultät für Biologie

der Ludwig-Maximilians-Universität

München

prepared at the

Research Unit – Stem Cell Dynamics

Helmholtz-Zentrum München

Submitted by

Dirk Löffler

26 September, 2013

The presented work was conducted as a member of the Research Unit Stem Cell Dynamics at the Helmholtz-Zentrum in München and was supervised by Prof. Dr. Timm Schroeder.

Erstgutachter: Prof. Dr. Heinrich Leonhardt
Zweitgutachter: Prof. Dr. Angelika Böttger

Tag der mündlichen Prüfung: 12 September, 2014

Part of this study has been published as:

Montrone, C., Kokkaliaris, K.D., Loeffler, D., Lechner, M., Kastenmüller, G., Schroeder, T., and Ruepp, A. (2013). **HSC-Explorer: A Curated Database for Hematopoietic Stem Cells.** PloS One *8*, e70348.

Kokkaliaris, K.D., Loeffler, D., and Schroeder, T. (2012). **Advances in tracking hematopoiesis at the single –cell level.** Current Opinion in Hematology 19, 243-249.

Loeffler, D., Kokkaliaris, K.D., and Schroeder, T. (2011). **Wnt to notch relay signaling induces definitive hematopoiesis.** Cell Stem Cell *9*, 2–4.

Acknowledgements:

I would like to thank Prof. Dr. Heinrich Leonhardt for being my official supervisor at the Ludwig-Maximilians-Universität München and for being a critical participant in my thesis committee.

Thanks to Prof. Dr. Timm Schroeder for introducing me into the exciting field of hematopoietic stem cells and electronic (time-lapse) imaging and for all the critical discussions regarding my project.

Thank you Prof. Dr. Magdalena Götz and Dr. Arndt Kieser for being critical members of my thesis committee and for organizing seminars and retreats in the Institute of Stem Cell Research at the Helmholtz-Zentrum München.

Thanks to Christian Raithel, Angelika Ziegler, Sandra Ammersdörfer and Bianca Vogel for generating viruses, for your help with bone marrow preparation and molecular cloning as well as your general technical support and the thousand little things you did in the lab.

Special thanks to my fiancé Heide Oller for her love, support and patience, without which this work wouldn't have been possible.

I would also like to thank all former and current members of the lab for creating the nice working atmosphere I could experience over the last years. Thank you also for critical discussions during and after lab meetings. Thank you, Konstantinos Kokkaliaris, Dr. Laura Skylaki, Max Endele, Philipp Hoppe, Dr. Daniel Coutu, Dr. Martin Etzrodt, Joost van den Berg, Dr. Adam Filipczyk, Prof. Dr. Michael Rieger and Dr. Masaki Shigeta.

Thanks also to Oliver Hilsenbeck, Bernd Streppel, Berndhard Straubinger, Michael Schwarzfischer and Konstantin Azadov for their efforts in programming and improving the data acquisition, processing and analysis tools used in this study: Timm´s Tracking Tool (TTT), QTFy, QTFy single, staTTTs.

And I would like to thank all members of the Institute for Stem Cell research (ISF) as well as the Institute for Diabetes and Regeneration (IDR) for their help, exchange of ideas as well as their support.

Table of contents:

Table of figures:

Table of tables:

1 Zusammenfassung

Die Töchter hämatopoetischer Stammzellen können verschiedene Schicksale annehmen. Ob die Entscheidung des Zellschicksals während der Zellteilung oder danach durch extrinsische Ereignisse die nicht im Zusammenhang zur Teilung stehen bestimmt wird konnte bisher nicht geklärt werden. Obwohl asymmetrische Zellteilung als möglicher Mechanismus dieser Entscheidung vorgeschlagen wurde, konnte weder die asymmetrische Vererbung von Faktoren die das Zellschicksal bestimmen noch deren Funktionen in hoch aufgereinigten, lebenden hämatopoetischen Stammzellen quantitativ demonstriert werden. Um dieses Problem zu addressieren haben wir 17 Kandidaten auswählt und deren Vererbung während der Teilung hämatopoetischer Stammzellen in vitro mit Hilfe eines neuen, kontinuierlichen und quantitativen biologischen Bildverarbeitungsverfahrens mittels mikroskopischer Zeitrafferaufnahmen analysiert. Drei verschiedene in vitro Verfahren um symmetrische und asymmetrische Zellschicksale im Hinblick auf Differenzierung und Linienentscheidung unterscheiden zu können wurden entwickelt und mit der Vererbung der Kandidaten während der ersten in vitro Zellteilung korreliert.

Durch die quantitative Analyse von über 6000 Zellteilungen konnte gezeigt werden das vier Proteine, CD63, VANGL2, SCA1 und LAMP1 während der Zellteilung von hämatopoetischen Stamm- und Vorläuferzellen asymmetrisch vererbt werden. Des Weiteren konnte gezeigt werden das diese Proteine mit Lysosomen kolokalisieren welche ebenfalls asymmetrisch während der Zellteilung von hämatopoetischen Stamm- und Vorläuferzellen vererbt werden. Die asymmetrische Vererbung ist dabei unabhängig von Zell-Zell oder Zell-Matrix Interaktionen, kann aber durch die Zugabe verschiedener Wachstumsfaktoren beeinflusst werden. Die asymmetrische Vererbung von Lysosomen scheint dabei weder mit Differenzierung noch mit der hämatopoetischen Linienentscheidungen zu korrelieren.

Die hier dargestellten Ergebnisse unterstützen die Theorie der asymmetrischen Zellteilung. Experimentelle Ansätze und Methoden zur kontinuierlichen und quantitativen Analyse von Zellteilungen und asymmetrischen Zellschicksalen werden diskutiert und dargestellt.

2 Abstract

Hematopoietic stem cells (HSC) give rise to daughters that adopt different cell fates. Whether these cell fate decisions are made during division or are determined by extrinsic post-mitotic events remains unclear. Although asymmetric cell division has been suggested as a mechanism to regulate these decisions, neither the asymmetric segregation of cell fate determinants, nor their function has been demonstrated quantitatively, in highly purified, living HSCs. To address this issue, we chose 17 putative cell fate determinants or markers and analyzed their protein segregation during in vitro HSC divisions by a novel, continuous, quantitative bioimaging approach. Three different in vitro read-outs to distinguish symmetric from asymmetric daughter cell fates were established for differentiation and lineage choice and correlated to the segregation of candidates during the first in vitro divisions of HSCs.

Over 6.000 cell divisions were analyzed, providing quantitative evidence that four proteins, CD63, VANGL2, SCA1 and LAMP1 are asymmetrically segregating in living hematopoietic stem and progenitor cells (HSPCs). We further demonstrate that these proteins colocalize to lysosomes which are asymmetrically inherited during HSPC divisions. We also show that the degree of asymmetry is independent of cell-cell or cell-matrix interactions, but can be actively modulated by the presence of secreted growth factors. However, the asymmetric segregation of lysosomes does not seem to correlate with differentiation or lineage choice.

These results contribute further evidence to the asymmetric cell division theory, and provide the tools to analyze cells divisions and asymmetric daughter cells fates quantitatively over time.

3 Introduction

3.1 Blood

Blood is an important tissue in higher organisms. Its functions are versatile and include the transport of various components (oxygen, carbon dioxide, water, nutrients, ions, hormones, etc.), thermoregulation, the regulation of the body pH, coagulation, osmoregulation, the immune response and hydraulics. Its constituents are divided into a liquid part, referred to as plasma, containing proteins, sugars and lipids, and a cellular part, named hematocrit, containing erythrocytes, thrombocytes and leukocytes. While erythrocytes are responsible for the efficient oxygen transport throughout the organism, leukocytes are specialized cells of the immune system. Thrombocytes are important for the coagulation process and prevent excess bleeding by clotting to close wounds. A healthy human has to generate 10^{11}-10^{12} new blood cells every day in order to maintain homeostasis, numbers that are even exceeded during challenge by injury or disease. The highly complex and plastic process of blood cell generation is called hematopoiesis.

A number of diseases are caused or associated with changes in hematopoiesis. Leukemia, myelomas and lymphomas are estimated to be the cause of death of over 54.000 people in the United States in 2013 (Howlader, 2012). A deeper understanding about mechanisms regulating hematopoiesis is therefore important to develop novel therapies and improve current treatments to reduce the mortality rate and to improve the quality of life of patients.

One of these treatments is based on the transplantation of bone marrow cells from either autologous or allogenic sources. The procedure involves the supralethal irradiation or chemotherapy of patients to eradicate their functionally compromised (i.e. leukemic, anemic) bone marrow. If successful, the eradication is complete and the transplant engrafts and repopulates the entire hematopoietic system of the recipient. Since its first application in 1959 the number of hematopoietic stem cells transplantations is increasing every year with an estimated global number of 50.417 in 2006 (Gratwohl et al., 2010; Jenq and van den Brink, 2010; Thomas and Blume, 1999; Thomas et al., 1959). Although techniques to harvest and transplant

hematopoietic stem cells are constantly refined, the available material is limited. This is especially true for allogenic sources such as umbilical cord blood which is increasingly used since incidences of graft-versus-host disease are less frequent and severe (Tse and Laughlin, 2005).

One way to overcome these limitations is the expansion of hematopoietic stem cells. However, until today no one was able to expand genetically unmodified HSCs for extended periods of time ex vivo. In fact even the prolonged maintenance of HSCs in defined stroma and serum free conditions has not been accomplished yet, illustrating that the underlying mechanisms are not understood. The reason for this is that the research of HSCs is hampered by their extremely low frequency (0.0008% of total nucleated BM cells) and their technically challenging analysis. Assays capable of reading out stem cell function are time consuming, expensive and allow only retrospective conclusions.

The prerequisite to expand hematopoietic stem cells is the generation of two identical daughters. It is generally assumed that this is accomplished by symmetric self-renewal divisions of the HSC mother cells. Additional division modes such as asymmetric cell division and symmetric differentiation division have been suggested to participate in the regulation of HSC numbers. However, neither of these modes has been observed directly and their role in the regulation of HSC numbers is unknown. In order to understand how self-renewal of HSC is regulated and can be controlled, a better understanding of HSC division modes is required. The elucidation of the underlying mechanisms might pave the way to unravel the mystery of HSC self-renewal in homeostasis and disease.

3.2 Hematopoiesis

3.2.1 Hematopoietic stem cells

3.2.1.1 Definition and functional readouts

Hematopoietic stem cells (HSCs) are able to maintain their numbers (self-renewal) while giving rise to all differentiated cells of the hematopoietic system for the entire life on an organism. This functional definition is based on studies demonstrating that the transplantation of a single HSC is sufficient to regenerate the hematopoietic system of lethally irradiated mice and that this potential is maintained over multiple rounds of consecutive transplantations into secondary or tertiary recipients (Dykstra et al., 2007a; Osawa et al., 1996; Sieburg et al., 2011). Although the functional definition is constantly redefined, the currently used criteria to demonstrate stem cell potential include ≥1% contribution to both myeloid and lymphoid progeny over at least 16 weeks in primary and secondary recipients (Dykstra et al., 2007a). Aside from their functional definition, HSCs have been demonstrated to be quiescent and enter the cell cycle infrequently about every 36-145 days in vivo (Wilson et al., 2008). They have been calculated to represent around 0.008% of total nucleated bone marrow cells (Osawa et al., 1996) and been shown to efflux dyes like Hoechst33342 and other chemicals due to the expression of multidrug resistance proteins (MDR) (Goodell et al., 1996). Multiple surface antigens have been identified allowing the prospective isolation of HSCs with purities around 50% as discussed in section 2.2.1.2. Although these populations are isolated based on a common immunophenotype, HSCs enriched by current purification schemes are highly heterogeneous in regard to their repopulation kinetics, lineage bias and durability of regenerative potential (Benveniste et al., 2010; Dykstra et al., 2007a; Müller-Sieburg et al., 2002; Sieburg et al., 2011).

In addition to transplantation assays, in vitro surrogate assays have been described to detect HSC potential in a shorter period of time, and without ethical constraints. Although these assays cannot replace transplantations, they represent a valuable tool for screening approaches. One of these assays is called Long-Term Culture-Initiating Cell (LTC-IC) assay. Hematopoietic cells are seeded in limiting dilutions or as single cells onto a stromal cell line (i.e. S17, AFT024) able to support the

maintenance of HSC in vitro. After several weeks in culture the number of colonies is either determined directly or after re-plating in semi-solid medium. Every colony formed is derived from a LTC-IC, of which 50% are able to repopulate the hematopoietic system of W41/W41 recipients after 3 weeks of culture on S17 (Cho and Müller-Sieburg, 2000).

Another assay is called Single-Cell Liquid Culture Colony Assay (SC-LCCA). Cells that are able to give rise to colonies containing megakaryocytes, erythrocytes, granulocytes and macrophages are considered to be multi-potent and have therefore been HSCs or early progenitors when initially isolated. The number of cells able to give rise to all four lineages correlates well with the number of freshly isolated cells capable of repopulating bone marrow upon transplantation. Since the culture conditions used only support the generation of myeloid cells, the lymphoid differentiation cannot be used as a criterion for multi-potency in this assay. Until today, no in vitro culture conditions are described that robustly support the generation of all hematopoietic lineages in vitro at the same time. However, keeping the limitations of the assay in mind, it provides the means to analyze myeloid lineage differentiation of individual cells over a short period of time and is therefore suitable for high throughput approaches.

3.2.1.2 Prospective isolation of hematopoietic stem cells

Technical advances in the 1960/70s, in particular the development and commercialization of the first fluorescence based flow cytometer (Dittrich W., 1971) and the generation of monoclonal antibodies with defined specificity (Köhler and Milstein, 1975) made it feasible to analyze and purify heterogeneous cell populations based on the presence of cell surface antigens. In 1986, Müller-Sieburg et al. was able to accomplish for the first time an enrichment of hematopoietic cells with radio-protective properties by sorting a Thy-1^{low} population negative for several lineage marker (Muller-Sieburg et al., 1986). Since then, various purification strategies utilizing fluorescent labeled antibodies or fluorescent dyes have been developed. Today, the combination of modern flow cytometers and sophisticated purification strategies enables us to reach HSC purities around 50% (Kent et al., 2009; Kiel et al.,

2005a).In the present study hematopoietic cells with the following immunophenotype were utilized: $CD150^{+}CD34^{-}CD48^{-}cKIT^{+}SCA1^{+}Lin^{-}$

Table 3.1: Overview about the most common HSC purification strategies.

Immunophenotype	purity	References
$CD34^{-}KSL$	21%	(Osawa et al., 1996)
KSL $Thy1.1^{low}$	18%	(Wagers et al., 2002)
SP^{+} Rho^{low} Lin^{-}	40%	(Uchida et al., 2003)
KSL SP^{+} $CD34^{-}$	96%	(Matsuzaki et al., 2004)
$CD150^{+}$ $CD48^{-}$ $CD41^{-}$	47%	(Kiel et al., 2005b)
KSL SP^{+} $CD34^{-}$	35%	(Camargo et al., 2006)
$CD48^{-}CD150^{+}$ $CD201^{+}$ $CD45^{+}$	56%	(Kent et al., 2009)

KSL: $cKIT^{+}SCA1^{+}Lin^{-}$. Population of hematopoietic stem and progenitor cells expressing the surface antigens cKIT+ and SCA1+ while being negative or low for several lineage marker of mature blood cells, SP: side population. Population enriched for HSCs that is not or weakly stained by the fluorescence dye Hoechst. Rho: Population that is weakly stained by the fluorescence dye rhodamine.

3.2.1.3 Niche

The major site of hematopoiesis in the adult is the bone marrow. HSCs have been found near the endosteum, the interface of bone and bone marrow, as well as adjacent to sinusoidal blood vessels (Kiel and Morrison, 2008; Kiel et al., 2005b). Cells of both sites have been described to influence the maintenance, quiescence, differentiation and migration of HSC by either secreted or membrane bound factors and are therefore thought to provide a specialized microenvironment (niche), a concept first proposed over 30 years ago (Schofield, 1978). If cells of the endosteum and sinusoids represent different parts of a single niche or if they are functionally different is currently controversial (Kiel and Morrison, 2008). Recently, these sites have been further subdivided by discriminating the sinusoids into vascular and perivascular niche, further complicating the issue (Nakamura-Ishizu and Suda, 2013). For simplicity we focus on endosteum and sinusoids and describe the cellular components of those two anatomical sites separately.

3.2.1.3.1 Endosteal niche

The endosteal surface is highly vascularized and is lined with cells of the osteoblastic lineage and osteoclasts. Since the number of HSCs increases with the number of osteoblasts in vivo, osteoblasts have been suggested to participate in their regulation (Calvi et al., 2003; Zhang et al., 2003). In line with this observation, it has been shown that the selective depletion of osteoblasts reduces HSC numbers (Visnjic et al., 2004). Angiopoietin (ANG1), Thrombopoietin (TPO) and CXC-chemokine ligand 12 (CXCL12) have been suggested to be secreted by osteoblasts. While TPO and ANG1 are thought to maintain HSC quiescence, CXCL12 affects their migration (Arai et al., 2004; Petit et al., 2002; Qian et al., 2007; Yoshihara et al., 2007). Notch signaling via JAGGED1 has been shown to promote HSC maintenance in vitro (Calvi et al., 2003). However, conditional deletion of *Jagged1* and *Notch1* does not affect maintenance of HSC in vivo (Mancini et al., 2005).

In addition to osteoblasts, osteoclasts have been shown to regulate HSC maintenance by secreting CXCL12 or proteases. Matrix metalloproteinase 9 (MPP9) and Cathepsin K play important roles in bone remodeling and the release of membrane-bound growth factors like stem cell factor (SCF) (Kollet et al., 2006). In a recent study, osteoclasts have been shown to be necessary for the initial formation of the niche. In this model, the absence of osteoclast activity leads to a reduction of osteoblast differentiation and an impaired homing of HSC to the bone marrow (Mansour et al., 2012).

3.2.1.3.2 Vascular niche

The vascular niche is thought to consist of specialized blood vessels carrying venous blood, referred to as sinusoids, and a variety of perivascular cells, including perivascular reticular cells, mesenchymal progenitors, and megakaryocytes (Ding et al., 2012; Méndez-Ferrer et al., 2010; Sacchetti et al., 2007; Sugiyama et al., 2006). The walls of the blood vessel are comprised of endothelial cells which allow HSC to enter or exit circulation. Endothelial cells were initially thought to regulate HSCs due to their close proximity in bone sections (Kiel et al., 2005b). This view is supported by

studies showing that endothelial cells can promote the maintenance of HSC in vitro (Li et al., 2004; Ohneda et al., 1998). Further evidence of this idea comes from a recent study showing that deletion of *Scf* in endothelial cells leads to a reduction of HSCs in vivo, highlighting their importance for HSC maintenance (Ding et al., 2012).

In addition to endothelial cells, several different cell types surrounding the sinusoids have been described to influence HSCs. Perivascular reticular cells have been shown to express high levels of CXCL12, a factor required for HSC maintenance. Interestingly, HSCs seem to localize to CXCL12 secreting cells in the endosteum as well as the sinusoids (Sugiyama et al., 2006). Functional evidence comes from a study showing that the deletion of *Scf* in *Lepr*-expressing perivascular stromal cells leads to a reduction of HSCs in vivo (Ding et al., 2012).

Other cell types such as $NESTIN^{+}$ perivascular mesenchymal progenitors have been associated with a reduction of HSCs in vivo as well (Méndez-Ferrer et al., 2010). Non-myelenating Schwann cells have been shown to regulate HSC dormancy via localized activation of transforming growth factor β1 (TGFβ1) (Yamazaki et al., 2011). In addition, megakaryocytes, monocytes and t-cells have been suggested to be parts of the vascular niche (Avecilla et al., 2004; Chow et al., 2011; Li et al., 2012; Winkler et al., 2010).

3.2.1.4 Signaling

Many either secreted or membrane bond growth factors have been suggested to regulate the maintenance of HSCs (Kent et al., 2008b; Yamazaki et al., 2007). Three of these growth factors, namely stem cell factor (SCF), thrombopoietin (TPO) and transforming growth factor β1 (TGFβ1) have commonly been used to study HSCs divisions in vitro and have been demonstrated in different combinations to be able to maintain HSCs for limited amounts of time (Ema et al., 2000a; Takano et al., 2004; Yamazaki et al., 2009).

3.2.1.4.1 Stem cell factor (SCF)

Stem cell factor (SCF) was among the first cytokines reported to affect HSC function. It binds the receptor tyrosine kinase c-KIT and is essential for HSC maintenance since stem cells isolated from mice deficient for *Scf* are not capable of maintaining repopulation activity (McCarthy et al., 1977). Mutations in c-KIT are frequently associated with impaired HSC function as well (Kent et al., 2008a). Almost all in vitro culture conditions used today intended to either maintain or expand HSCs contain SCF.

3.2.1.4.2 Thrombopoietin (TPO)

Thrombopoietin (TPO) is thought to regulate HSC self-renewal given that knock-out mice of either *Tpo* itself or its receptor *c-Mpl* have reduced numbers of HSCs (Alexander et al., 1996; Carver-Moore et al., 1996). The accelerated cell cycle kinetics of HSCs derived from *c-Mpl* deficient mice have led to the conclusion that TPO/c-MPL signaling is important for HSC maintenance by regulating their dormancy (Yamazaki and Nakauchi, 2009). Although TPO seems to be required for HSC maintenance in vivo its effects on in vitro cultured HSCs are controversial.

A study conducted by Ema et al. using single cell transplantation assays, suggested that HSCs cultured in SCF and TPO maintain their self-renewal capacity more efficiently than in other culture conditions using combinations of SCF, Interleukin-3 (IL3) and Interleukin-6 (IL6) (Ema et al., 2000a). These results were confirmed by Takano et al. who showed that HSCs cultured in SCF and TPO maintain their in vitro multi lineage differentiation potential more efficiently than in other culture conditions (Takano et al., 2004).

However, there are also reports suggesting that TPO exerts negative effects on the in vitro self-renewal of HSCs. NUP98-HOXA10hd is an engineered fusion protein capable of stimulating a >1000 fold in vitro expansion of murine HSCs. Sekulovic et al. demonstrated that the in vitro culture conditions influence NUP98-HOXA10hd mediated HSC expansion. Several cytokine combinations were compared and could

be grouped into positive and negative regulators. Interestingly, although the NUP98-HOXA10hd mediated expansion could be observed in all culture conditions, the expansion was significantly reduced as soon as TPO was present (Sekulovic et al., 2011). In another study CD34$^-$KSL transplanted after an extended in vitro culture for 7 days in SCF and TPO had strongly reduced repopulation activity suggesting that the presence of TPO alone is not sufficient to maintain HSCs for longer periods of time (Noda et al., 2008).

3.2.1.4.3 Transforming growth factor-β1 (TGFβ1)

Transforming growth factor β1 (TGFβ1) is a suppressive cytokine known to negatively regulate the proliferation of various cell types, including hematopoietic progenitor cells and populations enriched for hematopoietic stem cells (Keller et al., 1988; Sitnicka et al., 1996). In addition to its effect on proliferation, TGFβ1 has been shown to suppress HSC differentiation in vitro (Sitnicka et al., 1996; Yamazaki et al., 2009). It has also been reported to induce their hibernation by inhibiting the formation of lipid raft clusters, a process thought to be required for successful signal transduction (Yamazaki et al., 2009). The relevance of TGFβ1 signaling for the maintenance of HSC quiescence in vivo was recently demonstrated. HSCs isolated from TGFβRII ∆/-Rag2-/- mice have reduced long-term repopulation activity and enter the cell cycle more frequently (Yamazaki et al., 2011).

3.2.1.5 Heterogeneity

The HSC compartment was long thought to be homogenous, consisting of stem cells with equal self-renewal capacity and differentiation potential (Blackett et al., 1986; Muller-Sieburg et al., 2012). Early experimental results pointing towards heterogeneous behavior of HSCs were explained by stochastic or random events controlling self-renewal and differentiation (Ogawa et al., 1983; Suda et al., 1984b; TILL et al., 1964). It was only until about 10 years ago that carefully carried out single cell transplantation studies revealed a tremendous amount of heterogeneity in regard

to self-renewal capacity, differentiation propensity, kinetics of maturation and durability of contribution (Challen et al., 2010; Dykstra et al., 2007b; Morita et al., 2010; Müller-Sieburg et al., 2002). Although the degree of heterogeneity depends on the purification strategy used, patterns within the observed heterogeneities emerged, pointing towards the existence of HSC subsets biased in their differentiation potential. These subsets are defined by the ratio of lymphoid to myeloid cells in the peripheral blood of recipients. While balanced-HSCs have comparable numbers of lymphoid and myeloid cells, myeloid-biased HSCs have a lower lymphoid to myeloid cell ratio. Lymphoid-biased HSCs on the contrary are characterized by a high lymphoid to myeloid cell ratio (Müller-Sieburg et al., 2002). The interrelationship between different HSC subpopulations is currently not well understood and it has yet to be determined if the different HSC subsets are organized in a hierarchy or if they were initiated "independently" during the development of the hematopoietic system (Muller-Sieburg et al., 2012). Since the lineage bias is stably inherited over several rounds of self-renewal and even daughters transplanted into different recipients show the same lineage propensity, the lineage bias seems to be an intrinsic property of HSCs, arguing for the diversification of HSCs during development (Muller-Sieburg et al., 2012). Others have shown that $CD150^{high}$myeloid-biased HSCs are able to give rise to $CD150^{negative}$lymphoid-biased HSCs but not vice versa, implying a hierarchical relationship (Morita et al., 2010). The hierarchical model is further supported by the observation that myeloid-biased HSC have a higher self-renewal potential (Muller-Sieburg et al., 2004).

Recent studies were able to prospectively isolate myeloid and lymphoid biased HSCs by flow cytometry using the surface antigens CD150, CD41, CD86 and CD229 (Gekas and Graf, 2013; Morita et al., 2010; Oguro et al., 2013; Shimazu et al., 2012). Although these studies applied different purification strategies and further research is required, myeloid-biased HSCs seem to be $CD150^{high}CD41^{+}CD86^{-}CD229^{-/low}$ while lymphoid-biased HSCs are contained in the $CD150^{low/neg}$, $CD41^{-}CD86^{+}CD229^{+}$ population.

3.2.2 Classical model of hematopoiesis

In the classical model of hematopoiesis (Figure 2.1) (Akashi et al., 2000; Bryder et al., 2006) HSCs are divided into “long-term” (LT-HSC: $Lin^-c\text{-}KIT^+SCA1^+Flk2^-CD34^-CD150^+$) and “short-term” HSCs (ST-HSC: $Lin^-c\text{-}KIT^+SCA1^+Fkl2^-CD34^+CD150^{+/-}$) highlighting the fact that ST-HSCs are only capable to regenerate the hematopoietic system for periods shorter than 16 weeks (Dykstra et al., 2007a). In this model, ST-HSCs give rise to a cell population termed multipotent progenitors (MPP: $Lin^-c\text{-}KIT^+SCA1^+Flk2^+CD34^+CD150^-$), cells temporally even more restricted in their capacity to repopulate the hematopoietic system. Downstream of the MPPs, oligopotent progenitors called common myeloid progenitor (CMP: $Lin^-cKIT^+SCA1^-CD34^+FcγR^{low}$) and common lymphoid progenitor (CLP: $Lin^-c\text{-}KIT^{low}SCA1^{low}IL7Rα^+Flk2^{hi}$) with limited differentiation potential appear. While the CMP is limited to give rise to the Megakaryocytic-erythroid lineage and Granulocyte-Macrophage lineage, the CLP is restricted to give rise to lymphoid cells (B-Cells, T-Cells, Natural Killer Cells). Further differentiation of the CMP leads to the formation of Megakaryocyte-Erythrocyte Progenitors (MEP: $Lin^-cKIT^+SCA1^-CD34^-FcγR^-$), restricted to give rise to Megakaryocytes and Erythrocytes, and the formation of Granulocyte-Macrophage Progenitors (GMP: $Lin^-cKIT^+SCA1^-CD34^+FcγR^+$), restricted to give rise to granulocytes and macrophages. Further subsequent differentiation steps finally lead to the formation of all mature blood cells: erythrocytes, megakaryocytes, thrombocytes, granulocytes, macrophages, dendritic cells, B-Cells, T-Cells, Natural Killer cells and their various subtypes.

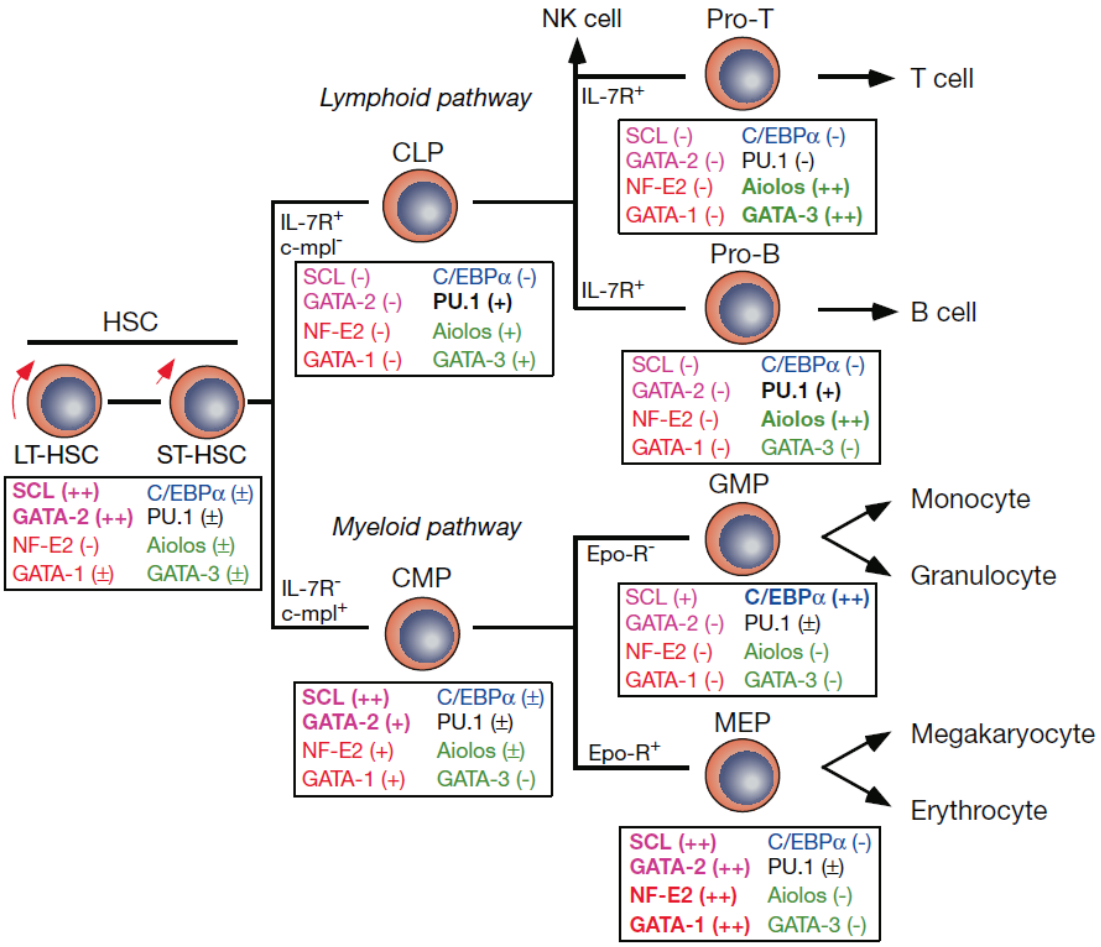

Figure 3.1: Classical model of the hematopoietic hierarchy (Akashi et al., 2000).

3.2.3 Revision of the hematopoietic hierarchy

Although widely used, the classical model of the hematopoietic hierarchy is highly controversial and constantly adjusted. Novel hematopoietic subpopulations are discovered by subdividing previously described ones and new branches are added while others are removed. One of these population is named the lymphoid primed multipotent progenitor (LMPP) and thought to have strongly reduced or no megakaryocytic-erythroid potential, while being capable of generating the granulocytic-monocytic as well as the lymphoid lineage, a feature clearly distinct from classical CMP and CLPs (Adolfsson et al., 2001; Luc et al., 2007). Another population is called pre-GMP to illustrate their appearance before the classical GMP (Pronk et al., 2007).

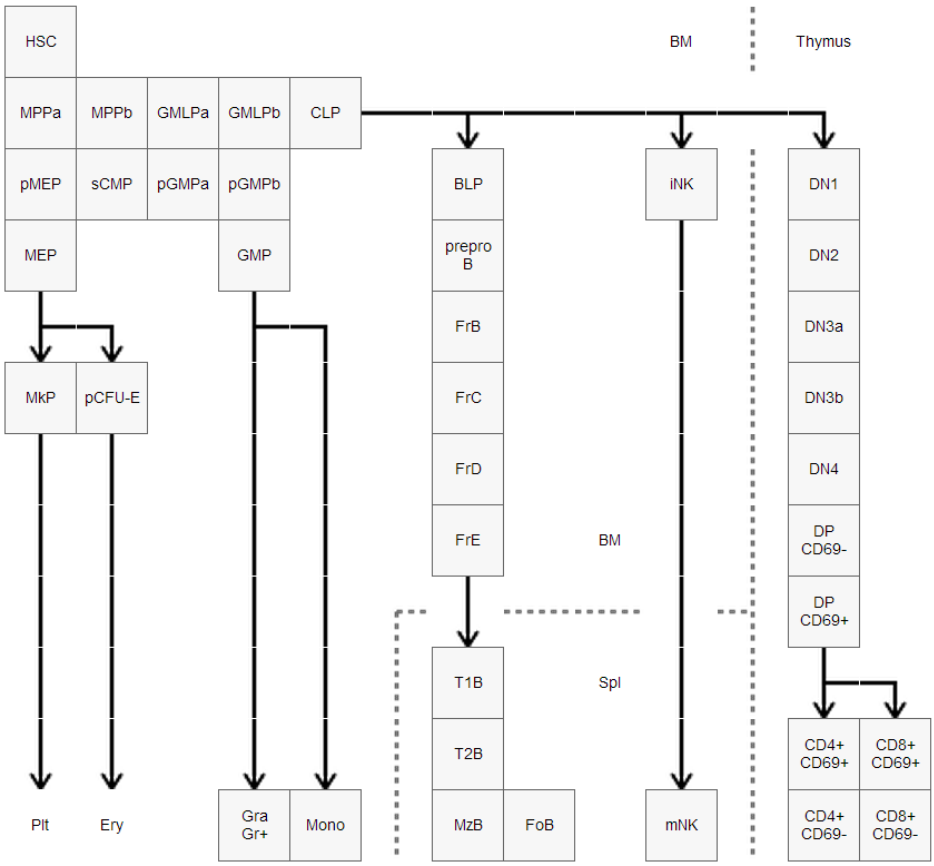

Figure 3.2: One of several revised models of the hematopoietic hierarchy (Seita et al., 2012).

A recent study, using a more comprehensive approach, combined the gene expression data of 39 hematopoietic populations in a common database. The gene expression levels were compared to >10.000 publicly available microarrays in order to assess absolute instead of relative gene expression levels (Seita et al., 2012). Based on the similarity of the populations, the authors deduced a novel hematopoietic roadmap (Figure 2.2) and combined elements of the classical hematopoietic hierarchy with more recently identified subpopulations.

3.3 Asymmetric cell division

3.3.1 The generation of cellular diversity – different modes of cell division

Heterogeneity within the hematopoietic system has long been appreciated. HSCs have self-renew potential while giving rise to cells committed to differentiation. These committed cells lose their self-renewal capacity and give rise to cells with more and more restricted lineage potential to finally generate all different cell types of the hematopoietic system. Recent work suggests that even the HSC compartment, previously thought to be rather homogenous, consists of a variety of stem cell subsets (Muller-Sieburg et al., 2012; Sieburg et al., 2006).
How this heterogeneity is established and maintained, and in particular how HSCs are able to self-renew to stably maintain HSC numbers, while simultaneously generating their differentiated progeny has been controversial for decades.

In principle, cellular heterogeneity can be achieved by two distinct mechanisms (Horvitz and Herskowitz, 1992):

1) A mother cell gives rise to identical daughters and cellular diversification is accomplished by some event later in their life time (symmetric cell division).

2) A polarized mother cell gives rise to daughters that are different from the moment of their generation (asymmetric cell division).

Early observations that distinct cytoplasmic domains of the leech egg differentially segregate to its progeny lead to the formulation of the hypothesis that two intrinsically different daughters can be generated during cell divisions (Horvitz and Herskowitz, 1992; Whitman, 1878). This idea was supported by later studies of the ascidian egg, where tracing of cytoplasmic pigmented areas over several cell divisions correlated with the generation of certain tissues (Conklin, 1905; Neumüller and Knoblich, 2009). In 1994, the asymmetric segregation of the protein NUMB in the sensory organ precursor (SOP) of Drosophila melanogaster could be functionally linked to future daughter cell fates for the first time (Rhyu et al., 1994). Since then, more

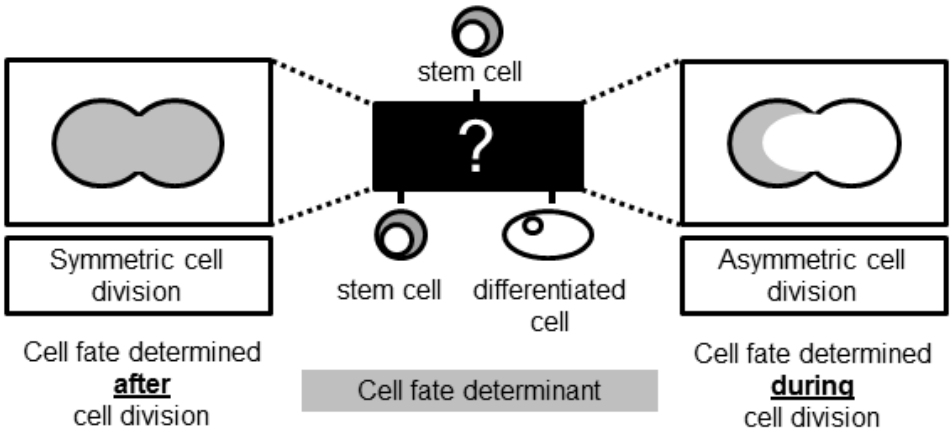

Figure 3.3: Cellular heterogeneity can be explained by two mechanisms

asymmetrically segregating proteins were identified and linked to their future daughter cell fates (Neumüller and Knoblich, 2009). Taken together, over a hundred years after the hypothesis has been formulated, experimental evidence clearly indicates that asymmetric cell division is a common mechanism for cellular diversification during development. It is important to point out that the majority of this data has been acquired through the observation of the development of organisms like Drosophila melanogaster and Caenorhabditis elegans and it is yet unclear if and how these concepts apply to somatic tissues, in particular somatic tissue stem cells, such as HSCs (Neumüller and Knoblich, 2009).

3.3.2 Different modes of asymmetric cell division

The prerequisite to give rise to daughters with different cellular compositions is the establishment of some kind of polarity in the mother cell before or during division. This polarity can in principle be established in two ways (Neumüller and Knoblich, 2009):

1) The polarization of the mother cell is preprogrammed and therefore cell-autonomous (intrinsic regulation).
2) The polarization of the mother cell is dictated by the microenvironment (extrinsic regulation).

Examples for both extrinsic and intrinsic regulation of asymmetric cell division have been described in invertebrates and are exemplified below.

3.3.2.1 Intrinsic regulation of asymmetric cell division

The Par protein complex is an example for intrinsically regulated asymmetric cell division. It is highly conserved and has been shown to control cellular asymmetry in Caenorhabditis elegans, Drosophila melanogaster and vertebrates.
In the C. elegans zygote the core components of the complex, PAR3, PAR6 and PKC3 (aPKC) are distributed along the entire cell cortex. After fertilization, PAR3 and PAR6 disappear from the cortex within close proximity to the sperm centrosome. This enables PAR2, another component of the complex, to locate to the cortex. The PAR2 area subsequently expands until an equally sized anterior PAR3/6 and posterior PAR2 domain is formed. After the domains have been formed, cortical polarity is maintained by inhibitory interactions between anterior and posterior Par proteins. While anterior PKC3 phosphorylates PAR2 to prevent its recruitment to the anterior part of the cortex, PAR2 inhibits PAR3´s localization to the posterior part. Once the cortical polarity is established it is used by a complex machinery to exert unequal pulling force upon mother and daughter centrosomes which result in the displacement of the mitotic spindle towards the posterior pole of the cells during mitosis. The displacement results in the generation of an larger anterior AB and a smaller posterior P1 daughter cells (Cowan and Hyman, 2004; Neumüller and Knoblich, 2009).

3.3.2.2 Extrinsic regulation of asymmetric cell division

The hub is a cluster of somatic cells located at the apical tip of Drosophila testis. It functions as the niche for germ line stem cells (GSC) by secretion of the signaling ligand Unpaired. Unpaired maintains GSC by activating the Janus kinase-signal transducer and activator of transcription (JAK-STAT) signaling pathway. During division the mitotic spindle orients perpendicular to the Hub-GSC interface resulting in the displacement of the daughter cell away from the niche (Kiger et al., 2001; Yamashita et al., 2003). Since the loss of contact to the niche induces differentiation,

GSCs are thought to be preprogrammed to differentiate. GSC differentiation is therefore repressed by signals emanating from the niche and differentiation is induced by derepression upon loss of contact (Morrison and Spradling, 2008).

While the maintenance of Drosophila GSC has been shown to depend on the contact to the hub, intestinal stem cells (ISC), scattered along the basement membrane of the mid gut have been suggested to require signals to differentiate (Morrison and Spradling, 2008). Upon ISC division, vesicles containing the NOTCH1 ligand DELTA are asymmetrically inherited, so that only one daughter receives notch signaling, specifying thereby its future fate (Morrison and Spradling, 2008; Ohlstein and Spradling, 2007).

Although there are several examples on how the microenvironment can modulate stem cell maintenance in invertebrates, it remains unclear if hematopoietic stem cells maintain themselves by displacing one daughter out of the niche (Morrison and Spradling, 2008).

3.3.3 Asymmetric inheritance

The asymmetric inheritance of cell fate determinants is a prerequisite for asymmetric cell division. Both intrinsically regulated asymmetric cell divisions as well as divisions regulated by the environment have been shown to segregate cellular components asymmetrically. The list of cellular organelles and proteins involved is this process has grown over the last decade and involves centrosomes (Yamashita and Fuller, 2008), midbodies (Gromley et al., 2005), midbody remnants (Schink and Stenmark, 2011), chromatin (Rando, 2007), various cell fate determinants (Rhyu et al., 1994; Spana et al., 1995), proteasomes (Chang et al., 2011), aggresomes (Lerit et al., 2013), various endosomes (Emery et al., 2005) and mitochondria (Lerit et al., 2013). Some asymmetric segregations have thereby been observed in various model organisms such as S. cerevisae, C. elegans and D. melanogaster suggesting that the underlying mechanisms are highly conserved throughout evolution (Neumüller and Knoblich, 2009). However, other mitotic asymmetries have so far only been observed

in cultured cells and their functional relevance remains to be demonstrated (Neumüller and Knoblich, 2009). As stated by Horvitz and Herskowitz, “any molecule that is asymmetrically segregated could in principle be used to distinguish sister cells and hence serve as a developmental determinant” (Horvitz and Herskowitz, 1992).

3.3.4 Asymmetric cell fates

Sister cells that show differences in size, shape or other morphological or biochemical features have acquired asymmetric fates. This also holds true for their subsequent patterns of cell division and the number or nature of descendants (Horvitz and Herskowitz, 1992). Asymmetric fates occur frequently in vivo as well as in vitro but it has only been possible for the last 20 years to demonstrate that events happening during cell divisions can be responsible for these future differences in sister cell fates (Neumüller and Knoblich, 2009; Rhyu et al., 1994; Spana et al., 1995). Not every asymmetric fate has to be caused by the asymmetric segregation of cell fate determinants. Alternative models trying to explain how HSCs decide between self-renewal and commitment have been formulated over 30 years ago (Ogawa et al., 1983). While some of these models suggested an underlying stochastic process, others proposed a more deterministic approach in which for instance the microenvironment or growth factors dictate the cellular fates (Korn et al., 1973; Ogawa et al., 1983; TILL et al., 1964; Trentin, 1971). The asymmetric cell division theory is another model proposed to explain how these decisions are made and is discussed below.

3.3.5 The hypothesis of asymmetric cell division of hematopoietic stem cells

The functional demonstration of asymmetric cell division during the development of several model organisms (S. cerevisae, C. elegans and D. melanogaster) led many scientists to conclude that the same principles apply to other organisms and somatic tissue stem cell, such as HSCs. Although it is still unclear if those mechanisms can be generalized, the concept of asymmetric cell division has evolved into a paradigm

and alternative explanations are often disregarded (Neumüller and Knoblich, 2009). The main reason for this is the inconsistent or even incorrect use of the terms asymmetric segregation/inheritance, asymmetric cell fate and asymmetric cell division.

As pointed out by others, the asymmetric segregation of cellular components during stem cell divisions is not sufficient to demonstrate its function (Horvitz and Herskowitz, 1992; Morrison and Spradling, 2008). In other words, asymmetric segregation has to be linked to future asymmetric cell fates to be regarded as an asymmetric cell division. This concept has been nicely applied to demonstrate functional asymmetric cell divisions in C. elegans and D. melanogaster and it is therefore surprising that these terms are confused in the hematopoietic field. Many examples for apparent asymmetric cell division in the blood field rely on the polarization of the mother cell or the asymmetric segregation of specific markers in cells fixed during mitosis by single snap shot analysis. Since these techniques are intrinsically static, dynamic processes such as cell divisions cannot be analyzed reliably. Proteins that are polarized during one phase of the cell cycle might change their localization and pattern of distribution in another cell cycle phase. Furthermore fixed cells are dead and the influence of putative asymmetrically inherited proteins on future daughter cell fates cannot be determined. These reports can therefore only be considered as circumstantial evidence (Horvitz and Herskowitz, 1992). Although circumstantial evidence might imply the occurrence of asymmetric cell division in hematopoietic stem cells, it has yet to be functionally demonstrated.

3.3.6 Circumstantial evidence for asymmetric cell division of hematopoietic stem cells

The two prerequisites, neither of which alone is sufficient, to show functional asymmetric cell division are the demonstration of

1) asymmetric segregation of cellular components during cell division (or asymmetric signaling inputs by asymmetric orientation towards the niche)
2) asymmetric daughter cell fates that correlate with the asymmetric inheritance of cellular components or signals

Asymmetric daughter cell fates have been demonstrated over 30 years ago, when Suda et al. showed that daughters of in vitro separated murine hematopoietic progenitors can differ in their differentiation potential as well as proliferative capacities (Suda et al., 1984a, 1984b). These observations were later confirmed with human hematopoietic progenitors (Leary et al., 1985) and more recently with populations highly enriched for murine HSCs (Ema et al., 2000a; Takano et al., 2004; Yamamoto et al., 2013).

Although asymmetric cell division is commonly assumed in many textbooks to be a property of HSCs the first reports of asymmetric segregation of cellular components in the hematopoietic system were published less than 10 years ago. In 2007, Beckmann et al. suggested CD53, CD62L, CD63 and CD71 as proteins that asymmetrically segregate in human hematopoietic progenitors in vitro (Beckmann et al., 2007). However, since their screen was based on immunofluorescence analysis of fixed samples, the future cell fates of the daughters could not be determined and the potential asymmetric inheritance in living daughters could not be proven. In addition, given the extremely low purity of the used human HSCs (with <1% being HSCs) no conclusions about HSCs were possible from this study. In another study Wu et al. claimed that numb, the notch signaling inhibitor involved in asymmetric cell division in Drosophila melanogaster SOP and neuroblasts, is also asymmetrically segregated during the in vitro culture of murine hematopoietic progenitors cultured on 7F2 or OP9 stromal cells. Although cells from a transgenic fluorescence *Notch* reporter mouse were used to indicate the differentiation status of $CD34^{-}$KSL by time-lapse imaging, the technique was solely applied to detect asymmetric cell fates (notch signaling hi/low). The asymmetric segregation of NUMB on the contrary was determined by classical immunofluorescence analysis of fixed cells. Although indirect evidence for its functional relevance was provided by the observation that GFP+ cells are in general lower in their NUMB expression level than GFP- cells, the asymmetric segregation of numb could not be directly linked to future daughter cell fates.
In a more recent study Ting et al. used time-lapse microscopy to demonstrate that the protein AP2A2, previously shown to bind NUMB and part of the adaptor-protein 2 (AP-2) heterotetrameric complex in clathrin coated pits can asymmetrically segregate during hematopoietic stem and progenitor cell divisions when overexpressed in vitro (Ting et al., 2012). Although transplantation assays indicated that AP2A2

overexpression slightly increases HSC capacity, which is indicative of AP2A2s putative role during HSC cell divisions, differences in daughter cell fates were not determined. Importantly, it must also be mentioned that only 7% of all cell divisions classified as asymmetric segregations completed mitosis successfully. If this unusual high mitotic failure rate is caused by the overexpression of AP2A2 or is indicative of an imaging artifact is unclear. Conclusions of this study therefore must be taken with caution. Interestingly, in contrast to the previous study of Wu (Wu et al., 2007a), HSPCs overexpressing a NUMB-mCHERRY fusion protein cultured on OP9 stromal cells did not show any signs of asymmetric segregation of NUMB (Ting et al., 2012).

Asymmetrically segregating proteins have also been identified in dividing T-cells upon stimulation by antigen presenting cells (Chang et al., 2007). T-cells labeled with CarboxyFluorescein Succinimidyl Ester (CFSE) were transferred into recipients infected with recombinant *Listeria monocytogenes* bacteria. After 32h the undivided T-cells were isolated and cultured with Cytochalasin B, an inhibitor of actin polymerization, before fixation for subsequent immunofluorescence analysis. Among other potential candidates, CD8, PKCζ, IFNγR and NUMB were found to localize asymmetrically to one pole of cell doublets arrested in telophase. Although the asymmetric segregation of these proteins was not monitored live via time-lapse imaging, subsequent flow cytometric analysis of living cells revealed populations distinguishable in several features. These populations were shown to differ in their protective ability upon transplantation and were therefore correlated with T-cell memory and effector fates. A more recent study using the same model was able to shed light on the underlying mechanism and could show that the transcription factor T-BET is asymmetrically segregated during T-cell division and that its unequal appearance is caused by the asymmetric segregation of the proteasome (Chang et al., 2011). Additional evidence for asymmetric cell division of T-cells comes from a study utilizing an in vitro T-cell / dendritic cell co-culture system. Since PAR3, SCRIBBLE, DLG, NUMB and PINS were shown to segregate asymmetrically this study suggests that the mechanisms controlling asymmetric cell division in Drosophila melanogaster are conserved and used by T-cells (Oliaro et al., 2010).

Recently, B-cells have been shown to asymmetrically segregate proteins via a different mechanism that does not seem to depend on prolonged interaction with an

antigen presenting cells (Thaunat et al., 2012). Upon activation, B-cells store antigens for extended periods of time in an intracellular compartment. This intracellular compartment can segregate during B-cell division in symmetric as well as asymmetric manner. B-cell daughters receiving more antigens are more potent in inducing T-cell proliferation than daughter receiving less.

3.3.7 Candidates for asymmetric segregation screen

All proteins previously suggested to be asymmetrically inherited during cell divisions in other model organisms, tissues or in hematopoietic cells were considered as putative candidates and a selection was cloned as fluorescence reporter fusions into lentiviral vectors (i.e. NUMB1, CD63, CD53, etc.). In addition, proteins described in other cell types to be either highly polarized themselves or to be part of a polarized complex were included (i.e. SCA1, VANGL2, Inversin, Inturned). While some of these proteins have been demonstrated to be expressed in HSCs, the expression of others was less clear. However, since even proteins that are not expressed in HSCs would be useful tools to trace divisions if asymmetric segregations were detected, we did not exclude these candidates. Most of the candidates have been reported to be associated with endosomes, lysosomes or the cell membrane but also proteins associated with the polarity complex (PRKCκ, PRKCζ), mitochondria (mito) or centrosomes (Centrin1) have been included. All these cellular compartments have been demonstrated or suggested in different cellular contexts to be asymmetrically segregated, polarized or associated with the occurrence of asymmetric daughter cell fates. A detailed description of all these candidates would exceed the scope of this study but a few are exemplified below. A complete list of all analyzed candidates can be found below.

Table 3.2: Candidates for asymmetric inheritance screen

candidate	ID	Expressed	Localization	Reference
NUMB1	1162	protein	endosomal	(Wu et al., 2007b)
CD63	1160	RNA	lysosomal	(Beckmann et al., 2007)
CD53	1283	protein	endosomal	(Beckmann et al., 2007)
Centrin1	1848	protein	centrosome	(Yamashita and Fuller, 2008)
Prominin1	596	protein	membrane	(Lathia et al., 2011)
LAMP1	1980	not reported	lysosomal	(Bergeland et al., 2001)
FYVE	1630	protein	endosomal	(Coumailleau et al., 2009)
SCA1	1687	protein	membrane	(Vannini et al., 2012)
TGFβRI	1979	protein	membrane	(Yamazaki et al., 2009)
Inscuteable	1983	Not reported	polarity complex	(Kraut et al., 1996)
PRKCκ	1282	protein	Polarity complex	(Lee et al., 2006)
PRKCζ	1385	protein	Polarity complex	(Chang et al., 2007)
Musashi-2	1373	protein	RNA	(Hope et al., 2010)
Mitochondria	1379	protein	mitochondria	(Lerit et al., 2013)
Inversin	1206	Not reported	PCP complex	(Sugimura et al., 2012)
VANGL2	1219	Not reported	PCP complex	(Sugimura et al., 2012)
Inturned	1218	Not reported	PCP complex	(Sugimura et al., 2012)

3.3.7.1 NUMB1

NUMB was the first protein shown to determine the fate of daughter cells upon its asymmetric segregation during mitosis (Rhyu et al., 1994; Spana et al., 1995). In Drosophila, the sensory organ precursor (SOP) gives rise to an external sensory organ consisting of a total number of 4 cells, a neuron, its sheath cell as well as two supporting cells forming the hair and socket. Upon its initial division the SOP gives rise to daughters referred to as pIIa and pIIb. The pIIb cell gives rise to a pIIIb cell

and a glial cell. While the glial cell undergoes apoptosis, the pIIIb divides to produce the neuron and its sheath cell. The pIIa on the contrary divides only once to generate the outer support cells (Neumüller and Knoblich, 2009; Rhyu et al., 1994). NUMB is asymmetrically segregated into pIIb, where is has been shown to interact with the notch receptor to inhibit signal transduction (Giebel and Wodarz, 2012; Guo et al., 1996). Although both daughters express NOTCH, only pIIa retains its responsiveness to NOTCH ligands due to the absence of NUMB (Guo et al., 1996; Santolini et al., 2000). The differences in signaling activity lead subsequently to the acquisition of asymmetric daughter cell fates.

NUMB's role as a cell fate determinant is based on its ability to control the endosomal trafficking of other proteins (Couturier et al., 2012; Giebel and Wodarz, 2012). NUMB binds the α-adaptin subunit of the adaptor protein complex 2 (AP-2), an interaction required for asymmetric cell division in the SOP (Berdnik et al., 2002). Since the AP-2 complex is a major component of clathrin-coated pits a regulatory role for endocytosis was suggested (Santolini et al., 2000). This role was confirmed when NUMB was found to regulate the internalization of NOTCH and its positive regulator SANPODO, thereby modulating the notch signaling responsiveness during asymmetric cell division (Couturier et al., 2012; Giebel and Wodarz, 2012).

Since its initial discovery as a cell fate determinant, numb has been shown to act in a similar fashion in other tissues of Drosophila (i.e. central nervous system, malphighian tubules, gut and muscles) and other organisms, for example mus musculus (Carmena et al., 1998; Neumüller and Knoblich, 2009). Since it possesses a high degree of conservation among different tissues and species, NUMB has been suggested to exert similar functions by being asymmetrically segregated during HSC divisions.

NUMB as well as NOTCH1 are expressed in HSCs and have been suggested to regulate their maintenance (Duncan et al., 2005; Stier et al., 2002; Wu et al., 2007a). This idea was supported by the observation that notch activation by its ligand JAGGED1 promotes HSC maintenance in vitro (Calvi et al., 2003). However, later reports showing that abrogation of notch signaling by either deletion of *Notch1* and/or *Jagged1*, or expression of dominant-negative *Mastermind-like1*, does not affect HSC self-renewal or differentiation. This demonstrates that notch signaling is not required

for HSC maintenance in vivo (Maillard et al., 2008; Mancini et al., 2005). In addition, simultaneous deletion of *Numb* and its mammalian homolog *Numblike* in HSCs did not affect HSC self-renewal or differentiation (Wilson et al., 2007). Although these reports highlight the controversy about the role of numb/notch signaling in HSCs, the later do not exclude a potential function under certain circumstances. However, it seems that numb and notch signaling is not required under homeostasis or that their loss might be compensated by other mechanisms.

Whether or not NUMB is segregated asymmetrically during HSC division is controversial. Wu et al. reported asymmetric segregation of NUMB in hematopoietic stem and progenitor cells, cultured on OP9 and 7F2 stromal cell lines in vitro, while a more recent study by Ting et al., using the same stromal cell line, could not confirm this observation (Ting et al., 2012; Wu et al., 2007a). This discrepancy might be explained by the different experimental approaches. Wu´s observation was based on the immunofluorescence analysis of fixed HSPCs (Wu et al., 2007a). Ting and colleagues on the other hand were using time-lapse microscopy of living HSPCs overexpressing a NUMB-mCHERRY fusion (Ting et al., 2012). Further research is required to clarify this issue. Even if Wu´s observations prove to be correct, the functional relevance of numbs asymmetric segregation remains to be demonstrated. The observation that NUMB low expressing cells tend to have in general lower *Notch* reporter levels is indicative of its function but not sufficient to meet the previously stated criteria required to prove asymmetric cell division (Giebel and Beckmann, 2007; Horvitz and Herskowitz, 1992).

However, evidence that NUMB is asymmetrically segregating in hematopoietic cells, although not necessarily in HSCs, is coming from studies demonstrating asymmetric cell division of T-cells (Chang et al., 2007; Oliaro et al., 2010). Interestingly, the asymmetric segregation of NUMB in these studies was shown in fixed cells via immunofluorescence analysis.

3.3.7.2 CD63/MLA1

CD63/MLA1 is an integral membrane protein belonging to the tetraspanin family. It is present in tetraspanin-enriched microdomains (TEMs) at the cell surface, but is also abundantly localized to late endosomes/multivesicular bodies, lysosome-related organelles, lysosomes and exosomes (Hemler, 2005; Pols and Klumperman, 2009; Tarrant et al., 2003). CD63/MLA1 is considered to be ubiquitously expressed and is used, due to its high abundance in LAMP1 and LAMP2 positive compartments, as a lysosomal marker (Metzelaar et al., 1991). It has also been demonstrated to interact with MHCII and a role in antigen uptake and/or presentation has been suggested (Engering and Pieters, 2001; Glickman et al., 1996; Mantegazza et al., 2004; Peters et al., 1991). In another study CD63 was shown to regulate the migration of human CD4+ T-Cells by locating CXCR4 from the cell surface to lysosomes, thereby reducing the SDF1 responsiveness (Yoshida et al., 2008). Further interaction partners include a variety of integrins (α4β1, α3β1, α6β1, LFA-1), tetraspanins (CD81, CD82, CD9, CD151), cell surface receptors (CD3. FcεRI), kinases and adaptor proteins, highlighting CD63s functional diversity (Pols and Klumperman, 2009).

CD63 has been shown to be expressed in murine HSCs at the RNA level (Akashi et al., 2003; Forsberg et al., 2005). Its asymmetric segregation has been suggested in fixed human cord blood derived $CD34^{+}CD133^{+}$ hematopoietic progenitor cells via immunofluorescence analysis (Beckmann et al., 2007). Beckmann demonstrated that in vitro cultured $CD63^{low}$ expressing $CD34^{+}CD133^{+}$ are more immature due to a higher LTC-IC frequency. The direct functional correlation between its asymmetric segregation and function however, was not demonstrated.

3.3.7.3 Stem cell antigen-1 (SCA1/Ly-6A/E)

SCA1 is a GPI-anchored surface protein expressed on murine hematopoietic stem and progenitor cells (Spangrude et al., 1988). Its function is largely unknown and its role in HSC regulation is controversial. It was initially reported that HSPCs derived from *Sca1*-/- mice have impaired competitive short-term repopulation activity as well

as a reduced self-renewal, determined by serial transplantation assays (Ito et al., 2003). However, a later study conducted by Bradfute et al., although confirming impaired short-term repopulation activity, did not observe defects in HSC self-renewal. Instead, a reduction of c-KIT expression, lineage skewing in B-cells, NK-cells as well as granulocytes and macrophages and a homing defect were reported (Bradfute et al., 2005). Although Ito et al. also observed differences in the lineage output after transplantations as well, the reported decrease in megakaryocytes and platelets does not agree with Bradfute´s observations (Bradfute et al., 2005; Ito et al., 2003). The differences between these studies might be explained by their use of different transplantation techniques. While Ito et al. utilized serial transplantations, commonly used as a readout for self-renewal, Bradfute used serial treatment of 5-Fluorouracil after one round of transplantation, arguing that serial transplantations might preferentially read out homing defects (Bradfute et al., 2005). Further studies are required to clarify if SCA1 is required for HSC self-renewal. Although it is not clear yet if SCA1 is required for self-renewal, it is highly expressed on stem cells and early progenitors, not only in the hematopoietic system, but also in other tissues, like the mammary glands, dermis, skeletal muscle and others (Holmes and Stanford, 2007). The down regulation of SCA1 is accompanied with a loss of self-renewal and sca-1^{low} expressing hematopoietic stem and progenitor cells have been shown to be committed to differentiation (Akashi, 2009).

Besides its potential role in self-renewal and/or homing, HSC derived from *Sca1*-/- mice have been shown to be insensitive to Interferon α (IFNα) stimulation. INFα activates quiescent HSC by activating STAT1 and PKB/AKT signaling which subsequently leads to an upregulation of SCA1 (Essers et al., 2009). SCA1 has also been suggested to act as a suppressor of TGFβ1 signaling by disrupting the heterodimerization of TGFβRI and TGFβRII in the NMuMG cell line (Upadhyay et al., 2011). A more recent study reported SCA1 having a negative effect on erythropoiesis (Azalea-Romero et al., 2012). This observation is in line with an earlier study investigating the differentiation propensities of SCA1^{low}, SCA1^{mid} and SCA1^{high} subpopulation, isolated from the EML cell line (Chang et al., 2008).

As other GPI-anchored proteins, SCA1 is believed to reside in lipid rafts (cholesterol rich membrane domains) thought to be involved in the modulation of signaling cascades (Horejsí et al., 1999). Lipid rafts, identified by the GM1 marker Cholera

toxin B, have been shown to be evenly distributed in the membrane of freshly isolated hematopoietic $CD34^{-}$KSL cells. After stimulation with growth factors in vitro, lipid rafts form clusters and intracellular signaling pathways are activated. Treatment of HSCs with the cholesterol depleting agent methyl-β-cyclodextrin (MβCD) prevents lipid raft clustering and abrogates intracellular signaling (Yamazaki et al., 2006).

SCA1 has not been shown to segregate asymmetrically so far. However, based on its location in lipid rafts we speculated that upon cytokine stimulation SCA1 might cluster along with other lipid raft associated proteins and that the clusters might segregate asymmetrically during HSC division in vitro. The idea is supported by a recent study, investigating the effect of different growth factors on lipid raft clusters in hematopoietic $CD150^{+}$KSL in vitro. As expected, cytokine stimulation induced SCA1 clustering, a process that was inhibited by MβCD treatment (Vannini et al., 2012).

3.3.7.4 Vang-like 2 (VANGL2/Loop tail)

VANGL2/Loop tail is a four-pass trans membrane protein and a core component of the Frizzled/planar cell polarity (PCP-) complex (Seifert and Mlodzik, 2007). The PCP-complex is evolutionary conserved from D. melanogaster to vertebrates and controls proper cell orientation within tissues. This orientation is achieved by the polarized localization of PCP-complex proteins within cells. In a recent study, Sugimura et al. demonstrated, using a Scl-tTA inducible H2B-GFP reporter mice to identify label retaining cells, that quiescent but not actively cycling hematopoietic $CD34^{-}CD135^{-}$KSL express the PCP-Components CELSR2/Fmi and Frizzled-8 (FZ8) (Sugimura et al., 2012). CELSR2 and FZ8 have been shown to be highly polarized and to predominantly localize at the interface to N-Cadherin (N-CAD) positive osteoblast progenitors in vivo. This observation could also be confirmed in vitro when quiescent HSCs were cocultured with the osteoblast progenitor cell line OP9 in vitro (Sugimura et al., 2012). Although the study did not address what happens with the highly polarized PCP-complex during HSC division we speculate that VANGL2 and other components of this complex are asymmetrically segregated during HSC divisions.

3.3.7.5 CD107a/LAMP1

CD107a/LAMP1 is an integral membrane glycoprotein highly abundant in lysosomes. Although it can be detected in the MHCII compartment, to a lesser extent in late endosomes and at the cell surface as well, it is generally considered to be a lysosomal marker (Escola, 1998; Williams and Fukuda, 1990). So far, LAMP1 has not directly been shown to segregate asymmetrically. However, Bergeland et al. demonstrated via life cell imaging of BSA-alexa594 pulsed MDCK cells that the observed segregation of the late endosomal/lysosomal compartment does not fit the expected stochastic distribution and concluded that there is no evidence “for a strict mechanism assuring an equal division of endosomes/lysosomes into the two daughter cells” (Bergeland et al., 2001). He suggested that the segregation of lysosomes might be ordered, although the accuracy would equal a stochastic process. Although not stated by the authors, the observation indicates that at least some part of the lysosomal compartment might segregate asymmetrically during MDCK cell divisions. Since CD63, another marker for late endosomes and lysosomes has been suggested to segregate asymmetrically during human hematopoietic progenitor divisions we speculated that LAMP1, labeling the same cellular compartment might show similar behaviors during hematopoietic stem cell division (Beckmann et al., 2007).

3.4 Experimental approach

3.4.1 The necessity for single cell analysis and its limitations

Classical biological assays are based on the analysis of thousands or even millions of cells and represent population averages. Although these assays can be used to address certain questions they are less useful for others. In fact, population averages can be interpreted in multiple ways, which led to controversies in the past. For example, the cytoplasmic to nuclear oscillations of NF-κb was missed until single cells were observed (Bakstad et al., 2012). The advent of clonal assays, immunofluorescence and high throughput single cell analysis by flow cytometry

demonstrated that even populations assumed to be rather homogenous, like embryonic stem cells, are highly diverse (Chambers et al., 2007).

Assays with single cell resolution are a prerequisite to study cell divisions. However since these assays are usually based on single snap-shot analysis the dynamics of the process are lost. This makes it difficult to judge if the observed polarization in mitotic cells would have led to asymmetric inheritance or is simply transient. In addition, most of these assays require fixation of the cells rendering any subsequent analysis and thereby proof of functional relevance for the observed asymmetry impossible. Furthermore, assays based on fixed cells are intrinsically artificial and are highly inefficient when rare cell populations such as HSCs have to be analyzed. In order to increase the frequency of mitotic cells upon fixation, cytokinesis inhibiting chemicals have been used in the past (Wu et al., 2007b). One of them, nocodazol, was recently shown to be inappropriate to study cell divisions due to its impact on cell viability and interference with proper centrosome localization (Nteliopoulos and Gordon, 2012). This demonstrates that results accomplished utilizing these reagents should be interpreted with care and that previously drawn conclusions based on these experiments require reevaluation.

3.4.2 Continuous single cell analysis – a prerequisite to study cell division

Single cell snap shot analysis has been useful in mapping cellular heterogeneity but is insufficient to elucidate dynamic processes like migration, differentiation, signaling or cell division. Although it is possible to study these processes indirectly by merging the analysis of independent samples at consecutive time points (time course analysis), single cell identity and cell viability are lost and subsequent functional assays are not possible. Simple single snap shot analysis of dynamic processes can therefore be interpreted in several ways. As with the interpretation of data derived from population averages this has led to decade long controversies about basic biological questions. It is thus not sufficient to analyze cell divisions by snap shot analysis, but a prerequisite to observe single living cells continuously over time.

3.4.3 Quantification of cell divisions

In order to assess if proteins are inherited in a symmetric or asymmetric fashion during cell division their abundance needs to be determined and compared between sister cells. Proteins of interest can either be genetically engineered and fused to fluorescent reporters or labeled directly with antibodies conjugated to fluorescent dyes. In both approaches, the amount of light emitted upon excitation of the fluorochrome is detected and used as a reporter for the presence, localization and abundance of the protein.

The most physiological way to express fluorescently tagged proteins is the generation of knock-in mice. Since the regulatory elements of the endogenous gene are maintained, the fusion protein is assumed to be expressed at physiological levels. Unfortunately, the generation of knock-in mice is time consuming and expensive and therefore not suited to screen a bigger number of candidate genes.

Viral delivery of fusion genes is a commonly used alternative. It is considerably faster and cheaper to generate viruses encoding fusion genes making it suitable for screening approaches. The technique comes with several drawbacks that need to be considered when experimental results are interpreted. The fusion protein is overexpressed, which might alter cellular behavior or protein localization itself. Clone to clone variability is likely since neither the number of viral integrations nor the viral integration site itself can be controlled. The detection of asymmetric fates is unlikely if the overexpressed protein acts as a cell fate determinant.

Manipulating cells by introducing genetically engineered fusion proteins might alter protein function and thereby cellular behavior. Although this is true for knock-in strategies as well, it is a major concern if fusion proteins are delivered virally. If the protein of interest is located at the cell surface, live antibody staining offers an alternative way to label proteins. In contrast to viral delivery, endogenous proteins levels are detected. Since live antibody staining circumvents the need for overexpression, the detection of asymmetric fates is more likely. Potential asymmetries established during mitosis are expected to be more stable since the expression of candidate genes and their downstream effects is not enforced in both daughters. Although live antibody staining avoids many issues associated with viral

delivery approaches it is not readily available for every surface antigen. For yet unknown reasons only some antibodies stain living cells during continuous observation. In addition, some antibodies may possess either blocking or activating properties and are therefore limited in their usability.

Based on careful evaluation of the advantages as well as drawbacks of the described approaches for our initial screen we decided to use virally delivered fluorescence reporter fusions and supplemented this approach with live antibody staining where ever possible.

3.4.4 In vitro maintenance of hematopoietic stem cells

Observing single, living hematopoietic stem cells continuously and quantitatively over time is a prerequisite to analyze dynamic processes such as cell divisions and should ideally be done in vivo, where the cells are undisturbed in their natural cellular environment. Imaging of living HSCs in vivo has been reported before (Lo Celso et al., 2009). However, the associated technical and ethical constraints limit the temporal as well as spatial resolution necessary to reliably detect and quantify the asymmetric segregation of proteins. In addition, the functional relevance of any putative asymmetry cannot be tested since cellular identities are soon lost using current technologies. We therefore decided to image HSC divisions in vitro where ethical and technical requirements can be fulfilled.

Despite repeated efforts around the globe, conditions that maintain or expand genetically unmodified HSCs indefinitely in vitro have not been described. However, several culture conditions have been shown to maintain HSCs for a limited period of time. These culture conditions are of particular interest for this study given that the limited maintenance of HSCs might be associated with asymmetric cell fates within single colonies and could therefore provide the functional relevance of putative asymmetric segregation. What is known about the behavior of HSCs in these culture conditions and why we intend to use them is discussed below.

3.4.4.1 In vitro model of the niche

Hematopoietic stem cells reside in a special microenvironment termed the “niche”. When the niche is ablated for instance by irradiation, HSC activity is lost. Stromal cell lines such as OP9 are frequently used as an in vitro model for the niche since they possess the capacity to maintain HSCs for limited amounts of time (Ueno et al., 2003; Wu et al., 2007a). The OP9 stromal cell line consists of osteoblast progenitors, a lineage that has been shown to be capable to support the maintenance of in vitro cultured HSCs (Taichman and Emerson, 1994). Increasing the number of osteoblasts by genetic manipulation has been shown to also increase the number of HSCs in vivo (Calvi et al., 2003; Zhang et al., 2003). In addition to their supporting abilities OP9s have been used in several other studies investigating in vitro cell divisions of hematopoietic stem and progenitor cells and has been shown to interact and polarize HSCs in a FZ8/CELSR2 dependent manner (Sugimura et al., 2012). This cell line has also been used in studies that suggested that NUMB and AP2A2 are asymmetrically segregating (Ting et al., 2012; Wu et al., 2007b).

3.4.4.2 Maintaining HSC in stromal cell free culture conditions

3.4.4.2.1 Culturing HSCs in SCF and TPO

Until today it is not possible to maintain HSCs for extended periods of time in stromal cell free culture conditions. However, several studies have reported culture conditions exerting positive effects on HSC activity. One of these culture condition contains SCF and TPO (Ema et al., 2000a; Takano et al., 2004). This combination has been demonstrated to be able to maintain in vitro cultured HSCs for at least 6 days (Ema et al., 2000b; Takano et al., 2004). In addition, daughters of HSCs cultured in these conditions have been demonstrated to differ in their differentiation potential (Takano et al., 2004). We therefore speculated that putative asymmetric segregation in these culture conditions might be correlated to the previous described asymmetric fates.

3.4.4.2.2 Culturing HSCs in SCF, TPO and TGFβ1

Another study used a cytokine cocktail containing SCF, TPO and TGFβ1 (Yamazaki et al., 2009). Interestingly, over an in vitro culture period of 5 days all differentiated $CD34^{+}$KSL died while 50% of the HSCs survived. Functional tests revealed that the surviving cells that had not been divided retained HSC activity in a similar fashion as freshly isolated $CD34^{-}$KSL. Based on this, the study concluded that TGFβ1 induces HSC hibernation. However, since HSCs were not observed continuously it cannot be excluded that HSCs underwent divisions followed by cell death of one daughter. Based on this we speculated that TGFβ1 selectively induces cell death of differentiated cells while maintaining HSCs and that apoptosis of one daughter after cell division could serve as an in vitro read out for asymmetric cell fates and loss of HSC activity.

3.5 Rational – Objective of the study

Hematopoietic stem cells have the ability to self-renewal and differentiate into all hematopoietic lineages. After cell division these properties can either be retained by both daughters (expansion), one daughter (maintenance) or can be completely lost (differentiation). It is currently not understood whether these outcomes are regulated by mechanisms that act during cell division or are determined by post mitotic events. Based on studies of invertebrates, symmetric or asymmetric segregation of cell fate determinants has been proposed to regulate the outcome of HSC divisions. However, this hypothesis has not been tested and neither the symmetric or asymmetric segregation of cell fate determinants, nor their functional relevance has been demonstrated in highly purified, living HSCs.

The objective of the study is to test this hypothesis. Therefore novel, continuous, quantitative bioimaging approaches were used. Fusion proteins of selected candidate genes previously suggested to be associated with asymmetric cell divisions were cloned and analyzed quantitatively for their segregation mode in HSCs as well as early hematopoietic populations under different culture conditions. In vitro read-outs

to distinguish symmetric from asymmetric daughter cell fates were established for differentiation and self-renewal potential and correlated to the segregation of candidates during initial in culture divisions.

4 Material

4.1 Devices

4.1.1 Centrifuges

Name	Company
Rotanta 460R	Hettich Holding GmbH & Co. oHG, Kirchlengern, Germany
Rotina 380R	Hettich Holding GmbH & Co. oHG, Kirchlengern, Germany
Mikro 200	Hettich Holding GmbH & Co. oHG, Kirchlengern, Germany
Mikro 200R	Hettich Holding GmbH & Co. oHG, Kirchlengern, Germany
Avanti-J-E	Beckman Coulter GmbH, Krefeld, Germany
Avanti-J30I	Beckman Coulter GmbH, Krefeld, Germany
Galaxy Mini Microcentrifuge	VWF International Inc.
Centrifuge/Vortexer	neoLab Migge Laborbedarf-Vertriebs GmbH, Heidelberg, Germany

4.1.2 Tissue culture hood

Name	Company
HERA safe KS	Thermo Electron Corporation

4.1.3 Incubators

Name	Company
Microbiol. Incubator CD210	Binder, Tuttlingen, Germany
Shaking incubator	Sheldon Manufacturing, Inc. Cronelius, USA

4.1.4 Transilluminator

Name	Company
UV Transilluminator 2000	Bio-Rad Laboratories, München, Germany
Geneflash	Syngene, Cambridge, UK
TM-300 Miniature CCD Camera	JAI A/S, Grosswallstadt , Germany

4.1.5 Freezer

Name	Company
-20°C Premium No Frost, small	Liebherr-International GmbH, Germany
-20°C Premium No Frost, big	Liebherr-International GmbH, Germany
-80°C Sanyo Ultra low	Panasonic Healthcare Company, USA
-80°C	New Brunswick Scientific, Germany

4.1.6 Pipettes

Name	Catalog no.	Company
Accujet Pro	26300	BRAND GMBH + CO KG, Germany
Pipetman Classic P2	F144801	Gilson, Inc. USA
Pipetman Classic P20	F123600	Gilson, Inc. USA
Pipetman Classic P200	F123601	Gilson, Inc. USA
Pipetman Classic P1000	F123602	Gilson, Inc. USA
Transferpette 20-200µL	703730	BRAND GMBH + CO KG, Germany
Pipet-LiteMultichannel	17013808	Rainin, USA
Pipette 2 - 20µL		

4.1.7 PCR Cycler

Name	Company
PCR sprint system	Thermo Fisher Scientific Inc. Schwerte, Germany
Px2 thermal cycler	Thermo Fisher Scientific Inc. Schwerte, Germany

4.1.8 Miscellaneous

Name	Company
Nanodrop	Thermo Fisher Scientific Inc. Schwerte, Germany
Vortex Genie 2	Scientific Industries, Inc., New York, USA
Heating block HBT-2-131	Heinrich Haep HLC, Bovenden, Germany
Cryo Freezing Containing	Nalgene, Rochester, USA
Gaswash bottleincl.filter	Carl Roth GmbH + Co. KG, Karlsruhe, Germany
Drossel-Rückschlagventil GR-QS-4	FESTO
Powerpac Basic Power Suppyly	Bio-Rad Laboratories GmbH, Germany
Reax top vortexer	Heidolph Instruments GmbH & Co.KG, Germany
inoLab pH-meter	WTW GmbH, Germany
ABS weight	Kern & Sohn GmbH, Germany
Microwave	Severin Elektrogeräte GmbH, Germany

4.1.9 Microscopes

4.1.9.1 Epifluorescence microscopes

4.1.9.1.1 Microscope body

Name	Catalog number	Company
Eclipse TS100	-	Nikon
Axiovert 40C	-	Carl Zeiss AG, Oberkochen, Germany
Axiovert 200M	000000 1312 732	Carl Zeiss AG, Oberkochen, Germany
AxioObserver Z1	431007 9902 000	Carl Zeiss AG, Oberkochen, Germany

4.1.9.1.2 Hardware autofocus

Name	Catalog number	Company
Definite Focusincl. Objective revolver mot. ACR	424533 9000 000	Carl Zeiss AG, Oberkochen, Germany

4.1.9.1.3 Optical filter

name	Ex. filter	Beam-splitter	Em. filter	Catalog number	Company
DAPI HC	387/11	BS 409	447/60	F36-513	AHF analysentechnik AG, Tübingen, Germany
38 HE	470/40	FT 495	525/50	489038-9901-000	Carl Zeiss AG, Oberkochen
GFP	470/40	495 LP	525/50	F46-002	AHF analysentechnik AG, Tübingen, Germany
46 HE	500/25	FT 515	535/30	489046-9901-000	Carl Zeiss AG, Oberkochen
YFP ET	500/20	515 LP	535/30	F46-003	AHF analysentechnik AG, Tübingen, Germany
43 HE	550/25	FT 570	605/70	489043-9901-000	Carl Zeiss AG, Oberkochen
mCherry HC	562/40	BS 593	641/75	F36-508	AHF analysentechnik AG, Tübingen, Germany
ET-SET Cy5	620/60	LPXR 660	700/75	F46-006	AHF analysentechnik AG, Tübingen, Germany
Dualband GFP/mCHERRY ET	474/25+ 570/40	ET 525/25 + 635/70	525/25 + 635/70	F56-019	AHF analysentechnik AG, Tübingen, Germany

4.1.9.1.4 Objectives

Name	Catalog number	Company
Fluar 10x/0,5 M27	420140-9900	Carl Zeiss AG, Oberkochen
Fluar 10x/0,50	440135-0000	Carl Zeiss AG, Oberkochen
EC Plan-Neofluar 10x/0,3 Ph1 M27	420341-9911	Carl Zeiss AG, Oberkochen
EC Plan-Neofluar 10x/0,3 Ph1	440331-9902	Carl Zeiss AG, Oberkochen
OEC Plan-Neofluar 10x/0,3 Ph1	440331-9902	Carl Zeiss AG, Oberkochen
ObjektivFluar 20x/0,75	440145-9901	Carl Zeiss AG, Oberkochen

4.1.9.1.5 Camera

Name	Company
AxiocamHRm Rev.2	Carl Zeiss AG, Oberkochen, Germany
AxiocamHRm Rev.3	Carl Zeiss AG, Oberkochen, Germany
Axiocam MRc5	Carl Zeiss AG, Oberkochen, Germany

4.1.9.1.6 TV-Adapter

Name	Catalog number	Company
Camera-Adapter 60C 1" 1,0x	456105 9901 000	Carl Zeiss AG, Oberkochen, Germany
Video-Adapter 60 C 2/3" 0,63x	000000 1069 414	Carl Zeiss AG, Oberkochen, Germany
Camera-Adapter 60N-C 2/3" 0,5x	426112 0000 000	Carl Zeiss AG, Oberkochen, Germany
Video-Adapter 60 C 1/3" 0,4x	456108 0000 000	Carl Zeiss AG, Oberkochen, Germany

4.1.9.1.7 Motorized Stages

Name	Catalog no.	Company
Ludl MAC5000 XY stage 130x100	000000 0431 478	Märzhäuser Wetzlar GmbH & Co. KG
Ludl MAC6000 XY stage 130x100	000000 1695 168	Märzhäuser Wetzlar GmbH & Co. KG
Motorized stage 130x85 mot P; CAN	432031 9902 000	Carl Zeiss AG, Oberkochen, Germany

4.1.9.1.8 Computer

Name	Catalog number	Company
Raidsonic Icy Box IB	IB-169SK-B	RaidSonic Technology GmbH, Ahrensburg, Germany
Siemens Workstation FSC Celsius R630-2	S26361-K680-V215	Fujitsu Technology Solutions GmbH, München, Germany

4.1.9.1.9 Hard drives

Name	Company
0.5TB HD501LJ	Samsung Electronics GmbH, Germany
1TB HD103SJ	Samsung Electronics GmbH, Germany
2TB Barracuda	Seagate Technology LLC, Germany

4.1.9.1.10 Temperature control

Name	Catalog number	Company
Heating Unit	000000 1116 061	Carl Zeiss AG, Oberkochen, Germany
Temperature Control Unit	000000 1052 320	Carl Zeiss AG, Oberkochen, Germany
Temperature Module S1	411860 9010 000	Carl Zeiss AG, Oberkochen, Germany
Heating Unit XL S1	411857 9030 000	Carl Zeiss AG, Oberkochen, Germany

4.1.9.1.11 Light sources

4.1.9.1.11.1 Transmitted light

Name	Catalog number	Company
Halogen bulb with collector	423000 000 000	Carl Zeiss AG, Oberkochen, Germany
Transmitted light VIS-LED	423053 9030 000	Carl Zeiss AG, Oberkochen, Germany

4.1.9.1.11.2 Reflected light

Name	Catalog number	Company
HXP 120C	423013 9000 777	Leistungselektronik JENA, Germany
Liquid light guide	000000 0482 760	Carl Zeiss AG, Oberkochen, Germany
SPECTRA X light engine™	-	Lumencor, Inc., Beaverton, USA

4.1.9.2 Confocal microscopes

Name	Company
Leica TCS SP5	Leica Microsystems GmbH, Germany

4.1.10 Flow cytometer

4.1.10.1 Model

Name	Company
BD FACS Aria III	Becton, Dickinson and Company, Germany

4.1.10.2 Filters and settings

561nm Laser (561)	beamsplitter	PMT voltage
582/15	-	
610/20	600LP	
670/14	630LP	
780/60 I	735LP	
Red Laser (633nm)		
660/20	-	
730/45	690LP	
780/60 II	755LP	
Blue Laser (488nm)		
530/30 I	502LP	
695/40	655LP	
Violet Laser (405nm)		
450/40	-	
530/30	502LP	
585/40	556LP	

4.2 Chemicals and reagents

4.2.1 General

Name	Catalog no.	Company
Agarose	870055	Biozym Scienfitic GmbH, Germany
Ampicillin sodium salt	K029.1	Carl Roth GmbH, Germany
BD Cellclean	349524	BD Biosciences, San Jose, USA
BD FACS Clean Solution	340345	BD Biosciences, San Jose, USA
BD FACSFlow Sheath Fluid	342003	BD Biosciences, San Jose, USA
DMSO	D2438	Sigma-Aldrich, USA
dNTP Set	R0181	Thermo Fisher Scientific, Germany

DPBS, -Ca, -Mg	14190-094	Life Technologies, Grand Island, USA
EDTA	CN063	Carl Roth GmbH, Germany
Ethanol 100%	100983	Merck KGaA, Darmstadt, Germany
Ethidiumbromid solution 1%	2218.2	Carl Roth GmbH, Germany
Gelatin from porcine skin	G1890	Sigma-Aldrich, USA
GeneRuler DNA Ladder Mix	SM0331	Thermo Fisher Scientific, Germany
Giemsa stain, mod. solution	48900	Sigma-Aldrich, USA
Hamster Fibronectin	IHMFBN	Dunn Labortechnik GMBH
Heparin	H3149	Sigma-Aldrich, USA
LB Broth Base	12780-029	Life Technologies, Grand Island, USA
Lichrosolv HPLC H2O	1.15333.1000	Merck KGaA, Darmstadt, Germany
May-Grünwald solution	T863.1	Carl Roth GmbH, Germany
Nail polish, essence gel-look	-	Cosnova GmbH, Germany
NaN_3	S2002	Sigma-Aldrich, USA
Paraformaldehyde	0335.3	Carl Roth GmbH, Germany
Pertex, Hist. mounting sol.	41-4010-00	Medite GmbH, Germany
Polyethylenimine, Lin (25k)	23966	PolySciences Inc., Germany
Poly-L-Lysine	P8920-100mL	Sigma-Aldrich, USA
Probumin	81-068-3	EMD Millipore Corporation, Billerica,USA
Roti-MagBeads Streptavidin	HP57.1	Carl Roth GmbH, Germany
Sodium chloride	1064060500	Merck KGaA, Germany
Taq DNA Polymerase	EP0072	Thermo Fisher Scientific, Germany
Triton-X	3051.3	Carl Roth GmbH, Germany
Trypan Blue Sol. 0.4%	15250	Life Technologies, Grand Island, USA
Tween-20	9127.1	Carl Roth GmbH, Germany

4.2.2 Tissue culture media and reagents

Reagent	Catalog number	Company
2-mercaptoethanol	M3148-25ML	Sigma-Aldrich, USA
EDTA Dinatriumsalz P.A	8043.2	Carl Roth GmbH + Co. KG, Karlsruhe, Germany
L-Glutamine	25030-081	Life Technologies, Grand Island, USA
Penicillin-Streptomycin (100X)	15140-122	Life Technologies, Grand Island, USA
Silicone oil AR 200	85419-100ML	Sigma-Aldrich, USA
Sodium Pyruvate Solution	S8636	Sigma-Aldrich, USA
StemPro®-34 SFM (1X), Liquid	10639-011	Life Technologies, Grand Island, USA
StemSpan™ SFEM	09650	STEMCELL Technologies SARL, Grenoble, France
StemSpan™ SFEM (phenol red free)	-	STEMCELL Technologies SARL, Grenoble, France
Trypsin-EDTA (1X), Phenol Red (0.05%)	25300-054	Life Technologies, Grand Island, USA

4.2.3 Serum

Reagent	Lot No.	Catalog no.	Company
FETAL BOVINE SERUM QUALIFIED (FCS 13)	S05130S1900	S1900-500	Biowest (Distributor Th.Geyer)
Fetal Bovine Serum (FCS 14)	A10108-2429	A15-101	PAA Laboraties, Velizy-Villacoublay, France
Fetal Bovine Serum (FCS 17)	-	30-2020	ATCC, Manassas, USA
Donkey serum	-	17-000-121	Dianova GmbH, Germany

4.2.4 Cytokines

Cytokine	Catalog number	Company
Recombinant human SCF	167300-07-B	Tebu Bio (Peprotech)
Recombinant human TPO	167300-18-B	Tebu Bio (Peprotech)
Recombinant mouse IL-3	167213-13-B	Tebu Bio (Peprotech)
Recombinant human EPOα	C-60022	Promokine
Recombinant human TGF-beta 1	240-B-010	R&D Systems, Miineapolis, USA

4.2.5 Antibodies

4.2.5.1 Flow cytometry

Antigen	conjugate	Clone	Catalog no.	company
B220	Biotin	RA3-6B2	13-0452-86	eBioscience
CD11b	Biotin	M1/70	13-0112-85	eBioscience
CD11b	eFluor® 450	M1/70	48-0112-82	eBioscience
CD150	PE	TC15-12F12.2	115904	Biolegend
CD16/CD32	Per-CP Cy5.5	93	45-0161-82	Biolegend
CD19	Biotin	eBio1D3 (1D3)	13-0193-85	eBioscience
CD34	eFluor® 450	RAM34	48-0341	eBioscience
CD3ε	Biotin	145-2C11	13-0031-85	eBioscience
CD41	Biotin	eBioMWReg30	13-0411-85	eBioscience
CD41	APC	eBioMWReg30	17-0411-82	eBioscience
CD48	FITC	HM48-1	103404	Biolegend
CD48	APC	HM48-1	17-0481-82	eBioscience
CD48	purified	HM48-1	16-0481-85	eBioscience
c-KIT	PE-Cy7	2B8	25-1171-82	eBioscience
c-KIT	APC eFluor®780	2B8	47-1171-82	eBioscience

Gr-1	Biotin	RB6-8C5	13-5931-85	eBioscience
Gr-1	FITC	RB6-8C5	11-5931-82	eBioscience
Gr-1	Alexa700	RB6-8C5	56-5931	eBioscience
Sca-1	Per-CP Cy5.5	D7	45-5981-82	eBioscience
Sca-1	purified	D7	14-5981-82	eBioscience
Streptavidin	APC eFluor®780	-	47-4317-82	eBioscience
Ter119	Biotin	TER-119	13-5921-85	eBioscience
Ter119	PE	TER-119	12-5921-81	eBioscience

4.2.5.2 Live cell labeling

Name	**Catalog no.**	**Company**
Hoechst33342	H1399	Life Technologies GmbH, Darmstadt, Germany
LysoTracker® Red DND-99	L-7528	Life Technologies GmbH, Darmstadt, Germany
Cyto-ID® Autophagy detection kit	ENZ-51031-K200	Enzo Life Sciences, Inc., Lörrach, Germany
Cholera Toxin Subunit B (Recombinant), Alexa Fluor® 488 Conjugate	C-34775	Life Technologies GmbH, Darmstadt, Germany
Cholera Toxin Subunit B (Recombinant), Alexa Fluor® 647 Conjugate	C-34778	Life Technologies GmbH, Darmstadt, Germany

4.2.6 Enzymes

Name	Catalog no.	Company
DNA Pol. Lg. Fragm. (Klenow)	M0210 S	New England Biolabs, Ipswich, USA
Taq DNA Polymerase	EP0072	Thermo Fisher Scientific , Germany
Advantage Polymerase Mix	639201	Takara Bio Europe
Antarctic Phosphatase	M0289 S	New England Biolabs, Ipswich, USA
T4 DNA Ligase	M0202 S	New England Biolabs, Ipswich, USA

All restriction enzymes used for molecular cloning were purchased either from New England Biolabs (NEB) or Fermentas.

4.2.6.1 Buffer solutions

Name	Catalog no.	Company
NEB1	B7001S	New England Biolabs, Ipswich, USA
NEB2	B7002S	New England Biolabs, Ipswich, USA
NEB3	B7003S	New England Biolabs, Ipswich, USA
NEB4	B7004S	New England Biolabs, Ipswich, USA
Blue	B30	Thermo Fisher Scientific Inc. Germany
Green	B30	Thermo Fisher Scientific Inc. Germany
Orange	B30	Thermo Fisher Scientific Inc. Germany
Red	B30	Thermo Fisher Scientific Inc. Germany
Yellow	B30	Thermo Fisher Scientific Inc. Germany
10X Advantage® 2 SA PCR Buffer	639147	Takara Bio Europe/Clonetech, France
T4 DNA Ligase Reaction buffer	B0202S	New England Biolabs, Ipswich, USA

4.3 Disposables

4.3.1 Multi well plates

4.3.1.1 Tissue culture

Name	Catalog no.	Company
Nunc Flat Bottom 96-well polystyrene plates	167008	Thermo Fisher Scientific Inc. Schwerte, Germany
Nunc™ MiniTrays, Nunclon™ Delta surface	163118	Thermo Fisher Scientific Inc. Schwerte, Germany
6-well Falcon microtiter plate, flat bottom	353046	Beckman Coulter GmbH, Krefeld, Germany
12-well Falcon microtiter plate, flat bottom	353043	Beckman Coulter GmbH, Krefeld, Germany
24-well Falcon microtiter plate, flat bottom	353047	Beckman Coulter GmbH, Krefeld, Germany
48-well Falcon microtiter plate, flat bottom	353078	Beckman Coulter GmbH, Krefeld, Germany
96-well Falcon microtiter plate, round bottom	353077	Beckman Coulter GmbH, Krefeld, Germany

4.3.1.2 Imaging

Name	Catalog no.	Company
12 well glass bottom plates	P12-1.5H-N	In Vitro Scientific, Sunnyvale, USA
SENSOPLATE, 24 WELL, glass bottom,flat	662892	Greiner Bio-One GmbH. Frickenhausen, Germany
µ-Plate 384 well	88401	Ibidi GmbH, München, Germany
SENSOPLATE, 1536 WELL, glass bottom, low base, flat	783892	Greiner Bio-One GmbH. Frickenhausen, Germany

4.3.2 Cell strainer

Name	Catalog no.	Company
Cell Strainer, 40 µm, blue	352340	Beckman Coulter GmbH, Krefeld, Germany
Cell Strainer, 100 µm, yellow	352360	Beckman Coulter GmbH, Krefeld, Germany
Cell strainer tubes 35 µm	FALC352235	Corning B.V. Life Sciences, Netherlands

4.3.3 Tissue culture silicon inserts

Name	Catalog no.	Company
Silicon inserts (4 chamber)	80246	Ibidi GmbH, München, Germany
Silicon inserts (2 Chamber)	80209	Ibidi GmbH, München, Germany

4.3.4 Sterile filter

Name	Catalog no.	Company
Minisart® high flow Syringe Filters (0.2µm pore size)	16532	Sartorius AG, Göttingen, Germany
“rapid” Filtermax	99250	TPP, Techo Plastic Products AG

4.3.5 Tubes

Name	Catalog no.	Company
15 ml high-clarity polypropylene conical centrifuge tube	352096	Beckman Coulter GmbH, Krefeld, Germany
50 ml high-clarity polypropylene conical centrifuge tube	352070	Beckman Coulter GmbH, Krefeld, Germany
17x100 mm, 14 ml high-clarity polypropylene round bottom tube	352059	Beckman Coulter GmbH, Krefeld, Germany
12 x 75 mm tube with cell strainer cap	352235	Beckman Coulter GmbH, Krefeld, Germany
12x75 mm, 5 ml high-clarity polypropylene round bottom tube	352063	Beckman Coulter GmbH, Krefeld, Germany

4.3.6 Syringes

Name	Catalog no.	Company
50ml Syringe Concentric Luer Lock x 60	300865	Beckman Coulter GmbH, Krefeld, Germany
1mL Omnifix Syringe	H999.1	Carl Roth GmbH + Co. KG, Karlsruhe, Germany
5 mL Syringe with Luor lock	0057.1	Carl Roth GmbH + Co. KG, Karlsruhe, Germany
20mL Syringe with Luor lock	0059.1	Carl Roth GmbH + Co. KG, Karlsruhe, Germany

4.3.7 Object slides

Name	Catalog no.	Company
µ-Slide VI 0.4	80606	Ibidi GmbH, München, Germany
Microscope slides “Elka”	2401	Glaswarenfabrik Karl Hecht GmbH & Co KG
Superfrost Plus microscope slides	10149870	Thermo Fisher Scientific Inc. Schwerte, Germany
Superfrost Gold Plus microscope slides	10609895	Thermo Fisher Scientific Inc. Schwerte, Germany

4.3.8 Tissue culture flasks

Name	Catalog no.	Company
12.5 cm² Cell Culture Flask, 25 ml, tissue-culture treated polystyrene	353018	Beckman Coulter GmbH, Krefeld, Germany
25 cm² Cell Culture Flask, 25 ml, tissue-culture treated polystyrene	353109	Beckman Coulter GmbH, Krefeld, Germany

4.3.9 Tissue culture dishes

Name	Catalog no.	Company
Cell culture Dish 60x15mm	150288	Thermo Fisher Scientific Inc. Schwerte, Germany
Cell culture Dish 100x15mm	150350	Thermo Fisher Scientific Inc. Schwerte, Germany
Cell culture Dish 150x20mm	168381	Thermo Fisher Scientific Inc. Schwerte, Germany
35mm TC-treated culture dish	430165	Corning, USA

4.3.10 Miscellaneous

Name	Catalog no.	Company
Breathe-Easy	BEM-1	Diversified Biotech, Deham, USA
The Big Easy EasySep™ Magnet	18001	STEMCELL Technologies SARL, Grenoble, France
Pressured air spray 67 NF	TC26.1	Carl Roth GmbH + Co. KG, Karlsruhe, Germany
BD™ Accudrop Fluorescent Beads	345249	Beckman Coulter GmbH, Krefeld, Germany
HXP-R 120W/45C VIS	8-12500302919345	Leuchtmittelmarkt
14mm round Coverslip	631-0899	VWR, Germany
Coverslips for hemocytometer	03-0000	Peske
Vectashield Hardset mounting medium with DAPI	H-1500	Vector Laboratories Inc., Burlingame, USA
Fisherbrand Pasteur pipets	FB50251	Thermo Fisher Scientific Inc. Schwerte, Germany
170µm precision coverslips 22x22mm	LH24.1	Carl Roth GmbH + Co. KG, Karlsruhe, Germany
170µm precision coverslips 24x60mm	LH26.1	Carl Roth GmbH + Co. KG, Karlsruhe, Germany
Cell culture cryogenic tubes	375418	Thermo Fisher Scientific Inc. Schwerte, Germany
reagent reservoirs	4870	Corning, USA
hemocytometer	0640010	Paul Marienfeld GmbH & Co. KG

4.4 Bacteria

Strain: DH5α

4.5 Cell lines

Name	Medium	Serum	Supplements
HEK293T	DMEM	10% FCS 13	1% P/S
NIH-3T3	DMEM	10% FCS 13	1% P/S
OP9	α-MEM	20% FCS 14	1% P/S
7F2	α-MEM(-nucleosides)	20% FCS 17	1% P/S

4.5.1 Commercial Kits

Name	Catalog no.	Company
QIAGEN Plasmid Maxi Kit (100)	12165	QIAGEN GmbH, Hilden, Germany
QIAGEN Plasmid Mini Kit (100)	12125	QIAGEN GmbH, Hilden, Germany
QIAquick PCR Purification Kit (250)	28106	QIAGEN GmbH, Hilden, Germany
QIAquick Gel Extraction Kit (250)	28706	QIAGEN GmbH, Hilden, Germany
Alexa Fluor® 488 Antibody Labeling Kit	A20181	Life Technologies, Grand Island, USA
Alexa Fluor® 555 Antibody Labeling Kit	A20187	Life Technologies, Grand Island, USA
Alexa Fluor® 647 Antibody Labeling Kit	A20186	Life Technologies, Grand Island, USA

4.6 Plasmids

4.6.1 Commercial

No.	Internal no.	Name	Catalog no.	Company / Reference
1	1515	pKOF2.Flag.msi2.PGK.GFP	-	(Deneault et al., 2009)
2	1241	pCMV-Prkci	IRAVp968F0244D	Source BioScience UK Limited, Nottingham
3	1280	pSPORT-CD53	IRAVp968A01108D	Source BioScience UK Limited, Nottingham
4	1380	pCR-BluntII-TOPO-Prkcz	IRCLp5011E1035D	Source BioScience UK Limited, Nottingham
5	1686	pCMV-SPORT6.sca-1	IRAVp968E033D	Source BioScience UK Limited, Nottingham
6	1852	pDNT-LIB.Centrin1	IRAWp5000B127D	Source BioScience UK Limited, Nottingham
7	1427	pYX-Asc.Lamp-1	IRAVp968G11125D	Source BioScience UK Limited, Nottingham
8	1428	pYX-Asc.EEA-1	IRAVp968A10135D	Source BioScience UK Limited, Nottingham
9	1430	pCMV-SPORT6.Inscuteable	IRAVp968B04167D	Source BioScience UK Limited, Nottingham
10	1628	pCMV-hSara	IRATp970D0956D	Source BioScience UK Limited, Nottingham
11	1855	pCMV-SPORT6.Rab11a	IRAVp968A0211D	Source BioScience UK Limited, Nottingham
12	1429	pYX-Asc.TGFβRI	IRAVp968C09115D	Source BioScience UK Limited, Nottingham

4.6.2 Generated in this thesis

No.	Internal no.	Name
1	445	pRRL.PPT.SF.VENUS.pre
2	596	pRRL.PPT.SF.Prom1VENUS SpeI pre
3	1162	pRRL.PPT.SF.Numb1VENUS.WPRE.SIN
4	1206	pRRL.PPT.SFFV.InversinVENUS.WPRE.SIN
5	1218	pRRL.PPT.SFFV.VENUSInturned.WPRE.SIN
6	1219	pRRL.PPT.SFFV.Vangl2VENUS.WPRE.SIN
7	1282	pRRL.PPT.SF.PrkciVENUS pre
8	1283	pRRL.PPT.SF.CD53VENUS pre
9	1373	pRRL.PPT.SF.msi2VENUS.PRE
10	1379	pRRL.PPT.SF.mitoVENUS.pre
11	1385	pRRL.PPT.SF.PrkczVENUS.PRE
12	1630	pRRL.PPT.SF.FYVE(Sara)VENUS.pre
13	1687	pRRL.PPT.SF.sca1VENUS.PRE
14	1848	pRRL.PPT.PGK.Centrin1VENUS.PRE
15	1851	pRRL.PPT.PGK.VENUSRab11a.PRE
16	1979	pRRL.PPT.SF.TGFbRIVENUS.PRE
17	1980	pRRL.PPT.SF.Lamp1VENUS.PRE
18	1981	pRRL.PPT.SF.EEA1VENUS.PRE
19	1983	pRRL.PPT.SF.InscVENUS.PRE
20	1530	pRRL.PPT.SF.MCS.linker.VENUS.PRE
21	1368	pRRL.PPT.SF.MCS.PRE

4.7 Primer

Internal no.	Sequence
1455	5´-ATATATCCGGATCCATGGAGGCAAATGGGAGCCCAGG-3´
1487	5´-ATCTCTACGGATCCGGCGTGGTATCCATTTGTAAAGGCCGTTGC-3´
1309	5´-ATTGGATCCCGGGGGAGTGAGGAGATG-3´
1303	5´-ACCGGATCCCGGCAAGCAGAACCAGACAC-3´
1305	5´-TACTACCGGTGTTGCAAGCCACAGCCCTAAAGC-3´
1308	5´-TTCACCGGTCACTGCCTTCAAAAGGG-3´
1425	5´-ATCGTCACTAGTATGAAAGTGACCGTGTGCTTCG-3´
1426	5´-ATATCCACTAGTCCGGAGTAGAAGGGCCGCCCTTTC-3´
1522	5´-ATATATATGGATCCATGGACACTTCTCACACTACAAAGTCCTGTTTGC-3´
1523	5´-ATATATATGGATCCACCGCCTCCACCGAGCAAGGTCTGCAGGAGGA-3´
1935	5´-TTAATTAAGGATCCATGGCGTCCACCTTCAGGAAG-3´
1936	5´-TTAACCGGTCTAGAGGATAAAGGTTGGTCTTTTTCATGATCTTAAGAAACTC-3´

2315	5´-TACCTATAGGATCCGCCGCCACCATGGCGGCCCCCGGCGCCC-3´
2316	5´-TACCTATATCTAGACCGATGGTCTGATAGCCGGCGTGACTCCTCTTCCTGCCAATG-3´
2317	5´-TACCTATAGGATCCGCCGCCACCATGTTTCGAAGGATCTTG-3´
2318	5´-TACGGCTATCTAGACCTCCTTGCAAATCATTGAAGCATG-3´
2319	5´-TAGGTATAGGATCCGCCGCCACCATGATGGCACTGCCTGGAG-3´
2320	5´-TACCTATATCTAGACCCACAAAACTCTCCTCCATATTGCTACACAGTAAGAAG-3´
1514	5´-ATATCCATGGATCCATGGTGGCTCCAGTATGGGTACC-3´
1515	5´-ATATCGATGGATCCGCCACCTCCACCCATTAGCACTGAATGGCAGATT-3´
1941	5´-TTAACTAAACCGGTGTATGGGCACCCGCGACGACGAG-3´
1942	5´-GCTCGCGCTTAATTAATTAGATGTTCTGACAGCACTGCACCTTTGGCTTG-3´
2323	5´-TACCTATAACCGGTGCCACCATGGAGGCGGCGGCCGCTG-3´
2324	5´-TACCTACCACTAGTCATTTTGATGCCTTCCTGTTGGCTGAGTTGTGACAATGTTT-3´
521	5´-GAACCGCATCGAGCTGAAGG-3´
522	5´-TCCATGCCGAGAGTGATCCC-3´

670	5´-TGCGCAACTACGGCAAGAC-3´
671	5´-GGGCGACGGGTTAATGCTATG-3´
672	5´-TCAGCTCGATGCGGTTCAC-3´
434	5´-GCATGGACGAGCTGTACAAG-3´
1451	5´-AGGTACTGCCCACCTCTATC-3´
1452	5´-GCAGGAGAATGGGAAATGTG-3´

4.8 Mice

Strain	Gender	Age [weeks]	Reference
C57Bl6/J	male	12-14	-
PU.1YFP/GATA1-mCherry	male	12-14	(Hoppe et al., 2013, submitted)
VWF2-eGFP	male	12-14	(Sanjuan-Pla et al., 2013)

4.9 Software

4.9.1 Commercial

Name	Version	company
Clone Manager Prof.	9	Scientific & Educational Software, Cary, USA
Microsoft Office	2007, 2010	Microsoft Corporation, Redmond, USA
Fiji/ImageJ	1.47b	Wayne Rasband, NIH, USA
Axiovision	4.5 – 4.8.2	Carl Zeiss AG, Oberkochen, Germany

Flowjo	10.0.0-10.0.6	Tree Star, Inc.
BD FACSDiva	4.1.1	BD Biosciences, San Jose, USA
GraphPad Prism	5.03	GraphPad Software, Inc., La Jolla, USA
FileZilla	3.5.3	Tim Kosse, http://filezilla-protect.org
LAS AF	2.60.7266	Leica Microsystems GmbH, Mannheim, Germany
Mendeley Desktop	1.8.4	Mendeley Ltd.
Bulk Rename Utility	2.7.1.2	TGRMN Software
VirtualBox Manager	4.1.2	Oracle Corporation
BOXIT		BOXIT LabSoftware

4.9.2 Custom made

name	**Programmed by**	
TAT – Timm´s Acquisition Tool	Prof. Dr. Timm Schroeder	Prof. Dr. Timm Schroeder
TTT – Timm´s Tracking Tool	Bernd Straubinger, Oliver Hilsenbeck	Prof. Dr. Timm Schroeder
staTTTs	Laura Skylaki, Bernd Streppel, Konstantin Azadov	Prof. Dr. Timm Schroeder
Qtfy – Quantify	Michael Schwarzfischer	Prof. Dr. Timm Schroeder Prof. Dr. Dr. Fabian Theis
Qtfy single – Quantify single	Michael Schwarzfischer	Prof. Dr. Timm Schroeder Prof. Dr. Dr. Fabian Theis

5 Methods

5.1 Molecular biology

5.1.1 DNA Preparation

The isolation of Plasmid DNA from a DH5α bacteria culture was done using the QIAgen Plasmid purification kit according to the manufacturer´s instructions. The principle of the kit is based on the alkaline lysis of bacteria and the purification of the released DNA by anion exchange chromatography, followed by its elution and precipitation. The negative charge of DNA enables a high affinity binding to the solid phase of the chromatography column in low pH and low salt solutions. Application of solutions having a high concentration of salts will lead to the release of the DNA.

Briefly, 300mL of LB-medium were inoculated with DH5α and incubated over night at 37°C. After centrifugation for 15min at 4600rpm, room temperature, the supernatant was discarded and the pellet was resuspended in 10mL P1 buffer (resuspension buffer). The RNase A in this buffer will lead to the selective degradation of RNA and therefore increase the DNA purity at the end of the procedure. The bacteria were lysed for 5min at room temperature by the addition of 10mL of P2 buffer (lysis buffer). After the reaction was neutralized by the addition of 10mL P3 (neutralizing buffer) the suspension was incubated for 20min on ice. Cell debris was pelleted in a 30min centrifugation step at 20.000xg, 4°C. The supernatant was afterwards transferred to a column that has been equilibrated with 10mL P4 (equilibration buffer) before and washed twice by the addition of 30mL QC-buffer (washing buffer), respectively. The addition of 15mL QF-buffer (elution buffer) induced the elution of DNA. In order to purify the DNA from salts present in the elution buffer, 10,5mL isopropanol were added. After an additional centrifugation of 10min at 4.600rpm, 4°C the precipitated DNA was pelleted. In an additional washing step with 5mL 70% EtOH and 10min at 4.600rpm, 4°C residual salts were removed. In order to remove EtOH the DNA was dried at room temperature before being resuspended in H_2O.

5.1.2 DNA Quantification

The concentration of all DNA containing solutions was determined with the Nano Drop ND-1000 spectrometer by loading the 1µL onto the device and comparing it´s absorbance to H_2O. In order to determine the DNA concentration the device determines the absorbance of the loaded sample across wavelengths and calculates based on the absorbance at λ=260nm and λ=280nm the concentration and purity of nucleic acids in the solution based on the Beer-Lambert law as follows:

$$E_\lambda = -log\frac{I_1}{I_0} = c \times d \times e_\lambda$$

E_λ *Extinction*

I_1 *Intensity of transmitted light*

I_0 *Intensity of*

c *Concentration in µg/mL*

d *Travel length of light*

e_λ *Molar extinction coefficient depending on λ (DNA: λ_{260}=50µg/mL; RNA:λ_{280} = 40µg/mL)*

The purity of DNA in the sample is thereby assessed by the $\lambda_{260}/\lambda_{280}$ ratio of absorbance. A ratio of 1.8 is considered to be “pure” for DNA, while a ratio of 2.0 is supposed to be “pure” RNA. Lower ratios indicate the presence of proteins, phenol or other contaminants that absorb at 280nm in the sample.

5.1.3 Digestion of DNA

The digestion of DNA is a controlled reaction catalyzed by enzymes referred to restriction endonuclease. It is commonly used to cut circular as well as linear DNA molecules into smaller fragments for analytical or preparative purposes. The catalytic

activity of restriction endonucleases requires specific buffer systems and cofactors. A typical digestion reaction is described below:

Table 5.1: Catalytic digestion of DNA with restriction endonucleases

Volume [µL]	Reagents
2	DNA (0,5µg/µL)
2	10x buffer
1	Restriction enzyme (5U/µL]
14,5	ddH_2O
20	Total volume

After the reaction mix is prepared it is incubated for 1-2h at 37°C. Depending on the restriction enzymes used this temperature might be different. In case a heat sensitive restriction enzyme was used the solution was incubated for 20min at 65°C to stop the reaction.

5.1.4 Agarose gelelectrophoresis

All DNA derived from either analytical or preparative digestions was separated on agarose gels based on its charge and size.Depending on the size of the expected DNA fragments agarose gels are casted at different concentrations. Higher agarose concentrations (>2%) are used to separate smallerDNA fragments (<100bp) while lower agarose concentrations (<1%) are used to separate bigger DNA fragments (>3kb).The desired agarose solution (0,5-3% (w/v)) is preparedin TAE-buffer (40mM Tris-Acetat, 1mM EDTA) and heated until the agarose is completely dissolved. Afterwards the agarose solution issupplemented with 0.1µg/mL ethidiumbromide and casted into a designated casting chamber. After the gel has been polymerized it was placed into the electrophoresis chamber which was afterwards filled with 1xTAE buffer until the gel was completely covered. Before the samples were loaded onto the gel, 0,17x volumes of a 6x loading buffer (15% (w/v) Ficoll, 0,25% (v/v) Bromophenolblue, 0,25% (v/v) Xylenocyanol) were added. In addition to the samples

a DNA ladder was loaded onto the gel.In order to separate the samples a voltage of 100-160V was applied for 10-30min. Analytical restrictions were afterwards analyzed by illuminating the gel with UV-light (λ=302) and documented with a TM-300 Miniature CCD Camera (JAI A/S, Grosswallstadt, Germany).

5.1.5 Gelextraction

The gel extraction reaction allows the recovery and purification of a DNA fragment from anagarose gel after it has been separated from other contaminating DNA fragments. The reaction is based on the QIAquick Gel Extraction KIT was performed according to manufacturer's instructions.

Briefly, the desired DNA fragment was isolated from the agarose gel by cutting the gel with a scalpel into pieces. In order to prevent the introduction of point mutations or double strand breaksthe DNA used for the subsequent extraction reaction was not illuminated with UV-light. Three gel volumes of QG-buffer were added to the isolated slice and incubated for 10min at 50°C until the gel has been completely dissolved. After 1 gel volume of isopropanol has been added the solution was transferred to a QIAquick spin column and centrifuged for 1min at 10.000rpm. Afterwards the column was washed by added 0,5mL of QG buffer and spinning for 1min at 10.000rpm. Two additional washing steps by adding 0,75mL of PE-buffer and centrifugation for 1min at 10.000 rpm respectively followed before the DNA was eluted by adding 20µL bidest. H_2O and spinning for 1min at 10.000rpm.

5.1.6 DNA purification

The purification of DNA was done using the QIAquick PCR purification kit according to the manufacturer´s instructions. The kit is based on the principle of ion exchange chromatography and uses the differential adsorption of DNA to chromatography matrix with changing pH-values to separate DNA from contaminants. The silica membrane used as a matrix in thiskits spincolumns is optimized to adsorb DNA in

aqueous solution with pH-value´sbelow 7.5, while solutions with higher pH-value lead to the elution of DNA. After loading the DNA to the columns a series of wash steps in low pH-buffers remove contaminants and are followed by the elution of purified DNA with H_2O.

5.1.7 Klenow fill-in reaction

The ends of two DNA fragments that have been cut with different restriction enzymes are usually not compatible during a ligation reaction (see section 5.1.10). However, it is possible to ligate these fragments by modifying their ends with the Klenow-Fragment of the DNA-Polymerase I. The enzyme catalyzes the addition of free nucleotides to the complementary strand of the 5´ extension by its 5´->3´ polymerase activity. 3´extensions on the contrary are modified by the 3´->5´exonuclease activity of the enzyme.

The reaction is prepared by mixing 50ng/µL DNA with 10x NEB buffer 2 (100mM, Tris-HCl, 10mM Dithiothreitol (DTT), 100mM MgCl, 500mM NaCl, pH7,9) and dNTPs to a final concentration of 33µM. The addition of 1U Klenow Polymerase per µg DNA starts the reaction which is stopped by heat inactivation for 10min at 75°C after 20min incubation at 25°C. Before processing with the ligation reaction the DNA was purified as described in section 5.1.6.

5.1.8 Dephosphorylation DNA

The dephosphorylation of DNA is an enzymatic reaction applied to linearized plasmids to prevent theirreligation before the integration of the insert. The reaction thereby significantly impacts the efficiency of the ligation reaction (see section 5.1.10) by reducing the frequency of false positive clones during selection to a minimum.

The reaction was carried out by mixing 1-5µg of DNA with 10x Antartic Phosphatase buffer (50mM Bis-Tris-Propane-HCl, 1mM $MgCl_2$, 0,1mM $ZnCl_2$, pH 6 at 25°C) and 5U of Antartic Phosphatase (NEB) and subsequent incubation for 15min at 37°C for

5´extension or blunt-ends or 60min for 3´extensions. Alternatively the enzyme and buffer were added directly to a heat inactivated digestion reaction. In order to stop the reaction the mixture was heat inactivated for 5 min at 65°C.

5.1.9 Polymerase Chain Reaction (PCR)

The purpose of the polymerase chain reaction(PCR) is the sequence specific amplification of DNA molecules for either analytical or preparative reasons. It has been described for the first time by Mullis in 1985/86 (Mullis et al., 1986).

The principle of the reaction is based on the sequence specific annealing of two oligonucleotides, usually referred to as primers, to a DNA template. The sequence of the primers has to be chosen in a way that they bind to the complementary strands of the template. The region lying between the primers defines the amplicon, the DNA sequence that is amplified during the PCR reaction.In addition to template and primers, desoxyribonucleotides (dNTPs), an enzyme catalyzing the reaction (DNA polymerase) and an appropriate buffer containing cofactors etc. are required for the reaction. The reaction is started by increasing the temperature to 95°C, a step called denaturation, which is supposed to induce separation of the complementary DNA strands of the template. In the second step the temperature of the reaction is reduced to enable the sequence specific annealing of the primers to the DNA template. The temperature of this step depends on the size and sequence of the primer pair and has to be determined for every reaction. After the primers have annealed the temperature is changed to meet the temperature optimum of the DNA polymerase which varies depending on the enzyme used in the reaction. During this step, the polymerase is catalyzing the sequence specific extension of both primers in 5´->3´direction. The dNTPs present in the solution are thereby used as a substrate. After the reaction is completed each DNA strand has been replicated once and is present as a double stranded DNA molecule. The reaction continues by changing the temperatures in the described order to induce an additional cycle of denaturation, annealing and extension until the desired degree of amplification is accomplished.

The reaction used in this work is based on the Advantage Polymerase Kit

(Clonetech) and was done according to the manufacturer´s instructions. Briefly, 500ng of template DNA were mixed with 320µM dNTPs, 5µM forward primer, 5µM reverse primer, 10x Advantage Polymerase buffer and H_2O. Optionally, DMSO was added to a final concentration of 2% (v/v) to prevent the formation of secondary structures in the DNA template. The reaction was started by the addition of 2U Advantage Polymerase and placed into a Thermo Cycler (PCR sprint system, Thermo Fisher Scientific) programmed as described below:

Table 5.2: Polymerase Chain Reaction – exemplified programm

Step	description	Temperature [°C]	Time [min]
1	Initial Denaturation	85	5
2	Denaturation	90	1
3	Annealing	*	1
4	Extension	68	**

The annealing temperature * strongly depends on the primer sequence and should be 5°C below the estimated melting temperature as determined by the simplified formula below. However, the optimal annealing temperature has to be empirically be determined and can deviate from the calculated value:

$$T_m = 2°C \times (A + T) + 4°C \times (G + C)$$

T_m *Melting temperature*
A *Number of adenine*
T *Number of thymidine*
G *Number of guanine*
C *Number of cytosine*

The elongation time ** varies with the size of the amplified sequence and depends on the processing efficiency of the Polymerase. In order to calculate the extension time

for the Advantage Polymerase a processing speed of 1kb/min was used.

The primers were used for the PCR reaction were designed using Clone manager 9 and are listed in section4.7.

5.1.10 Ligation

During the ligation reaction two linearized, doublestranded DNA molecules, usually referred to as insert and backbone/vector are connected to yield a circularized DNA molecule called plasmid.The backbone has been dephosphorylated as described in section 5.1.8 while the insert is usually derived from a digestion (see section 5.1.3) or PCR reaction (see section 5.1.9). The reaction is catalyzed by the ATP dependent enzyme T4- ligase and carried out as follows. 20-100ng of vector and insert DNA are added in molar ratio of 1:3 to 1x T4 ligase buffer (50mM Tris-HCl, 10mM $MgCl_2$, 1mM ATP, 10mM DTT, pH 7,5) and H_2O. The amount of DNA required to accomplish the molar ratio was thereby calculated as follows:

$$\frac{Vector\ [ng]}{Vector\ [kb]} \times \frac{1}{3} = \frac{Insert[ng]}{Insert[kb]}$$

The reaction is started by the addition of 1U T4-Ligase (NEB) and incubated either for 1-2h at room temperature or at 16°Covernight. In order to stop the reaction and inactivate the ligase the solution was incubated for 20min at 65°C.

5.1.11 Generation of chemocompetent bacteria

In order to generate chemocompetent bacteria an overnight culture DH5α was started in 20mL LB-medium and incubated at 37°C. The next day the bacteria culture was transferred to 250mL LB-medium and incubated at 37°C until an Optical Density (λ=600nm) of 0,65-0,8 ($OD_{\lambda 600}$)was reached. Next, the bacteria culture was

centrifuged for 10min at 5.000xg and washed once with 1 volume of precooled H_2O. After an additional washing step with 0.5 volumes of H_2O the bacteria were centrifuged for 10min at 5000xg and resuspended in 30mL of precooled 10% glycerin.After an additional centrifugation step the bacteria were resuspended in 1mL glycerin and distributed in 50µL aliquots. The aliquots were frozen in liquid nitrogen and afterwards stored at -80°C.

5.1.12 Transformation

An aliquot in chemo competent DH5α (see section5.1.11) was thawed for 30min on ice and mixed with 50ng of DNA derived from a ligation reaction. After 30min on ice the bacteria were heat shocked for 90s at 42°C and incubated on ice for another 2min. Next, 200µL of LB-medium without antibiotics were added and incubated for 1h at 37°C. Afterwards the solution was plated on a pre-warmed agar plate containing the antibiotic required for selection and incubated over night at 37°C.

5.1.13 Preparation of glycerol stocks

Glycerol stocks are prepared to store successfully transformed bacteria and are used to circumvent the transformation reaction when more DNA of a previously cloned plasmid has to be generated.Glycerol stocks can be used directly to inoculate a culture of bacteria by adding a small amount to LB-medium containing the desired antibiotics required for successful selection. In order to prepare a glycerol stock, 700µL of bacteria culture were mixed with 300µL of a 50% glycerol solution and frozen/stored at -80°C.

5.1.14 Sequencing

All sequencing reactions were performed using the BigDye Terminator 3.1 Cycle Sequencing Kit (Applied Biosystems) and analyzed in the sequencing facility of the

Helmholtz-Zentrum München using an ABI 3730 48-capillary sequencer. The sequencing results were manually analyzed using Clone Manager Software 9 (Sci-Ed).

The sequencing reaction consists of the following 4 consecutive steps which are described below: (1) Polymerase Chain Reaction (2) Ethanol precipitation of the PCR products (3) Analysis by electrophoresis in (4) manual analysis of sequencing results.

5.1.14.1 PCR - Sequencing reaction

The PCR reaction was carried out in a total volume of 5µL as described below using the BigDye Terminator 3.1 Cycle Sequencing Kit (Applied Biosystems).

Table 5.3: PCR reaction for DNA sequencing

Reagent	**Volume [µL]**
Big Dye (incl. dTNPs, polymerase)	0.5
5x BigDye buffer	1
DMSO	0.1
Primer	1
DNA template	x (= 150-300ng)
H_2O	x
total	**5**

Table 5.4: PCR program for sequencing reactions

Step	description	Cycle	Temp. [°C]	Time [s]
1	Initial Denaturation	1	96	60
2	Denaturation	35	96	10
	Annealing		50	5
	Extension		60	240
3	-	-	12	-

5.1.14.2 Ethanol precipitation of sequencing product

After the PCR reaction 0.5µL of 125mM EDTA, 2µL 3M Na-Acetate and 50µL 100% EtOH were added to each reaction in order to precipitate the DNA. After 15min incubation at RT in the dark the samples were centrifuged for 30min at 2.000xg at 4°C and the supernatant removed by spinning the inverted plate briefly at 180xg. After an additional wash step with 70µL 70% EtOH and a subsequent incubation step for 2min in the dark to ensure its complete evaporation the DNA was resuspended in 20µL HLPC water (LiChrosoly, #1.15333.1000, Merck).

5.2 Cell culture

5.2.1 General cell culture conditions

All cell lines or freshly isolated hematopoietic cells were cultured in sterile conditions in a standard humidified tissue culture incubator at 37°C, 5% (v/v) CO_2 (Microbiological Incubator CD210; Binder, Tuttlingen, Germany). Media exchanges and passages were done under were carried out under a standard tissue culture flow hood (HERA safe KS) using sterile plastic, glassware and media.

5.2.2 Freezing of cell lines

OP9 and 7F2 cell lines were trypsinized and resuspended in their standard tissue culture medium and pelleted by centrifugation for 5min 1.200rpm. After the supernatant had been discarded the cells were resuspended in FCS containing 10% DMSO and transferred into cryotubes. The cryo tubes were put into with 100% isopropanol containing Cryo Freezing container (cat no 5100-0001, Nalgene, Rochester, USA) and stored at -80°C to allow a gradual decrease in temperature at a rate of -1°C/min. After 24h the cryotubes were transferred into a liquid nitrogen tank for long term storage.

5.2.3 Thawing of cell lines

In order to thaw OP9 and 7F2 cell lines the cryotubes were removed from the liquid nitrogen tank and opened slightly to allow depressurization. Afterwards the cryotubes were transferred to a 37°C water bath until almost the entire vial was thawed. Next, 9mL of standard tissue culture medium were added and the cells were centrifuged for 5min 1200rpm at 4°C. After the supernatant was discarded the cells were plated at an approximate density of $1.6x10^4$ / cm^2.

5.3 Transfection

The term transfection is used for a series of procedures by which DNA is introduced into eukaryotic cells. It can be accomplished by a variety of techniques, but is mainly achieved by the application of certain chemicals, mechanical forces or particles. The transfection methods used in this work are all chemically based and are described below. The transfections were done using HEK293T cells to determine the localization of the fluorescence fusion reporters cloned in this study.

5.3.1 Polyethylimine (PEI)

Transfections using polyethylimine (PEI) are based on its properties to condense DNA into positively charged aggregates (Boussif et al., 1995). Due to their charge the particles are able to attach efficiently to anionic residues at the cell surface and are subsequently taken up via endocytosis. For transfections HEK293T were seeded in 500µL of standard tissue culture medium in a 24 multi well plate and incubated overnight. At the next day, the transfection reagent was prepared by adding 300-500ng of DNA to 66µL of a previously prepared PEI solution (4µM PEI (PolySciences Inc., cat. no.: 23966), 15mM NaCl, pH 7.8). After the solution had been vortexed and incubated 10min at RT it was added directly onto the cells and incubated for at least 6h prior to medium exchanged. The cells were incubated for another 24h at 37°C, 5%CO_2 before analysis.

5.3.2 Lipofectamine

The transfection of cells with Lipofectamine is based on the formation of a DNA-liposome complex which can be taken up by various cell types. The transfection was carried out using the Lipofactamine 2000 Transfection Reagent (Life technologies) following the manufacturer´s instructions. Briefly, 10µL Lipofectamin2000 were added to 90µL Opti-MEM. After 15min incubation at RT, 100µL Opti-MEM containing 2µg DNA were added and vortexed. After an additional incubation for 15min at RT the standard tissue culture medium from a previously prepare 10cm^2 dish containing HEK293T cells was discarded and replaced with the prepared solution. The cells were incubated for 24h at 37°C, 5%CO_2 before analysis.

5.3.3 $CaPO_4$Transfection

The $CaPO_4$ transfection has been described for the first time in 1973 and is based on the formation of a DNA-$CaPO_4$ co-precipitate which is bound and internalized by cells(Graham and van der Eb, 1973). The procedure was carried out using the

Calcium Phosphate Transfection Kit (Sigma-Aldrich, CAPHOS-1KT) following the manufacturer´s instructions. Briefly, HEK293T cells were plated at a density of $5x10^6$ cells/$60cm^2$ in DMEM (10%FCS13, 1%P/S). After 24h 5µg of DNA were mixed with 50µL of 2,5M $CaCl_2$and H_2O to a final volume of 500µL. Next, 500µL of 2x HBS (50mM HEPES, 280mM NaCl, 1,5mM Na_2HPO_4) were added drop wise while vortexing the solution. After 20min incubation at room temperature, the HEK293T standard tissue culture medium was discarded and replaced with transfection medium (DMEM, L-Gln, 100mg/mL sodium pyruvate, 10%FCS13, 1%P/S, 2mM HEPES).After 6-12h incubation at 37°C, 5%CO_2 the medium was replaced and the cells were incubated for additional 24h at 37°C, 5%CO_2.

5.4 Virus production

5.4.1 Generation of lentiviral supernatants

The production of viral particles is based on the parallel transfection of 4 plasmids and was done as previously described (Schambach et al., 2006). Briefly, the four plasmids are transiently cotransfected, (1) a lentiviral vector plasmid (2) a plasmid encoding for the HIV-Rev gene, (3) for the HIV-gag/pol genes and (4) the viral envelope (i.e. VSG-g). As basic lentiviral vector plasmid we used the previously published pRRL.PPT.PGKGFP.pre packaging plasmid and modified it according to our needs (i.e. exchange of promoter, fluorescence protein, etc.). The transfection was carried out using the CaPO4 methods as described before (section 5.3.3). Once transfected, the viral genes and the gene of interest are expressed and the latter mRNA is packaged into viral particles.

The viral supernatants were collected 36 hours after transfection and were centrifuged for 5min at 240xg, 4°C and filtered to remove cellular debris (0.2µm pore size). After filtration the concentration of viral particles by ultracentrifugation at 50.000xg for 1h at 4°C and resuspended in 200µL SFEM, aliquoted and frozen and stored at -80°C.

Table 5.5: Transfected plasmid for the generation of lentiviral supernatants

[µg]	no.	Name	Function
2	495	pMD2.VSVG	VSVG pseudotyped envelope protein
5	392	PRSC_Rev	Regulator of expression of virion proteins (Rev)
10	393	pMDLg_pPRE	Gag, pol
5*	-	-	Transfer vector containing genes of interest

**the amount of vector DNA was adjusted according to its size. The indicated amount of DNA was used for a 7kb vector.*

5.4.2 Virus Titration

In order to determine the number of infectious viral particles per volume (titer),2x10^{4}NIH3T3 cells per well were seeded into a 24 well plate and incubated for 16h at 37°C, 5%CO_2. Afterwards, NIH3T3 cells were counted and previously concentrated and aliquoted viral supernatants were thawed and added in several dilutions (ranging from 1x10^{-1} to 1x10^{-4}). After 48h of incubation at 37°C, 5%CO_2, NIH3T3 cells were trypsinized, harvested, washed and analyzed by flow cytometry. The titer was subsequently determined using the following formula:

$$titer = \frac{\frac{\%\ positive}{100} \times cell\ number}{Volume\ [\mu L]}$$

Abbrev.	***Description***
Titer	*Number of virus particle / µL*
Cell number	*Number of NIH3T3 when virus supernatant was applied*
% positive	*Percentage of positive cells as analyzed by flow cytometry, gated according to the negative control*
Volume	*Volume of viral supernatant used for infection*

The virus titer were determined in 3 technical replicates and only dilutions yielding infection rates between 3% and 30% were regarded for the titer determination to minimize inaccuracies caused by multiple infections.

5.5 Flow cytometry

5.5.1 Analysis

Flow cytometric analysis was done using the BD FACS Aria III. All samples were washed, resuspended in 50µL FACS buffer (PBS, 2% FCS, 2mM EDTA, 0.1% NaN_3) and stained for 60-90min by addition of fluorescently labeled antibodies at 4°C in the dark. Afterwards cells were washed and filtered through a 100µm mesh to get a single cell suspension and to prevent clogging of the flow cytometer. Unstained and single stain controls were always included and used to correct for fluorescent channel bleed through by manual compensation. Unless otherwise indicated populations were gated according to the negative control.

5.5.2 Sorting

Flow cytometric sorting of cells was done using the BD FACS Aria III. All cells were prepared as described above (section 5.5.1). The machine was cleaned prior to every sort by flushing the cytometer for at least 5min with BD FACS Clean, rinsing the flow cell for 5min with BD FACS flow by activating the stream when the nozzle was not inserted and by sonification of the nozzle itself. Afterwards the machine was calibrated by determining the drop delay using BD Accudrop beads and the “auto drop delay” option. The calibration was controlled by sorting and reanalyzing a “test” population and only accepted if purities over >99% were accomplished. Afterwards the electric field strength was adjusted to ensure the proper localization of sorted cells in tubes or multi well plates. All tubes and multi well plates were cooled to 4°C during the whole procedure to maximize cell viability. All sorts were done using the single cell mode to achieve the highest purity possible. Purities of all sorts were controlled by reanalyzing at least one sorted population and were always ≥98%.

5.6 Isolation of hematopoietic stem and progenitor cells

Hematopoietic stem and progenitor cells were isolated as described earlier with minor modifications as described below (Ema et al., 2006). Briefly, femur, tibia and coxae were isolated, mortared in FACS buffer (PBS, 2% FCS, 2mM EDTA, 0.1% NaN_3)and filtered through a 100µm mesh. After the cell number was determined, cells were washed (5min, 1200rpm, 4°C) and resuspended in FACS buffer to $1x10^8$cells/mL. Next, 0.1µL/$1x10^6$ cells biotin conjugated B220, CD3e, CD19, CD41, CD11b, Gr-1, and ter-119 antibodies were added and incubated for 10-20min on ice. In order to remove unbound antibodies the cells were washed once and resuspended to $1x10^8$ cells/mL FACS buffer. Next, 0,1µL/$1x10^6$ cells streptavidin conjugated magnetic particles were added and incubated 20min on ice. After filling up the volume to 10mL the cells were placed for 5-7min into a magnet where the lineage marker expressing cells were selectively retained due to their association with the magnetic particles. Inversion of the magnet therefore selectively transferred cells negative or low in expression for lineage marker into a new tube, a process called lineage depletion. The lineage depleted cells were counted, washed resuspended in 50µL FACS buffer and stained with 0.1µL/$1x10^6$ cells CD150-PE, CD34-eFluor450, c-KIT-PECy7, sca-1-PCPCy5.5, CD48-FITC and Streptavidin-APCeFluor780 for 60-90min on ice. After washing and resuspension in 200µL/$1x10^7$ cells the suspension was filtered, analyzed and sorted into SFEM, 1%P/S.

5.7 Transduction of hematopoietic stem and progenitor cells

Sorted hematopoietic stem and progenitor cells were washed with PBS, counted and resuspended in 100µL infection media (SFEM, 10ng/mL SCF, 20ng/mL TPO, 1µM 11R-VIRVIT). 11R-VIVIT is a cell permeable NFAT inhibitor and is supposed to keep hematopoietic stem cells in a quiescence state (Sugimura, 2011). Next, titrated lentiviral particles were added to achieve a multiplicity of infection (MOI) of 300-600

and cells were incubated for 24h at 37°C and 5% CO_2. The MOI was thereby calculated as follows:

$$MOI = \frac{\text{Volume(Virus)} * \text{Virus titer [virusparticles/mL]}}{\text{Volume(Medium)} * \text{Cell concentration } [\frac{\text{cells}}{\text{mL}}]}$$

The next day the cells were washed 2-3 times in 15mL PBS to remove residual virus particles and resuspended in the medium required for subsequent assays.

5.8 Colony assays

5.8.1 Cytospins and May-Giemsa-Grünwald staining

In order to determine the cell identity of hematopoietic cells based on their morphology independently of antibodies, cells were spun onto object slides and stained consecutively with May-Grünwald and Giemsa solutions. The May-Grünwald solution consists out of acidic eosin, alkaline methylene blue and methanol and colors granules blue-violet, acidic granules red and neutral granules light red-purple. The cytoplasm of erythrocytes is staining light red while thrombocytes are colored as light blue. The Giemsa solution on the other hand consists of azure A-eosinat, azure B-eosinat, methylenblue-eosinate and methylenblue chloride and colors the nuclei purple while the cytoplasm acquires a bluish coloration. The combination of both solutions allows the discrimination of different hematopoietic cells based on nuclear morphology, coloration, appearance of granules and the nuclear:cytoplasm ratio.

The reaction was carried out as follows. Cells were washed in PBS, 5%FCS and transferredinto a cytospin chamber containing a standard objective slide and centrifuged for 3min at 270RCF and RT. Afterwards the supernatant was discarded andthe slide was centrifuged for 1min at 1100RCF at RT. Next, the slide was stained for 4 min in concentrated May-Grünwald solution and washed twice in H_2O bidest.,before the 5% Giemsa solution (diluted in H_2O bidest.) was added. After 16min incubation at RT and 3 washes in H_2O bidest. the slides were air dried and mounted onto a coverslip.

5.8.2 Single cell Liquid Culture Colony Assay (SC-LCCA)

The Liquid Culture Colony assay was done as described earlier (Takano et al., 2004). Briefly, single hematopoietic stem cells or multipotent progenitors were sorted into a 96 well plate containing 150-200µL of LCCA media and incubated for 14 days at 37°C and 5% CO_2. At day 14 the colonies were harvested and either stained with May-Giemsa-Grünwald solution for morphological analysis or with CD11b-eF450, Ly6G-FITC, FcyR-PCP-Cy5.5, c-KIT-APCeF780, CD150-PE, CD41-APC and ter119-PECy7 antibodies for flow cytometric analysis.

Liquid culture colony assay medium:

- StemPRO34
- 1:40 BIT (media supplement)
- 10% pre-tested FCS(14)
- 100ng/mL SCF
- 100ng/mL TPO
- 10ng/mL IL-3
- 2U/mL EPO
- 2mM L-Glutamine
- 50µM β-mercaptoethanol
- 1%P/S

5.9 Daughter cell separation assay

The daughter separation assay was established to compare the differentiation potential of individual daughter cells and to investigate its correlation to the asymmetric segregation of proteins. It consists of 4 consecutive steps: (1) Isolation of hematopoietic stem and progenitor cells (see section 5.6); (2) Stochastic separation of daughter cells (3) Quantification of daughter fluorescence intensities (4) Liquid culture colony assay of individual daughter cells (see section:5.8.2)

First hematopoietic stem and progenitor cells were isolated and sorted as single cells into a round bottom 96-well plate containing 20µL of liquid culture colony assay medium (see section5.8.2) supplemented with 100ng/mL Cholera Toxin B-a488and

incubated at 37°C, 5%CO_2. After 40h the majority of the cells have divided once so that 2 cells were expected to be present per well. In order to separate the two daughters, the content of each individual well was mixed and 10µL of the cell suspension transferred into two adjacent wells of a 1536 glass bottom well plate, respectively. It is important that both daughters were situated in the same volume since different media volumes above cells would affect the background intensities differentially therefore influence the quantification of absolute fluorescence intensities.

Next, the plate was centrifuged for 5min at 1200rpm, 4°C to sediment the cells and to remove air bubbles.A gas permeable foil was applied to prevent evaporation. Every well of the plate was then imaged completely using a 10xPlan-NeoFluar Objective, a 0,4x TV-Adapter and a 38HE filter set. Each picture was acquired at a resolution 1388x1024pixels and saved in the uncompressed file format .png. During the imaging process the plate was continuously gassed (5%CO_2, 5%O_2, 90%N_2) to avoid acidification of the media.

After 3 pictures of each individual wells had been acquired the plated was incubated for additional 12 days at 37°C, 5%CO_2 after which the daughter colonies were harvested, stained and analyzed by flow cytometryas described for the single cell - Liquid culture colony assay (see section:5.8.2)

5.10 Immunofluorescence analysis

Immunofluorescence analysis were performed as previously published with the following minor modifications (Ema et al., 2006). HSC were isolated as described above (see section 5.6). After the indicated times of in vitro culture the cells were transferred in a total volume of 10µL to four chamber silicon inserts (Ibidi, #cat 80246) placed onto object slides. Before loading, the wells were coated with Poly-L-Lysine according to manufactures instructions (1h, 37°C 1:10 diluted). After 30min incubation at 37°C, 5%CO_2 cells were fixed by addition of 10µL of 4%p-formaldedyd (PFA). In order to assure that all cells are fixed the object slide was spun for 10s at 500 rpm. After 20min incubation at RT cells were washed with PBST (PBS, 0.05% Tween-20) and permeabilized for 20min in PBS, 0,1% Triton-X 100, 0,1% NaN_3). After one wash with PBST cells were incubated for 1h at RT in blocking solution

(PBST, 10% donkey serum, 1:1000 FcyR block) before primary antibodies diluted in blocking solution were added. Primary antibodies used were chicken anti-GFP at 1:500 (Aves Lab) and rat anti-sca-1 at 1:200 (eBioscience).
After overnight incubation at 4°C in a moisture chamber cells were washed at least three times with PBST before secondary antibodies (all used as 1:500 dilution) were added. After an additional incubation for 2h at RT cells were washed at least three times in PBST and mounted under a coverslip using VECTASHIELD hard set mounting medium + DAPI (Vector Laboratories, #cat H-1500). The coverslip was fixed to the object slide by application of nail polish.

5.11 Time-lapse microscopy

5.11.1 General imaging parameters and microscope settings

Imaging and quantification of fluorescence signals of living cells requires the careful optimization and prioritization of the following parameters: (1) photo toxicity (2) temporal resolution (3) spatial resolution (4) dynamic range (5) noise and (6) signal to noise. Depending on the addressed questions, the priorities and therefore the applied microscope settings are different. The described settings below have been optimized to image hematopoietic stem and progenitor cell divisions over several days and might not be applicable to other cell types and/or experimental approaches.

However, when imaging living cells the most pressing concern is always the photo toxicity. The reduction of photo toxicity is mandatory for cell survival during imaging and has been accomplished by (1) increasing the gain of the CCD camera to level 1-2 when possible (2) setting the white point for image acquisition to a value of 0.12 when 14-bit to 8-bit conversion was used (3) adjusting the diaphragm to minimize exposure of adjacent, currently not imaged positions (4) optimizing the order of commands required to take a picture (5) usage of glass bottom plates to improve the signal to noise ratio by reducing background fluorescence (6) using phenol-red free medium to improve the signal to noise ratio by reducing background fluorescence (7) application of fast fluorescence shutter (response time <50ms) or LED based systems (response time <5ms) (8) favoring low exposure times over a high dynamic

range (9) using epifluorescence imaging instead of confocal microscopy (10) using low magnification objectives to reduce the exposure of adjacent, currently not imaged positions (11) minimizing the imaging frequency to the smallest amount required to keep cell identity.

Another important consideration is the temporal resolution. After the survival of the cells has been ensured by reducing the photo toxicity to a minimum the temporal resolution is the main factor determining the data throughput and quality. Imaging the cells more frequently than required not only increases the photo toxicity but also decreases the amount of data that can be acquired per experiment. Imaging the cells less frequently than required will lead to the loss of cell identities over time and there for reduce the data quality. The requirements for the temporal resolution depend strongly on the cell type and the length of the experiment. While a lower temporal resolution might be sufficient to keep the cell identity at the beginning of an experiment it might not be sufficient after several days. In order to keep cell identity, adherent cells, which are usually less motile, can be imaged less frequently than highly motile suspension cells.
Hematopoietic stem and progenitor cells are suspension cells and therefore highly motile. The motility of these cells can be reduced by either coating the plates with an extracellular matrix components like fibronectin, collagen etc. or by co-culturing them with stromal cells. Experiments using fibronectin coating were usually done with a temporal resolution between 1-3min, while images acquired in experiments using a coculture system were taken every 2-5min.Another way to restrict the motility of hematopoietic stem and progenitor cells is the application of micro wells or micro well inserts restricting essentially the maximum distance a cell can migrate by reducing the dimension of the well and there for the imaging area. This can be favorable since the imaging area and temporal resolution are inversely correlated. In other words, the higher the temporal resolution the less area can be imaged and vice versa.

5.11.2 HSC/OP9 coculture – time lapse experiments

Glass bottom 12 or 24 well plates were equipped with silicon inserts (ibidi) and coated with 0.1% gelatine for 5-10 min at room temperature. Afterwards$3x10^3$OP9

stromal cells were plated per microwell in OP9 medium (see section4.5) and incubated for 24h at 37°C, 5%CO_2. Before the time-lapse experiment was started the OP9 medium was removed and replaced with 100µL of hematopoietic stem and progenitor cell suspension. The cells were allowed to settle down for 30min at 37°C, 5%CO_2. Next, coculture medium was added until the silicon insert was completely covered with medium. In order to maintain a stable atmosphere while imaging the plate was sealed with adhesive tape and gassed (5%CO_2, 5%O_2, 90%N_2) through a hole in its lid. Depending on the experiment either a 10xFLUAR Objective was used in combination with a 0,63x-TV-Adapter or a 20xFLUAR Objective with a 1x-TV-Adapter.

HSPC/OP9 Coculture imaging medium:

- *SFEM*
- *20% FCS 14*
- *100ng/mL SCF*
- *1%P/S*

5.11.3 Stromal cell free – time lapse experiments

Stromal cell line free time-lapse experiments were done in glass bottom multi well plates coated with 50ng/mL fibronectin for 1h at 37°C, 5%CO2. Two chamber silicon inserts were used when necessary to reduce the imaging area. Before the time lapse movie was started cells were transferred in the indicated media into the wells and incubated for 30min at 37°C, 5%CO_2 to allow the cells to sink to the bottom of the wells. In order to maintain a stable atmosphere while imaging the plate was sealed with adhesive tape and gassed (5%CO_2, 5%O_2, 90%N_2) through a hole in its lid. Depending on the experiment either a 10xFLUAR Objective was used in combination with a 0,63x-TV-Adapter or 0,5x-TV-Adapter.

Table 5.6: Stromal cell free imaging media

[ng/mL]	ST	STT	SI	SIT
SCF	100	100	100	100
TPO	100	100	-	-
IL-3	-	-	10	10
EPO	-	-	-	-
TGFβ1	-	100	-	5

All media were based on phenol red free SFEM and supplemented with 50µM β-mercaptoethanol, 2mM L-Glutamine and 1%P/S.

5.11.4 Live antibody / dye staining

For live antibody staining, fluorescently labeled antibodies were added in dilutions ranging from 1:5.000-1:10.000 (100-200ng/mL) to the imaging medium. If several live antibodies were used in parallel, non-overlapping fluorescent dyes were used with optimized filter sets to avoid spectral bleed-through. In order to avoid degradation of fluorescent dyes over time during time lapse movie only Alexa-Fluor dyes were used. Other live cell dyes were used in the following dilution: LysoTracker Red - 1:20.000 (50µM), Cyto-ID green - 1:5.000, Hoechst33342 - 1:200.000 (50ng/mL).

5.12 Image acquisition, processing and data analysis

5.12.1 Data Acquisition – Timm´s Acquisition Tool (TAT)

Brightfield and fluorescence pictures were acquired using Zeiss Axio Observer Z1 microscopes (Carl Zeiss), equipped with Spectra-X (Laser2000) or HXP fluorescence light sources, the monochromatic 14-bit CCD camera AxioCam HRm (native resolution of 1388x1040 pixel), motorized stages, automated temperature control units and transmitted light LEDs. The microscope itself and the peripheral devices

were controlled by a custom made VBA (Visual Basic Application), named Timm´s Acquisition Tool (TAT), controlling Axiovision 4.8.2 microscope imaging software, thereby allowing for fully automated image acquisition using predefined settings. Images were saved as 8-bit in portable networks graphics (.png) format and transferred directly onto removable 0.5-2TB hard drives. Brightfield images were acquired every 1 to 3min at 50-100ms, fluorescence pictures using optimized filter sets every 5 to 30min at 50-500ms, depending on the channel used. The camera gain was increased from 0 two 2 when fluorescence images were acquired with low time intervals in order to minimize photo toxicity. Depending on the experiment 12-1536 glass bottom multi well plates were used, sealed with adhesive tape and constantly gassed (5%CO_2, 5%O_2, 90%N_2) through a custom made inlet in the multi well plate lid for the entire duration of an experiment. The duration of the time-lapse experiments ranged depending on the question from 0.5-10days.

5.12.2 Generation of cellular genealogies - Timm´s Tracking Tool (TTT)

The acquired brightfield and fluorescence images were loaded into a custom made program, called Timm´s Tracking Tool (TTT), where the x,y coordinates of cells and their fates (division, death, fluorescence, etc.) were manually annotated over time (tracking). The program integrates the annotated information to generate the cellular genealogy of single cells or whole colonies in form of pedigrees. Tracks with uncertain single cell identity were marked as lost and not considered for analysis.

5.12.3 Background correction

All fluorescence pictures were corrected and normalized to eliminate position and time dependent quantification artifacts as previously described (Schwarzfischer et. al, submitted). Briefly, each fluorescence image was subdivided into tiles to identify and remove cellular signals using a machine-learning algorithm. The pixel intensities of the remaining gaps were interpolated based on the properties of the surrounding tiles

and estimated background pictures generated.

In order to remove position dependent artifacts, the changes in pixel intensities over time derived from the estimated background pictures were integrated for every field of view. Plotting these changes against the mean background signal of a given field of view illustrates that the intensities of pixels located at different positions in a fluorescence picture change differently over time (Figure 1D). This change of pixel intensity per mean background signal is individually described by the slope of linear regression and is used to generate a time independent correction factor (=gain) for every field of view. Fully normalized and corrected fluorescence pictures were generated by subtracting the estimated background intensities from the raw fluorescence pictures for every time point and dividing the result by the calculated gain function (Figure 1E).

5.12.4 Quantification of fluorescence pictures (QTFy)

The quantification of fluorescence intensities was done as previously described (Schwarzfischer et al., submitted). Briefly, a custom made program termed QTFy, was used to semi-automatically calculate the corrected fluorescence intensities as described in section 4.11.3. The results were integrated with the previously generated cellular genealogies as described in section 4.11.2. All quantification were manually inspected and corrected if necessary before used for further analysis.

5.12.5 staTTTs

Data derived from cellular genealogies generated by TTT as well as quantifications generated by QTFy were integrated into a common source by using the custom made software termed staTTTs. In staTTTs, the data was filtered and sorted exported for further analysis.

5.13 Statistical analysis

Statistical analysis was performed using Graphpad Prism 5. Whenever the distribution of data points was normal (=Gaussian) two-tailed student´s t-test or student´s t-test with Welch´s correction (in case of unequal variances) was used. For not normally distributed data one- or two-tailed Mann Whitney U test was used as indicated. Statistical significant results are indicated with: * $p<0.05$, ** $p<0.01$, *** $p<0.001$. ns refers not significant ($p>0.05$).

6 Results

6.1 Isolation and quantitative imaging of single hematopoietic stem cells over time

In order to test the hypothesis that HSC self-renewal and differentiation is controlled by asymmetric cell division, a list of putative candidate genes was compiled (see table 2). Some of these candidates have previously been suggested to segregate asymmetrically during cell division in non-hematopoietic tissues of other model organisms (i.e. NUMB, inscuteable, centrin1). Others are known parts of complexes that have been shown to be highly polarized during the interphase of hematopoietic cells (i.e. VANGL2, Inversin, Inturned). In order to quantify and compare the amount of candidate protein inherited by both daughters after HSC division, the proteins need to be visualized. This has previously been done by antibody staining of fixed cells (Giebel and Beckmann, 2007; Wu et al., 2007a). However the fluorescence intensities of both daughter were not quantified and the functional relevance of any putative asymmetric segregation could not been demonstrated since the daughter cells were fixed and therefore not available for subsequent analysis. In order to circumvent this problem we required a technique allowing us to quantify protein levels in living cells. Since mice expressing these candidates fused to a fluorescence reporter were not available and the generation of these mice for an initial screen

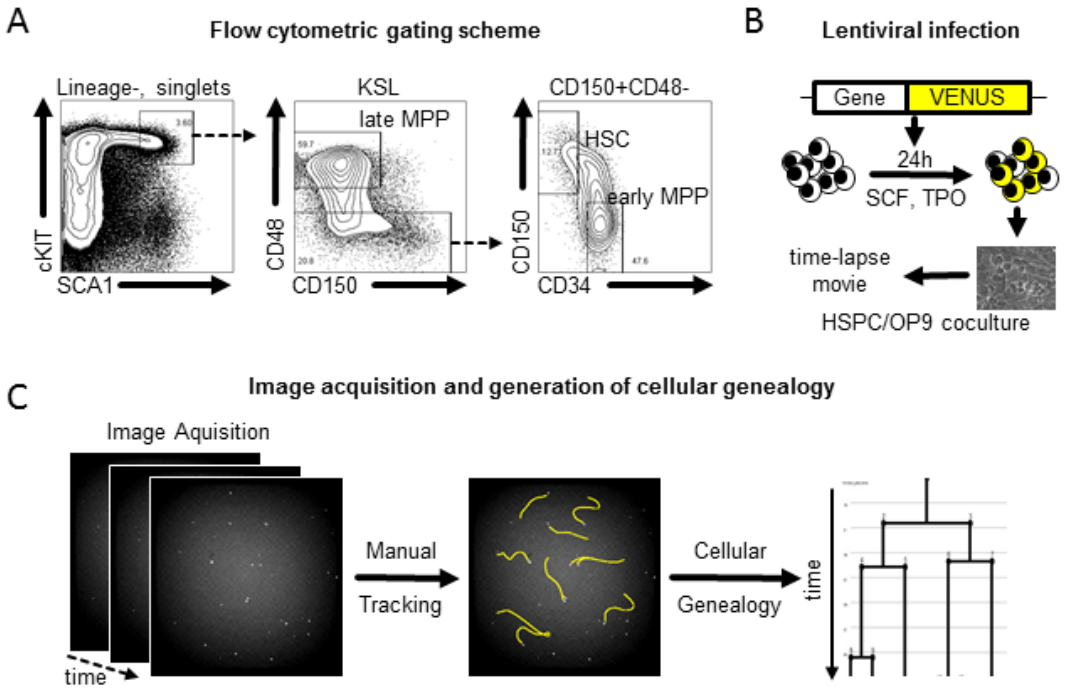

Figure 6.1: Isolation and quantitative imaging of single hematopoietic stem and progenitor cells over time.

(A) Gating scheme for the flow cytometric isolation of HSC, early and late MPPs by flow cytometry. (B) Lentiviral transduction of HSPCs and their OP9 coculture for time-lapse imaging. (C) Generation of cellular genealogy by manual tracking of HSPCs over time.

would be time consuming and expensive we decided to clone lentiviral constructs in which the candidate genes are fused to the fluorescence reporter VENUS. HSCs ($CD150^+CD48^-CD34^-KSL$), early ($CD150^-CD48^-CD34^+KSL$) or late MPPs ($CD150^-CD48^+CD34^+KSL$) were isolated from 12-14 week old C57BL/6J males (Figure 5.1A), transduced and subsequently transferred onto an OP9 stromal cell layer for quantitative time lapse imaging over several days (Figure 5.1B). Brightfield and/or fluorescence images were acquired in constant time intervals allowing us to keep the single cell identity for over 10 days. The cellular genealogy of whole colonies was deduced by manually annotating the x, y coordinates and kinship of cells at every given time point (Figure 5.1C).

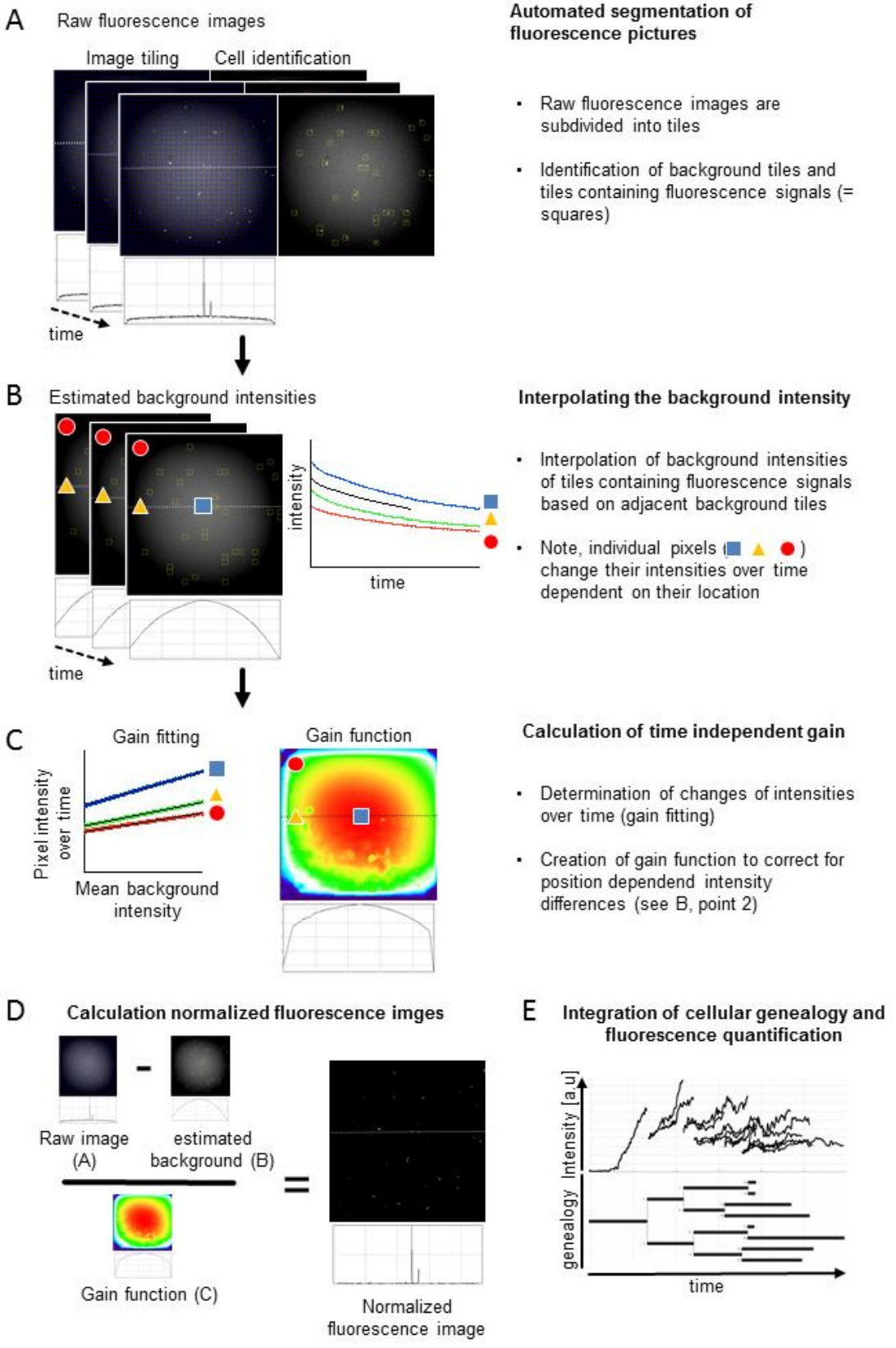

Figure 6.2: Normalization of fluorescence images is required for reliable quantifications of fluorescence signals

(A) Raw fluorescence images are subdivided into tiles and segmented to indentify fluorescence and background signals. (B) The background intensity of tiles containing fluorescence signals in interpolated based on the background intensities of adjacent tiles. Intensities of pixels at the edge or

center of the images changes differently over time and need to be corrected if fluorescence signals want to be quantified reliably (C) Changes of pixel intensities over time yield a linear regression, when plotted again mean background intensity over a given pictures. The slope represents the gain for each individual pixel. The combination of all slopes according to the x,y coordinates of the pixels yields the gain function used to correct for position dependent differences (D) Normalized fluorescence images are generated by subtracting the estimated background (B) from the raw images (A) and dividing the results by the gain function (C). (E) Quantification of normalized cellular fluorescence intensities over time can be integrated with cellular genealogies. This allows the correlation of changes in fluorescence intensities with previous and/or future cellular behavior.

The physical properties of light result in an uneven illumination of fluorescence images making reliable quantifications difficult. In time-lapse experiments where fluorescence images are acquired over several days or weeks these difficulties are even enhanced. Bleaching effects, position differences and intensity changes of the fluorescence light source over time negatively affect the accuracy of quantification results and need to be corrected (Figure 5.2 A-D) before cellular genealogy and the results of fluorescence quantifications can be integrated (Figure 5.2E). The corrections were done using specialized software (Schwarzfischer et al., in preparation) by normalizing every fluorescence image according to position and time dependent changes of pixel intensities. Briefly, using a machine-learning algorithm, raw fluorescence images were divided into subimages (tiles) and subsequently clustered according to their fluorescence intensities to filter out images containing cellular signals and retain images containing background only (Figure 5.2A). The background intensities of filtered subimages were interpolated based on the intensities of adjacent images creating estimated background images (Figure 5.2B). The rate pixel intensities change over time depends on the location of every pixel. Pixels in the center of images change their intensities at different rates as pixels located at the edges or corners (figure 5.2 B). The intensity changes over time can be used to estimate the relationship between pixel intensities and the mean background intensity (Figure 5.2C). The combination of these relationships results in the gain function which corrects for location dependent intensity changes and normalizes the fluorescence intensities to the same intensity scale. In order to generate normalized fluorescence images estimated backgrounds were substracted from raw images and subsequently divided by the gain (Figure 5.2D). The integration of continuous quantification of normalized fluorescence images and cellular genealogies (Figure 5.1C) allows us to correlate changes in fluorescence intensities to previous and/or future cellular behaviors (Figure 5.2E).

6.2 Proteins can be asymmetrically inherited during in vitro HSC divisions

A variety of proteins has been demonstrated to segregate asymmetrically in other tissues and model organisms and is therefore assumed to behave in a similar fashion in HSCs. The most prominent of these proteins is NUMB, which has been shown to segregate asymmetrically in the Drosophila SOP (Rhyu et al., 1994). However although one report suggests, importantly, without showing its functional relevance, that NUMB is asymmetrically segregating in HSC as well (Wu et al., 2007b), another report could not confirm this observation (Ting et al., 2012). In order to clarify if NUMB is asymmetrically segregating during HSC divisions in vitro we overexpressed NUMB1VENUS by lentiviral transduction in freshly isolated HSCs and (Figure 5.1A and 5.1B) imaged them on OP9 stromal cells as previously described (Ting et al., 2012; Wu et al., 2007b). Besides NUMB1, 16 other fluorescence fusion constructs were transduced (Figure 5.3A) and their inheritance quantified during the first in vitro HSC divisions. Among the analyzed proteins, PRKCζVENUS, InversinVENUS, Centrin1VENUS, InturnedVENUS, FYVEVENUS, InscuteableVENUS mitoVENUS and PRKCκVENUS did not differ from the control and therefore do not show any sign of asymmetric segregation in the culture conditions used in this study. However since these proteins are overexpressed we cannot exclude that asymmetric segregation of the wild type proteins occurs at endogenous protein levels. The other proteins, namely CD63VENUS, SCA1VENUS, VANGL2VENUS, LAMP1VENUS, NUMB1VENUS, PROM1VENUS, MSI2VENUS, CD53VENUS and TGFβRIVENUS differed despite their overexpression from cells overexpressing VENUS (Figure 5.3A). As with the symmetrically segregating candidates, the possibility that the observed asymmetric segregation is caused by the overexpression or the FP fusion cannot be excluded. It is interesting to note that in contrast to other studies the

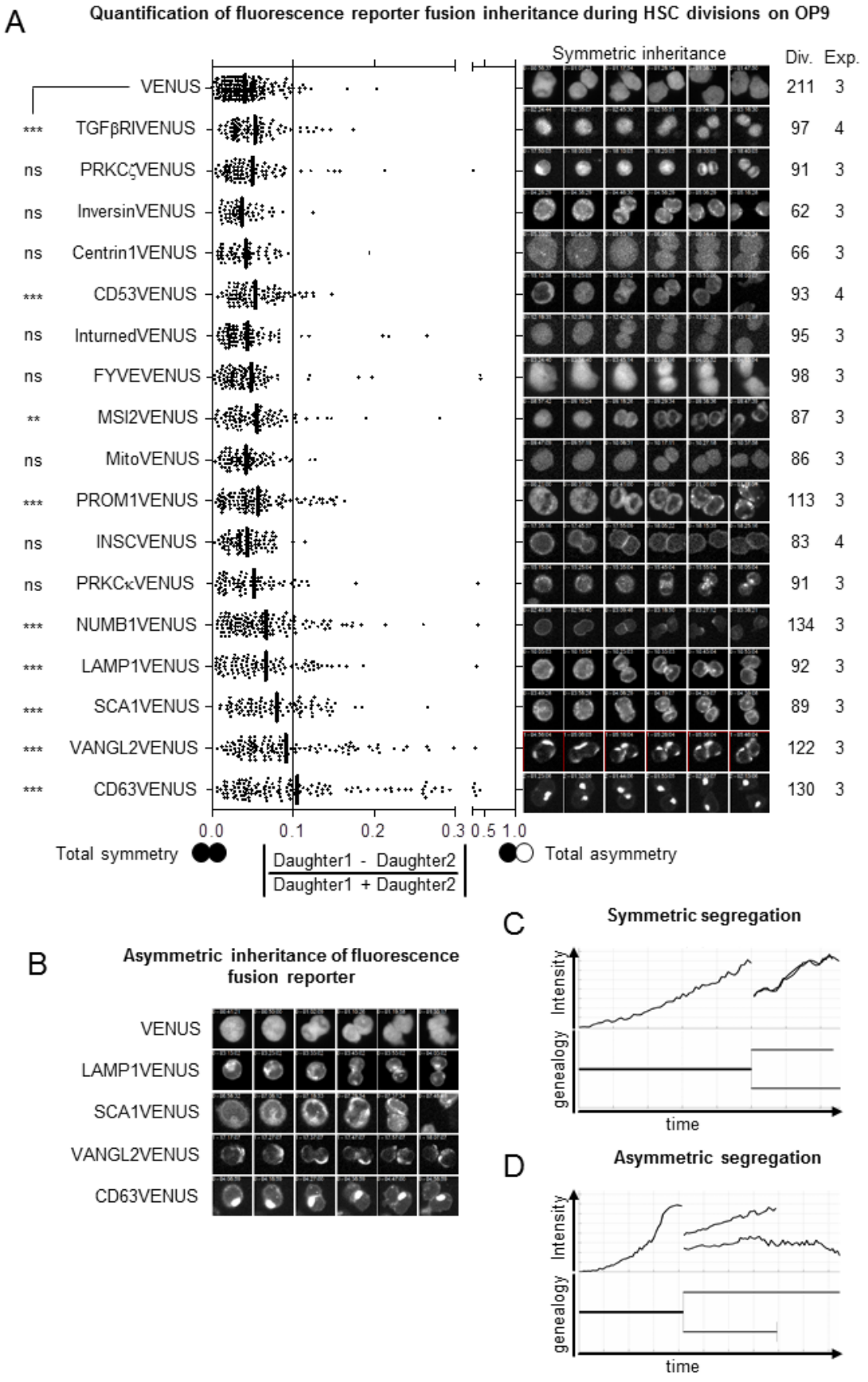

Figure 6.3: Asymmetric inheritance of fluorescence fusion reporter during HSC divisions.

(A) Quantification of asymmetric and symmetric inheritance of fluorescence fusion reporter during cell

divisions by continuous, quantitative imaging of living HSCs in vitro (B) Asymmetric inheritance can be confirmed visually (C and D) Representative examples of symmetric and asymmetric segregeation of fluorescence reporter fusions during HSC divisions as determined by quantitative time-lapse imaging. (C) Quantification of HSC daughter intensities demonstrates that some fluorescence reporter fusions can segregate asymmetrically during in vitro divisions.

majority of daughter cell intensities range from 0 (absolute symmetric segregation) to 0.3 (2:1 daughter ratio) and are thereby much smaller than what one would expect based on the pictures shown in previous reports (Giebel and Beckmann, 2007; Wu et al., 2007b). However, since these reports did not quantify the fluorescence intensities inherited by the daughters it is difficult to judge whether the few shown pictures are representative. Anyways, our results suggest that a difference as small as 0.1 (10% of mother cell fluorescence intensity or 1.22:1 daughter intensity ratio) can only be observed in 1-2% of divisions in the control and that these differences are stable over hours (Figure 5.3C and D). It should be mentioned that even smaller stable differences have been observed. However, since these differences do not exceed the values of the control they are not considered as asymmetric segregations in this study.

In order to investigate if the quantification results could be confirmed visually, transduced HSCs cultured for 3-4 days were imaged with higher spatial and temporal resolution. In line with the quantification results, symmetric as well as asymmetric segregation of CD63VENUS, VANGL2VENUS, SCA1VENUS and LAMP1VENUS could be observed (Figure 5A right and 5B). With the high temporal resolution we were thereby able to confirm that the differences in daughter cell intensities are indeed caused by their asymmetric segregation and are not the result of a rapid protein production immediately after division in one daughter. However, we were not able to confirm the asymmetric segregations of TGFβRIVENUS, CD53VENUS, MSI2VENUS, Prominin1VENUS and NUMB1VENUS visually (Figure 5.3A right). The reasons for this discrepancy are unclear, but might reflect a quantification artifact. Alternatively, it is possible that these proteins are asymmetrically inherited, but that there localization is less concentrated and therefore less obvious. However, the differences in normalized sister intensity ratio are less pronounced when compared to CD63VENUS, VANGL2VENUS, SCA1VENUS and LAMP1VENUS.

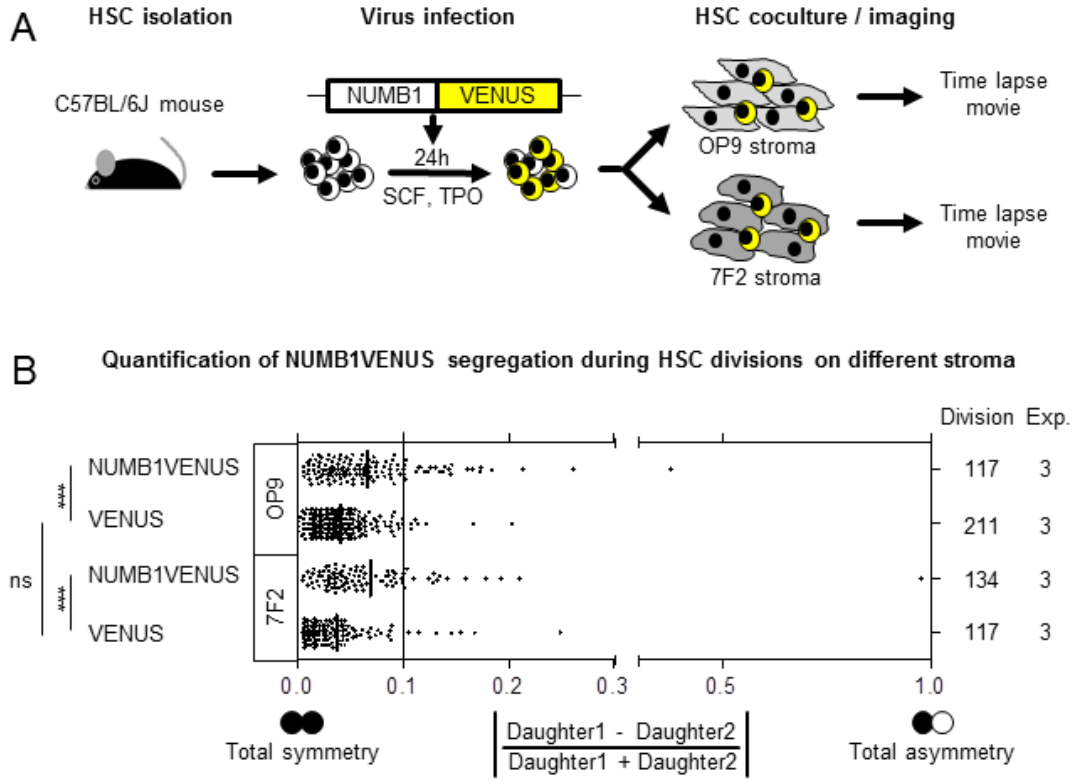

Figure 6.4: Asymmetric inheritance is a generic feature of HSPCs and is not influenced by the microenvironment.

(A) HSCs were isolated, transduced with NUMB1VENUS and cultured in medium containing 20%Serum, 100ng/mL SCF on either OP9 or 7F2 stromal cells. (B) Asymmetric inheritance of NUMB1VENUS does not differ between HSCs cultured on OP9 and 7F2. Statistical results were calculated using one-tailed Mann-Whitney U test and are indicated with: * $p<0.05$, ** $p<0.01$, *** $p<0.001$. ns refers to not significant ($p>0.05$).

NUMB has previously been suggested to segregate more asymmetrically when cultured on 7F2 instead on OP9 stromal cells in vitro (Wu et al., 2007b). If this difference could also be quantified using our imaging technique one could conclude that the lack of visual confirmation is negligible since it is a rather subjective than objective criterion. We transduced HSCs, cultured them on OP9 and 7F2 stromal cells and quantified the amount of NUMB1VENUS that was inherited by the HSC daughters (Figure 5.4A). Although both differed from the VENUS control we could not detect any difference between OP9 and 7F2 stromal as previously described (Figure 5.4B). The reasons for this discrepancy are unclear. One possibility would be that the overexpression of NUMB1VENUS alters its subcellular localization. However, cell-cycle dependent changes in the localization of the fusion protein were exactly as previously described for wild type NUMB protein (Schmit et al., 2012), strongly suggesting normal localization of the NUMB1VENUS fusion protein.

Since the asymmetric segregation of CD63VENUS, VANGL2VENUS, SCA1VENUS and LAMP1VENUS was detected by image quantification and could be seen by eye in living (Figure 2D) as well as fixed cells (data not shown) we decided to analyze these candidates in more depth.

6.3 Asymmetric inheritance of CD63, VANGL2, SCA1 and LAMP1 is a generic feature of HSPCs and is not influenced by the microenvironment

HSCs reside in a specialized microenvironment. Although the exact location and cellular architecture of the niche in vivo is controversial, it has been speculated to provide external cues required to induce polarity and asymmetric HSC divisions. This assumption is based on observations made in other model systems, like D. melanogaster (Morrison and Spradling, 2008; Oliaro et al., 2010). In order to test whether the observed asymmetric segregations of CD63VENUS, VANGL2VENUS, SCA1VENUS and LAMP1VENUS are induced by the in vitro microenvironment, HSCs overexpressing these proteins were cultured on OP9 stromal cells, or only fibronectin or glass (Figure 5.5A). Similar frequencies of asymmetric and symmetric segregations were observed in all three culture conditions, suggesting that the segregation of these proteins is not influenced by the microenvironment (Figure 5.5B). Interestingly, VENUS was inherited more symmetrically when HSCs were cultured in stromal cell free conditions. Although the differences are minute it might indicate a potential interaction with the microenvironment. However, since we did not observe differences in CD63VENUS, VANGL2VENUS, SCA1VENUS and LAMP1VENUS cultured HSCs this putative influence does not seem to alter the segregation of these proteins.

In order to investigate if the observed asymmetric segregation is restricted to HSCs, we overexpressed VENUS, CD63VENUS, VANGL2VENUS, SCA1VENUS and LAMP1VENUS in early and late MPPs and cultured them on OP9 (Figure 5.6A). The frequencies of asymmetric and symmetric segregation in early as well as late MPPs are comparable to what has been observed in HSCs (Figure 5.6B). This suggests

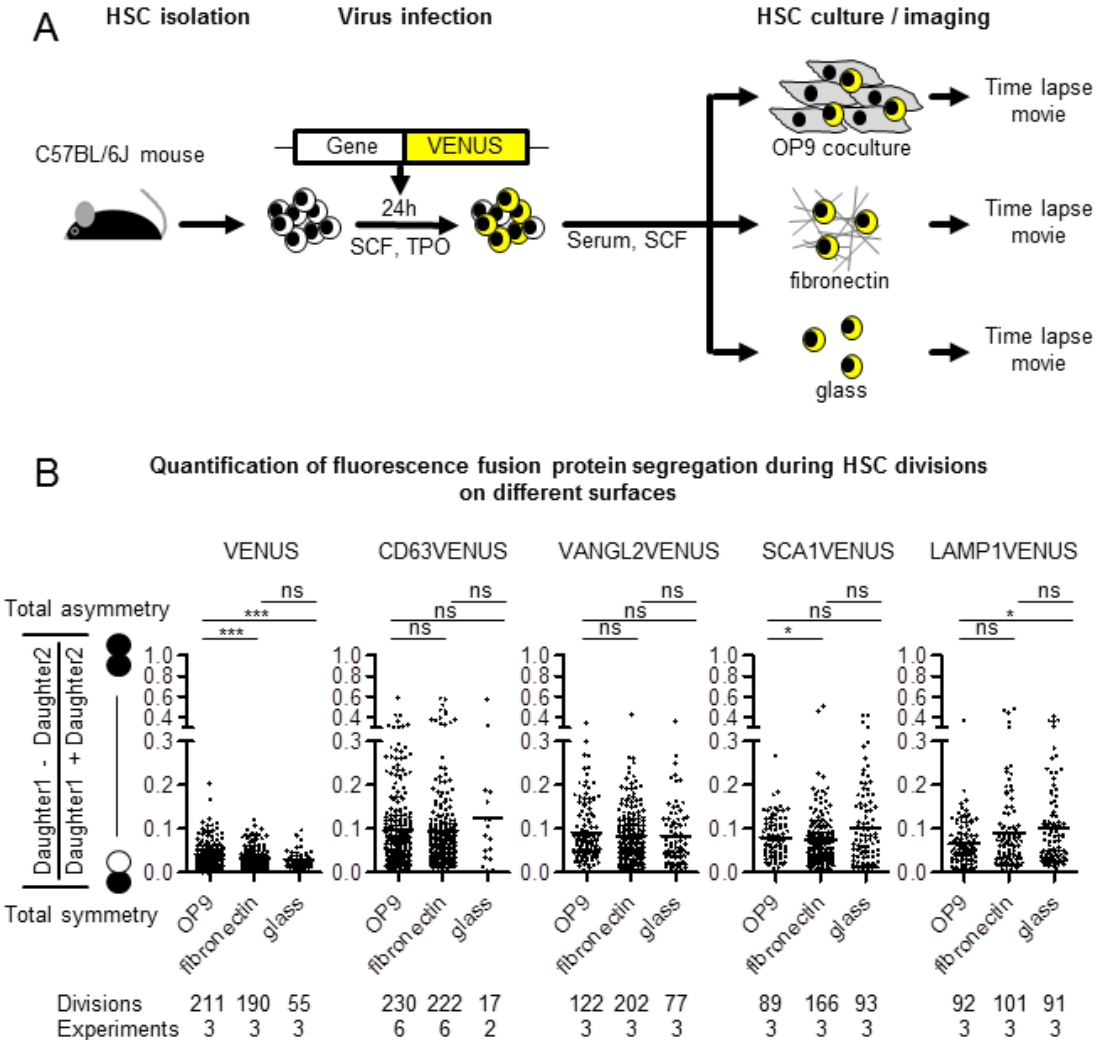

Figure 6.5: Asymmetric inheritance is a generic feature of HSPCs and is not influenced by the microenvironment.

(A) HSCs were isolated, transduced with fluorescence reporter fusions and cultured in medium containing 20% Serum, 100ng/mL SCF on OP9 stromal cells, fibronectin or glass only to determine whether the asymmetric segregation is influenced by the environment. (B) The environment does not influence the inheritance of fluorescence fusion reporters. Each dot represents the normalized daughter intensity ratio of a single HSC division calculated by the indicated formula. Statistical results were calculated using one-tailed Mann-Whitney U test and are indicated with: * p<0.05, ** p<0.01, *** p<0.001. ns refers to not significant (p>0.05).

that the observed asymmetric segregations are a more generic feature of hematopoietic cells and are not restricted to stem cells.

As mentioned above we cannot exclude that the observed asymmetric segregations were caused by the overexpression of fluorescence fusion reporters. We therefore cultured HSCs, early and late MPPs on fibronectin and labeled endogenous SCA1 with live antibody staining (Figure 5.7A). Live antibody staining of CD63, LAMP1 and

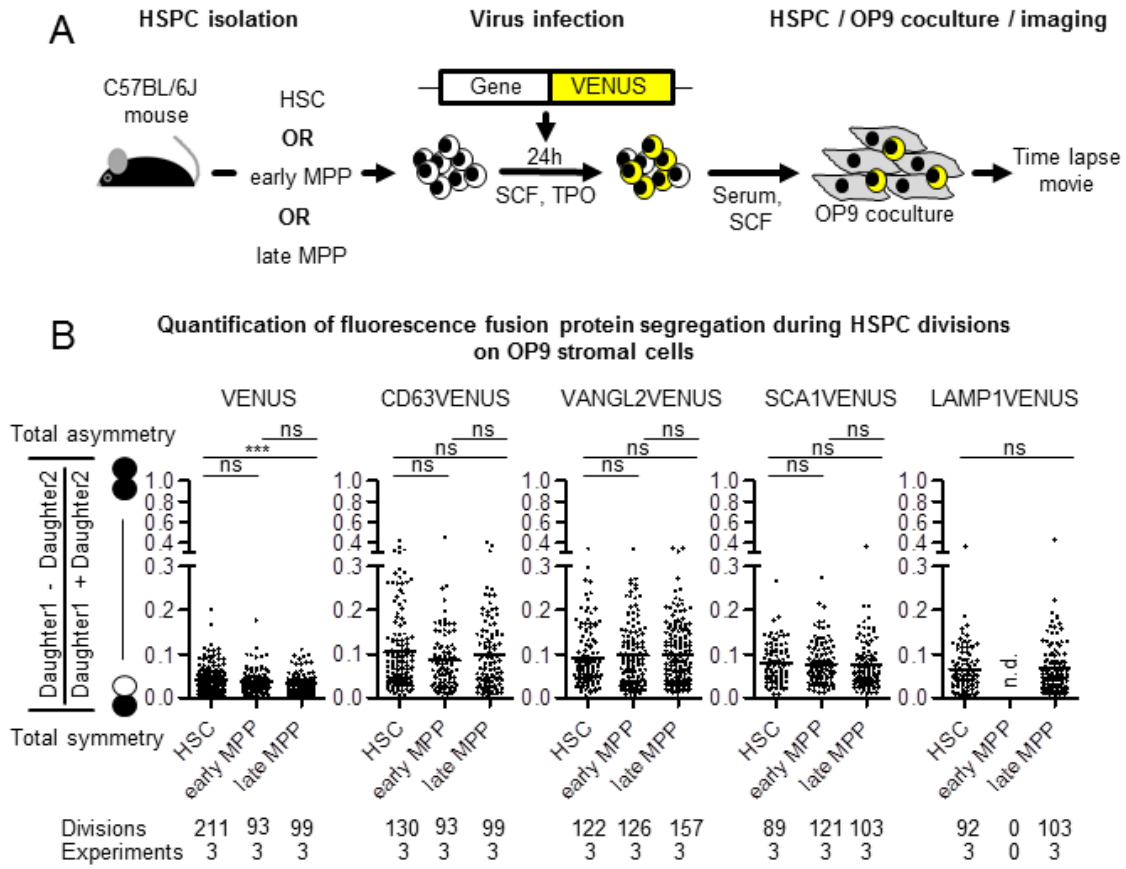

Figure 6.6: Asymmetric inheritance of different proteins is a generic feature of early hematopoietic populations

HSC, early and late MPPs were isolated, transduced with fluorescence reporter fusions and cultured in medium containing 20%Serum, 100ng/mL on OP9 stromal cells to determine whether the asymmetric segregation is cell type specific. (B) Asymmetric inheritance of fluorescence reporter fusions during HSPC divisions on OP9 in not cell type specific. Each dot represents the normalized daughter intensity ratio of a single HSPC division calculated by the indicated formula. Statistical results were calculated using one-tailed Mann-Whitney U test and are indicated with: * $p<0.05$, ** $p<0.01$, *** $p<0.001$. ns refers to not significant ($p>0.05$).

VANGL2 was tested as well but no signals could be detected (data not shown). However, asymmetric segregation of endogenous SCA1 could be observed and quantified even with live antibody staining (Figure 5.7B-D). Interestingly, the degree of asymmetric inheritance although present in all 3 populations was more pronounced in early and late MPPs compared to HSCs (Figure 5.7B). The staining pattern between these 3 populations differed already during interphase showing a highly localized SCA1 signal in late MPPs and an increasingly more evenly distributed signal across the plasma membrane in early MPPs and HSCs (Figure 5.7C). Interestingly the localized signal could also be observed in HSCs and early MPPs and was asymmetrically inherited during cell divisions of all 3 populations

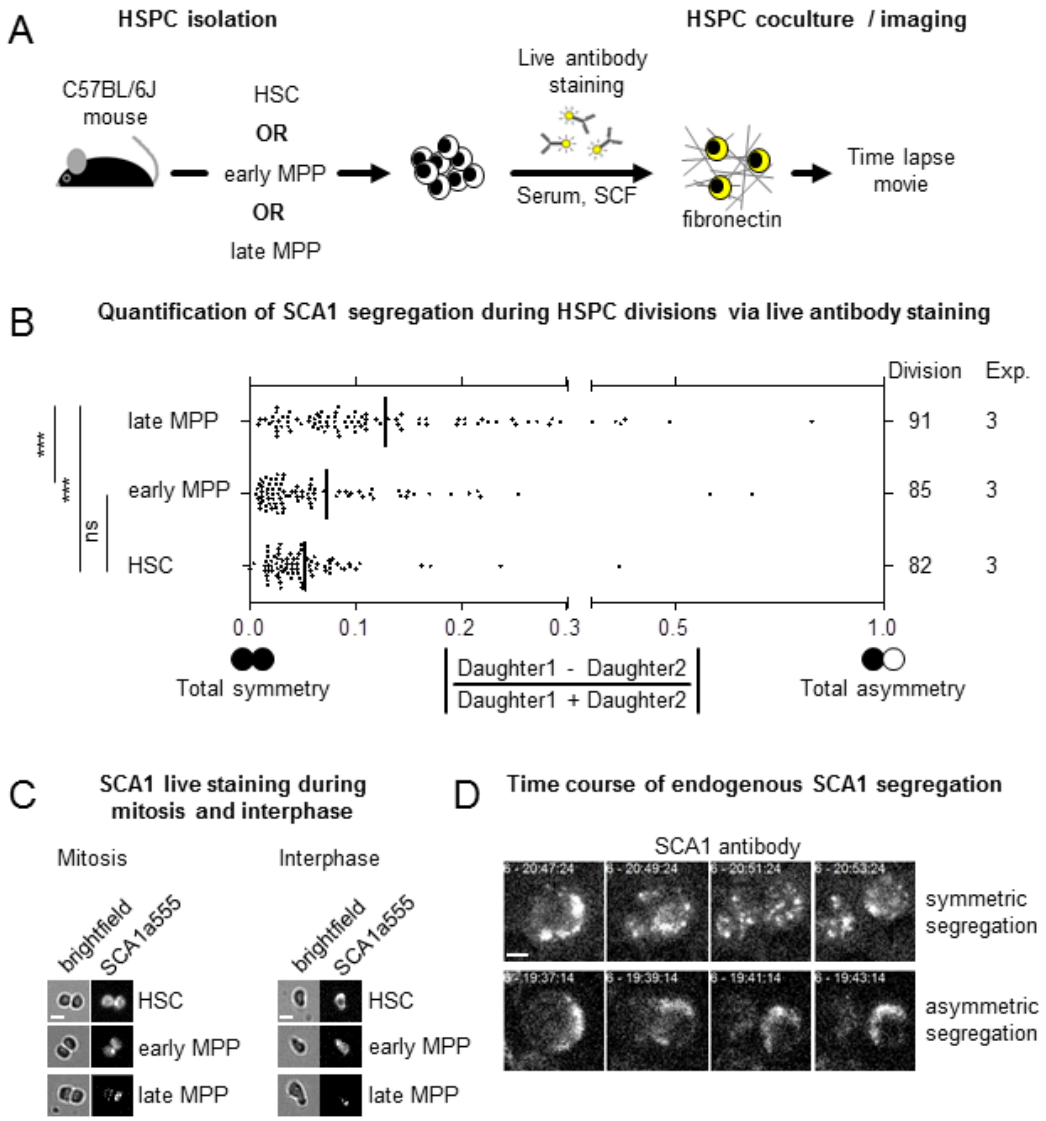

Figure 6.7: Live antibody staining reveals asymmetric inheritance of endogenous SCA1

(A) HSCs, early and late MPPs were isolated and cultured on fibronectin in medium containing 20%Serum, 100ng/mL SCF supplemented with fluorescently tagged SCA1 antibody to determine whether endogenous SCA1 is asymmetrically inherited as well. (B) Quantification of HPSC cell divisions shows that asymmetric segregation of endogenous SCA1 can be detected and is more pronounced in early and late MPPs. Each dot represents the normalized daughter intensity ratio of a single HSPC division calculated by the indicated formula. (C) Representative images of endogenous SCA1 in living HSCs, early and late MPPs during mitosis and interphase demonstrate that endogenous SCA1 is accumulating already during interphase and that this accumulation is asymmetrically segregated during cell division. Scale bars: 10µm. (D) High temporal and spatial resolution time-lapse movie demonstrates that endogenous SCA1 is accumulating in subcellular compartments and confirms asymmetric segregation occurs indeed during cell division. Scale bar: 20µm. Statistical results were calculated using one-tailed Mann-Whitney U test and are indicated with: * $p<0.05$, ** $p<0.01$, *** $p<0.001$. ns refers to not significant ($p>0.05$).

(Figure 5.7C). The localized signal resembled the previously observed signal accumulation in virally transduced cells (Figure 5.3B), and therefore is not an effect of overexpression. The fact that the signal accumulation is present in all four

overexpressed fluorescent fusion reporters as well as endogenous SCA1 labeled by live antibody staining points towards a common subcellular localization and mechanism. This idea is supported by the observation that the frequencies of asymmetric segregations were comparable between different fluorescence fusion reporters (Figure 5.3A, 5.5B and 5.6B).

6.4 Lysosome like compartments are inherited asymmetrically during HSPC divisions

In recent years, lipid rafts have been reported to be involved in the activation of quiescent HSCs. Upon cytokine stimulation the evenly distributed lipid rafts form highly polarized clusters (Vannini et al., 2012; Yamazaki et al., 2006, 2009). SCA1 as a GPI-anchored protein has been reported to be located in lipid rafts (Horejsí et al., 1999). We therefore speculated that the highly localized SCA1 signal observed by overexpression of SCA1VENUS (Figure 5.3B) or by live antibody staining (Figure 5.7C and D) might colocalize with the commonly used lipid raft marker Cholera toxin B (CTxB). To test this hypothesis HSCs were transduced with SCA1VENUS and stained live with fluorescently labeled CTxB. SCA1/CTxB colocalization could be observed in SCA1VENUS expressing HSCs as well as HSCs labeled by SCA1 live antibody staining (Figure 5.8A and B). Asymmetric and symmetric cosegregation of both SCA1 and CTxB during HSC divisions could be detected (Figure 5.8B). Furthermore we were able to confirm the colocalization by high spatial resolution confocal imaging of fixed HSCs after cytokine stimulation (Figure 5.8C). Surprisingly, also CD63VENUS, VANGL2VENUS and LAMP1VENUS showed a strong colocalization with the lipid raft marker when imaged in living HSCs (Figure 5.8A). This suggests that CD63, VANGL2, LAMP1 and SCA1 localize to the same subcellular compartment and that their asymmetric inheritance is based on a common mechanism. This idea is supported by the previously described similarities in form of a single localized fluorescence fusion reporter accumulation (Figure 5.3A and B) and the comparable frequencies of asymmetric inheritance between different fluorescence fusion reporters (Figure 5.3A, Figure 5.5B and 5.6B).

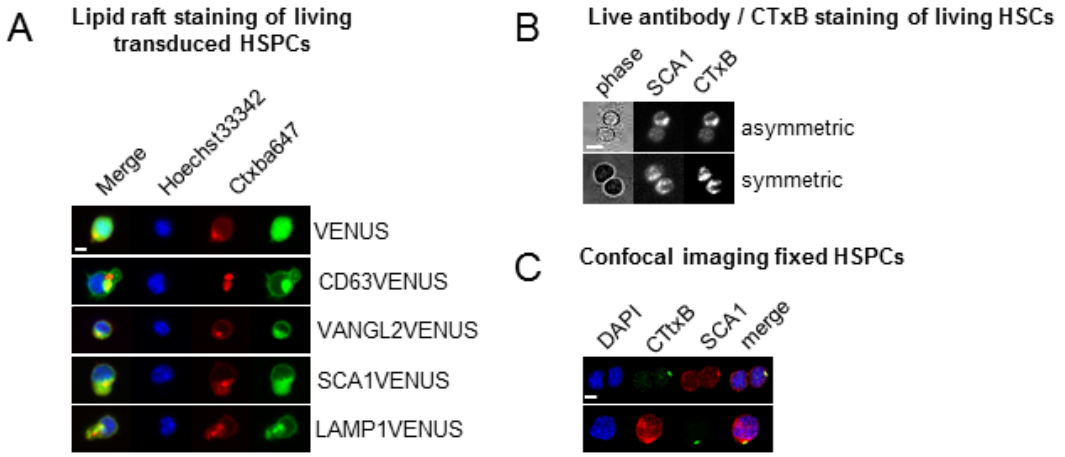

Figure 6.8: Fluorescence fusion reporter and endogenous SCA1 colocalize with lipid raft marker CTxB.

(A) Representative images of living HSPCs transduced with fluorescence fusion reporters stained with Hoechst33342 and CTxB. Fluorescence fusion reporters strongly colocalize with the lipid raft marker CTxB. Scale bar: 5µm (B) Representative images of symmetric and asymmetric inheritance of endogenous SCA1 and CTxB in 100ng/mL SCF, 100ng/mL TPO demonstrates that both markers cosegregate during HSC divisions in vitro. Scale bar: 10µm (C) Representative confocal images of fixed HSPCs demonstrating that CTxB and SCA1 colocalizes in freshly isolated cells (stimulated for 30min with 100ng/mL SCF, 100ng/mL TPO). Scale bar: 10µm.

Since CD63VENUS and LAMP1VENUS are commonly used marker for lysosomes we tested the colocalization of all asymmetrically segregating fluorescence fusion reporters with the lysosomal marker LysoTracker Red in living HSCs. CD63VENUS and LAMP1VENUS colocalized with the lysosomal marker as expected (Figure 5.9A). Surprisingly, also SCA1VENUS and VANGL2VENUS colocalized with LysoTracker Red (Figure 5.9A). This observation is in line with the previously mentioned idea that the asymmetrically segregating fluorescence fusion reporter localize to the same subcellular compartment. Furthermore, since all fluorescence fusion reporter colocalize with CTxB as well (Figure 5.8A), the presented results suggests that the specificity of CTxB to mark lipid rafts has been grossly overestimated in previous studies and that the previously described lipid raft clusters are most likely part of the degradative machinery. The accumulation of fluorescence fusion reporters in the degradative machinery would explain why CD63VENUS, VANGL2VENUS, SCA1VENUS and LAMP1 show similar, highly localized signal accumulations (Figure 5.3B) and why this accumulation is more pronounced when endogenous SCA1 is labeled by live antibody staining in late MPPs (Figure 5.7B). In contrast to HSCs and

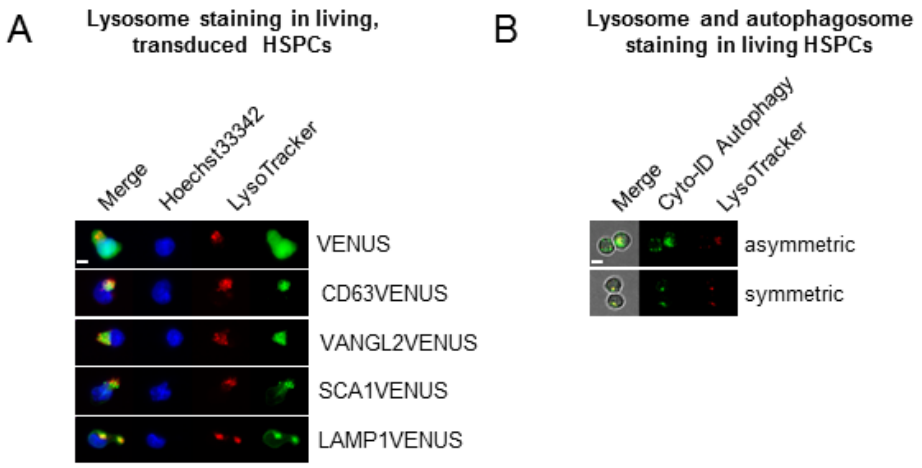

Figure 6.9: Lysosomes colocalize with fluorescence fusion reporter and are inherited asymmetrically during HSPC divisions in vitro

(A) Representative images of living HSPCs transduced with fluorescence fusion reporters stained with Hoechst33342 and LysoTracker Red. Fluorescence fusion reporters colocalize with the lysosomal marker LysoTracker Red. Scale bar: 5µm (B) Representative images of living HSPC stained with LysoTracker and the autophagosomal marker Cyto-ID demonstrate colocalization of both markers It demonstrates that lysosomes can asymmetrically segregate also in the absence of live antibody staining or viral overexpression. Scale bar: 5µm.

early MPPs which actively produce SCA1, its production in late MPPs is downregulated. SCA1 therefore disappears shortly after isolation of late MPPs from the plasma membrane and accumulates in lysosomes. In contrast, in HSCs and early MPPs, where SCA1 is abundantly expressed, the accumulation is less obvious since it is masked by the SCA1 expression on the plasma membrane (Figure 5.7C). The asymmetric inheritance of lysosomes would also explain why fluorescence fusion reporters as different as CD63VENUS, VANGL2VENUS, SCA1VENUS and LAMP1VENUS are asymmetrically inherited in similar frequencies (Figure 5.3A, Figure 5.5B and 5.6B). However, if fluorescence fusion reporters accumulate in lysosomes which can be asymmetrically inherited during cell division, it is surprising that only 4 out of 17 candidates show this behavior. The reasons for that are currently unclear.

A recent report demonstrated the importance of autophagy for HSC maintenance (Warr et al., 2013). Since the autophagosomal and lysosomal pathways merge to form the autolysosome we wanted to determine whether autophagosomes are asymmetrically segregating as well. We therefore used the autophagosome marker Cyto-ID and imaged HSCs live. Asymmetric as well as symmetric segregation of

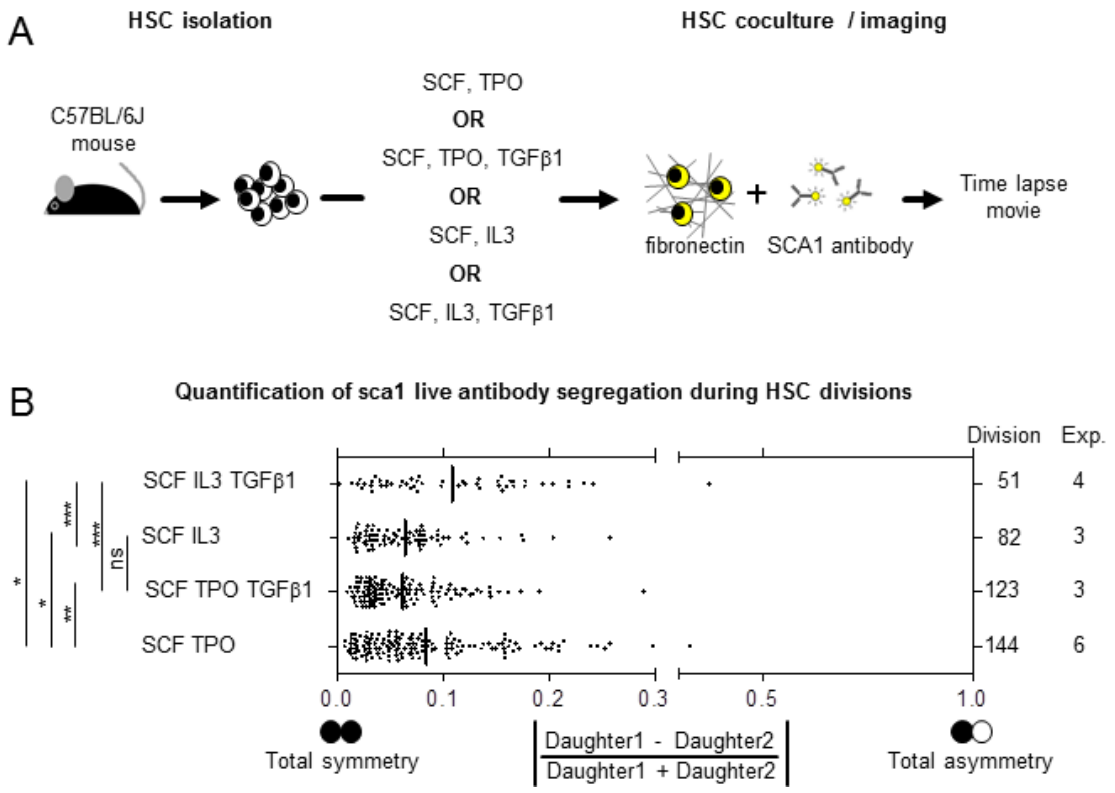

Figure 6.10: Asymmetric inheritance of endogenous SCA1 can be modulated by cytokines.

(A) To determine whether its segregation influenced by different extracellular derived signals, HSCs were isolated and cultured on fibronectin using the indicated cytokine conditions supplemented by fluorescently tagged SCA1 antibody. (B) The asymmetric segregation of endogenous SCA1 can be modulated by the cytokine conditions used. The occurrence of asymmetrically inherited endogenous SCA1 more pronounced in SCF, TPO and SCF, IL3, TGFβ1 compared to SCF, TPO, TGFβ1 and SCF, IL3. Each dot represents the normalized daughter intensity ratio of a single HSC division calculated by the indicated formula. Statistical results were calculated using one-tailed Mann-Whitney U test and are indicated with: * $p<0.05$, ** $p<0.01$, *** $p<0.001$. ns refers to not significant ($p>0.05$).

autophagosomes could be detected (Figure 5.9B). However, since this marker strongly overlaps with the lysosomal marker we assume that the specificity of these dyes is limited. Nevertheless, taken together the presented evidence suggests that CD63VENUS, VANGL2VENUS, SCA1VENUS and LAMP1VENUS as well as endogenous SCA1 accumulate in lysosomal-like organelles that can asymmetrically segregate during HSPC divisions in vitro.

It has recently been reported that the frequency of lipid raft cluster formation in HSCs can be increased or decreased depending on the cytokines used (Vannini et al., 2012). We therefore speculated that different cytokines might influence the degradative machinery and its segregation during HSPC divisions. HSCs were therefore labeled with SCA1 live antibodies and cultured in SCF/TPO, SCF/TPO/TGFβ1, SCF/IL3 and SCF/IL3/TGFβ1 on fibronectin (Figure 5.10A). The

SCA1 inheritance of the HSC daughters was quantified and compared. Interestingly, SCF/TPO and SCF/IL3/TGFβ1 showed a more pronounced asymmetric segregation compared to SCF/TPO/TGFβ1 and SCF/IL3 (Figure 5.10B). The meaning of these differences is currently unclear and requires further investigation. Even though the frequencies of asymmetric inheritance are increased in SCF/TPO and SCF/IL3/TGFβ1, HSCs do not react in a unified manner. It will therefore be interesting to see if the asymmetric segregation of the degradative machinery is a stochastic event with a certain probability depending on the culture conditions used or if the different responses are based on different subpopulations.

6.5 Asymmetric segregation of SCA1 does not correlate with early in vitro differentiation

We could demonstrate that SCA1 and other proteins are asymmetrically segregating during HSPC divisions in vitro. As a next step, its functional relevance had to be tested. We were therefore looking for ways to identify asymmetric daughter cell fates allowing us to identify differentiation and lineage choice in vitro. Linking asymmetric fates to the observed asymmetric segregation would allow us to prove the control of HSPC fates through asymmetric cell division.

It has previously been published that in vitro cultured HSCs change their immunophenotype (Zhang and Lodish, 2005). It is therefore not trivial to find reliable in vitro marker as indicators of differentiation. The expression of SCA1 and CD48 has been shown to correlate with loss of HSC capacity and differentiation in vitro as well as in vivo (Noda et al., 2008; Zhang and Lodish, 2005). As in vivo, all in vitro cultured HSCs are contained within the $SCA1^{+}CD48^{-}$ fraction while the downregulation of SCA1 or the CD48 onset are indicative of their differentiation (Figure 5.11A-C).

It has previously been suggested that HSCs divide asymmetrically when cultured in SCF and TPO (Ema et al., 2000; Takano et al., 2004). However since cell divisions were not observed directly it was not clear if the cause for these asymmetries is

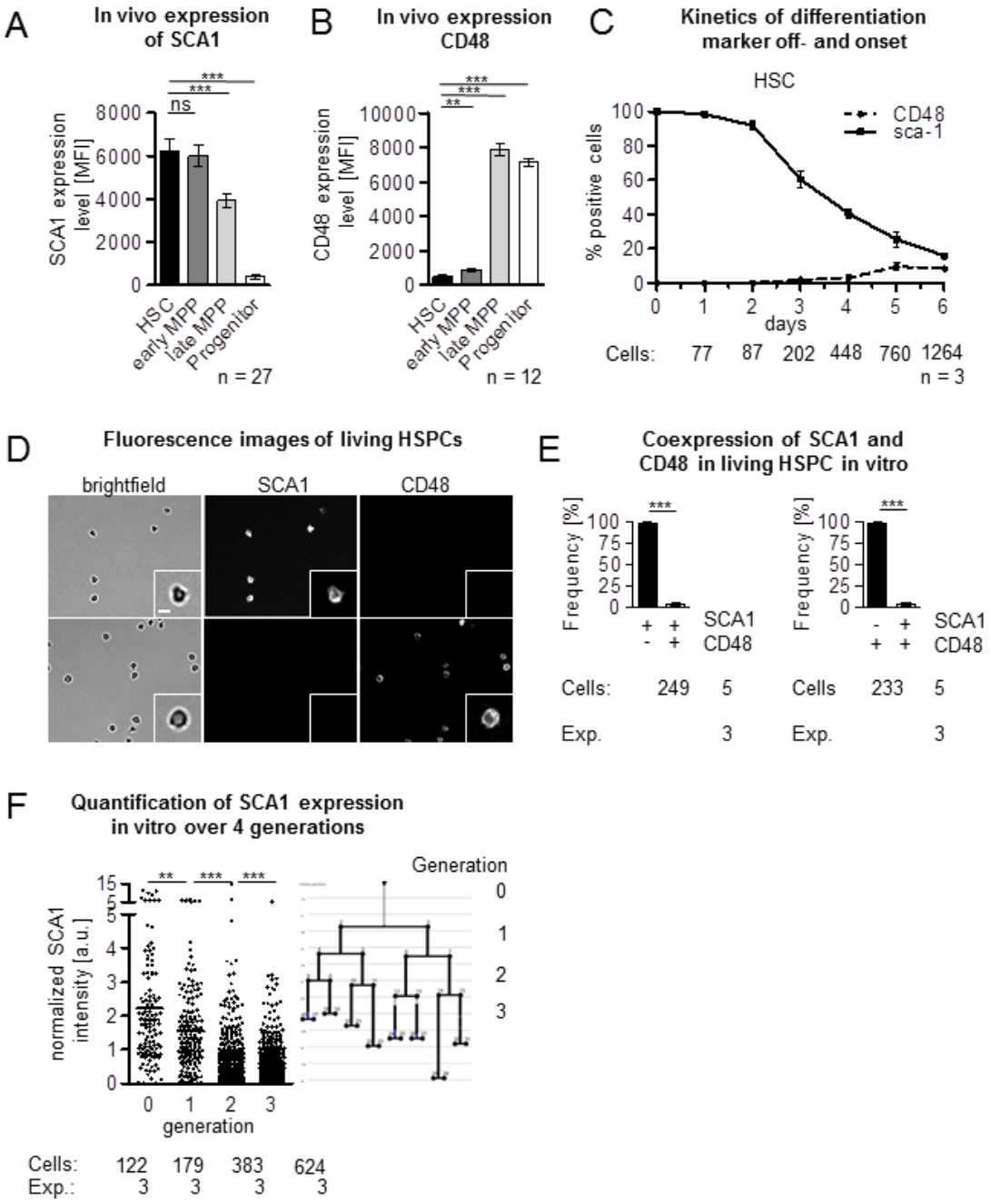

Figure 6.11:SCA1 offset is an early, quantifiable event indicative of differentiation.

(A-B) Freshly isolated HSCs, early and late MPPs and hematopoietic progenitors were stained with antibodies and analyzed by flow cytometry for SCA1 and CD48 expression demonstrate the SCA1 downregulation and CD48 upregulation during differentiation in vivo. (B) Culturing HSCs for 7 days in SCF, TPO on fibronectin shows that SCA1 downregulation precedes CD48 upregulation. Thus, SCA1 is the earlier differentiation marker. (C-E) SCA1 is downregulated before CD48 onset occurs. Representative fluorescence images and quantification of double positive living HSPCs stained by live SCA1 and CD48 antibodies. Scale bar: 10µm. (F) Analysis of SCA1 fluorescence intensities in living HSPCs over 4 generations show that the downregulated of SCA1 can be detected and quantified. Each dot represents the normalized SCA1 intensity at the end of the cell cycle. Statistical results were calculated using two-tailed unpaired student´s t-test and are indicated with: * $p<0.05$, ** $p<0.01$, *** $p<0.001$. ns refers to not significant ($p>0.05$).

linked to events happening during HSC division or caused post mitotically. We speculated that asymmetric daughter cell fates might have been caused by asymmetric segregations and decided to use these culture conditions for our further analysis. As a first step, we determined the SCA1 offset and CD48 onset kinetics on a population level as markers for differentiation. While SCA1 levels were rapidly downregulated, CD48 positive cells did not emerge before day 5-6 (Figure 5.11C). After 7-8 days, a massive upregulation of CD48 could be observed (data not shown). However, the majority of HSCs had become SCA1 negative days before that (Figure 5.11C). In fact, we rarely observed double positive cells, indicating that SCA1 downregulation precedes the CD48 onset (Figure 5.11D and E). This idea is supported by the rapid downregulation of SCA1 protein levels over 3 generations (Figure 5.11F).

The rapid downregulation of SCA1 in these culture conditions was also found when individual HSC colonies were tracked over time (Figure 5.12B). While some of the colonies can be characterized by a rapid downregulation of SCA1 which is almost always associated with symmetric SCA1 segregations (Figure 5.12B left), other colonies are more heterogeneous and give rise to cells of various SCA1 intensities (Figure 5.12B middle/right). These colonies are sometimes, but not always associated with asymmetric SCA1 segregations. In summary, the loss of SCA1 expression precedes the CD48 onset and is therefore an earlier and potentially more reliable marker for differentiation than CD48.

In order to correlate the asymmetric segregation of SCA1 with its downregulation as an indicator for differentiation or other cellular attributes, HSC divisions were sorted according to their normalized daughter sister intensity ratio into symmetrically (normalized sister intensity ratio: <0.05) and asymmetrically segregating HSCs (normalized sister intensity ratio: >0.1) (Figure 5.12C). Next, the sister cells receiving more or less SCA1 in asymmetric segregations were pooled and the SCA1 production of the daughter cells themselves as well as the total SCA1 production of their future progeny (for 3 generations) compared (Figure 5.12D and E). The SCA1 production was calculated by subtracting the SCA1 intensities at the beginning of the cell cycle from the SCA1 intensities at the end and added over several generations in case of the total sister colony SCA1 production. Negative values would thereby be

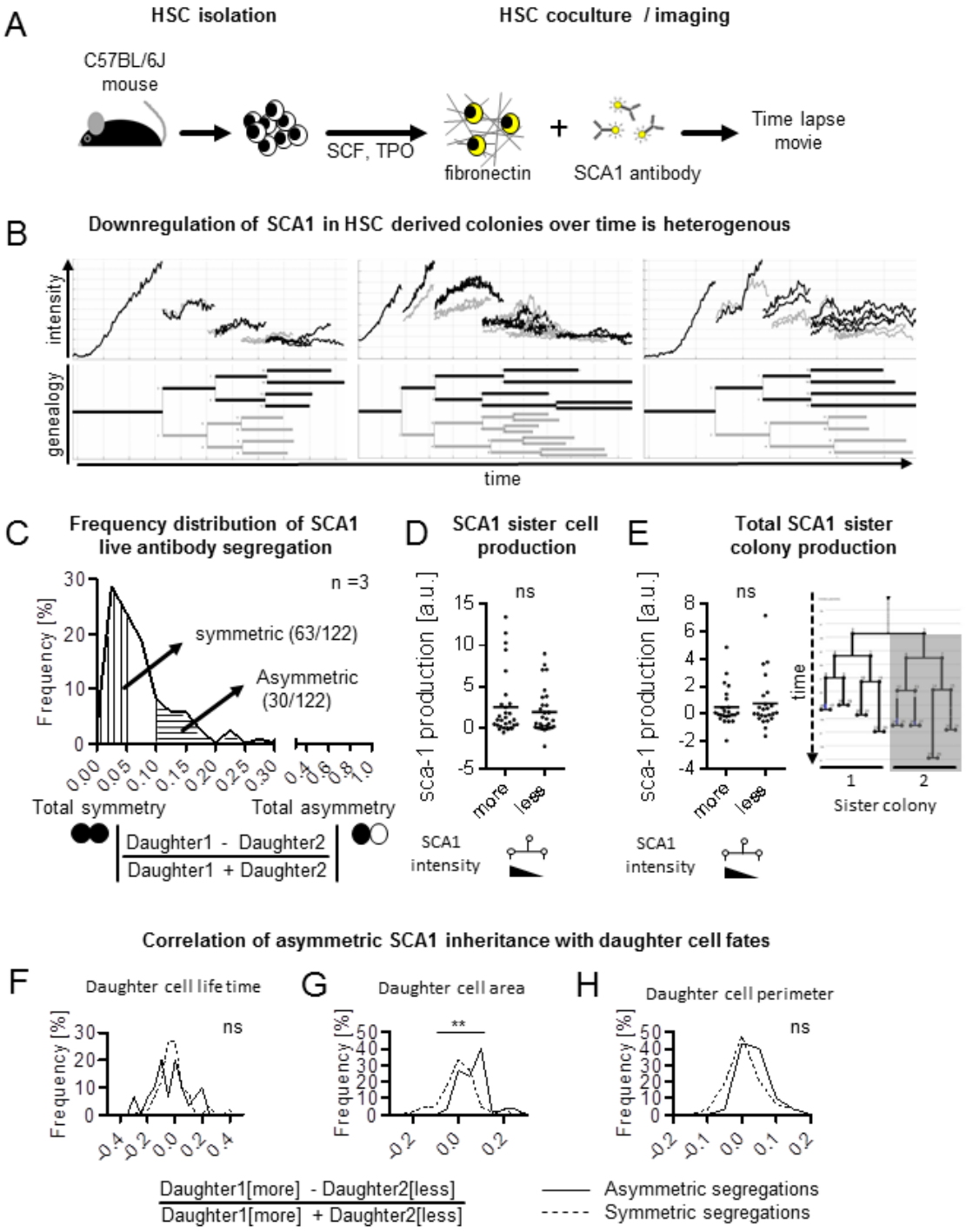

Figure 6.12: Asymmetric inheritance of endogenous SCA1 does not correlate with future daughter cell fates

(A) HSCs were isolated and cultured in SCF, TPO on fibronectin supplemented by fluorescently tagged SCA1 antibody to determine whether its asymmetric inheritance correlates with future daughter cell fates. (B) Representative examples of HSC derived colonies with integrated SCA1 quantification demonstrates highly heterogeneous SCA1 offset behaviors between different colonies. (C) SCA1 inheritance during HSC divisions was quantified using the depicted formula and clustered into symmetric and asymmetric segregations based on arbitrary thresholds as indicated. (D-E) Asymmetric SCA1 inheritance does affect the SCA1 production or maintenance of individual daughter cells or daughter cell derived colonies. Daughters of asymmetric divisions receiving more or less SCA1 were pooled the SCA1 production of the daughters themselves or the total SCA1 production

(=maintenance) of their future progeny compared. (F) Asymmetric SCA1 inheritance does not affect the cell life time or morphology (=perimeter) of the daughters, but correlates with daughter cell size or adherence (=area). Statistical results were calculated using one-tailed Mann-Whitney U test and are indicated with: * $p<0.05$, ** $p<0.01$, *** $p<0.001$. ns refers to not significant ($p>0.05$).

indicative of active degradation of SCA1, positive values for a net production. However, we were not able to detect differences in the production and maintenance of SCA1 intensities between HSC daughter cells or HSC daughter colonies (Figure 5.12D and E).

In addition to the loss of SCA1 other cellular attributes like HSC daughter cell life time and area as an indicator of size were normalized and analyzed in a way, that a random set of variables (in case of a symmetric segregation it is random which daughter is defined as the one that receives [more] or [less]) would give a Gaussian distribution centered around 0. An ordered data set (in case of asymmetric segregation, where it is clearly defined which daughter receive [more] or [less]) on the contrary would deviate from this distribution if the attributes where correlated with the segregation. If the distribution would shift towards the right (positive) the daughter cell receiving more SCA1 would have also have bigger numerical values in this attributes (positive correlation). If the distribution would shift towards the left (negative) the cell receiving more SCA1 would have the smaller numerical value and vice versa (negative correlation). Since the distributions of the neither the cell life time nor their shape (=perimeter) in asymmetric segregation deviate from the distribution of symmetric segregations we conclude that the asymmetric segregation of SCA1 does neither influence the cell cycle length of the daughters nor their shape (=perimeter) (Figure 5.12F and H). However, the daughters receiving more SCA1 tend to occupy a bigger area than the daughter receiving less SCA1 (Figure 5.12G). This might either indicate that HSPCs receiving more SCA1 give rise to bigger daughters, or that the daughters differ in their ability to adhere to the fibronectin coated surface. The meaning of this observation is currently unclear.

6.6 The asymmetric inheritance of SCA1 does not correlate with TGFβ1 induced apoptosis

TGFβ1 is considered to be an inhibitory cytokine controlling proliferation, differentiation and quiescence. It has been suggested to induce hibernation of HSCs while inducing apoptosis in differentiated $CD34^+$ cells when cultured with SCF and TPO (Yamazaki et al., 2009). Interestingly, HSC self-renewal and differentiation potential were maintained for a period of 5 days. We speculated that apoptosis would be indicative of differentiation in these culture conditions and could therefore be used as a marker in our time-lapse experiments. If this assumption would be correct, any asymmetric occurrence of apoptosis in the cellular genealogy might correlate with the asymmetric segregation of SCA1 in case it is associated with this process.

In order to test this hypothesis we cultured HSCs, early and late MPPs in SCF, TPO and TGFβ1 (Figure 5.13A). HSC derived colonies were able to survive longer than their counterparts derived from early or late MPPs (Figure 5.13B), which were rarely able to divide at all in these culture conditions (data not shown). If TGFβ1 were to induce apoptosis of differentiated cells one would expect a selective enrichment of SCA1 high expressing cells. In order to test that, we cultured freshly isolated HSC for 3 days in SCF/TPO and SCF/TPO/TGFβ1 and analyzed their SCA1 expression level by flow cytometry (Figure 5.13C). As expected, HSCs cultured with TGFβ1 maintained high SCA1 expression levels when compared to HSCs cultured in SCF/TPO only. This observation is in line with a recent publication suggesting that SCA1 inhibits TGFβRI mediated signaling by preventing its hetero dimerization with TGFβRII (Upadhyay et al., 2011). In order to determine if asymmetric cellular genealogies can be observed we tracked HSCs cultured in SCF and TPO with and without TGFβ1 (Figure 5.14A). The frequency of asymmetric apoptotic genealogies up to generation 2 increased from 4.2% (7/168) in SCF/TPO to 22.6% (30/133) in SCF/TPO/TGFβ1 (Figure 5.14B). This strongly suggested that cells inheriting less SCA1 were more sensitive to TGFβ1 mediated apoptosis. In order to test this hypothesis we tried to correlate the occurrence of asymmetrically segregating SCA1 with the occurrence of cell death. As described before (section 5.5) the quantified

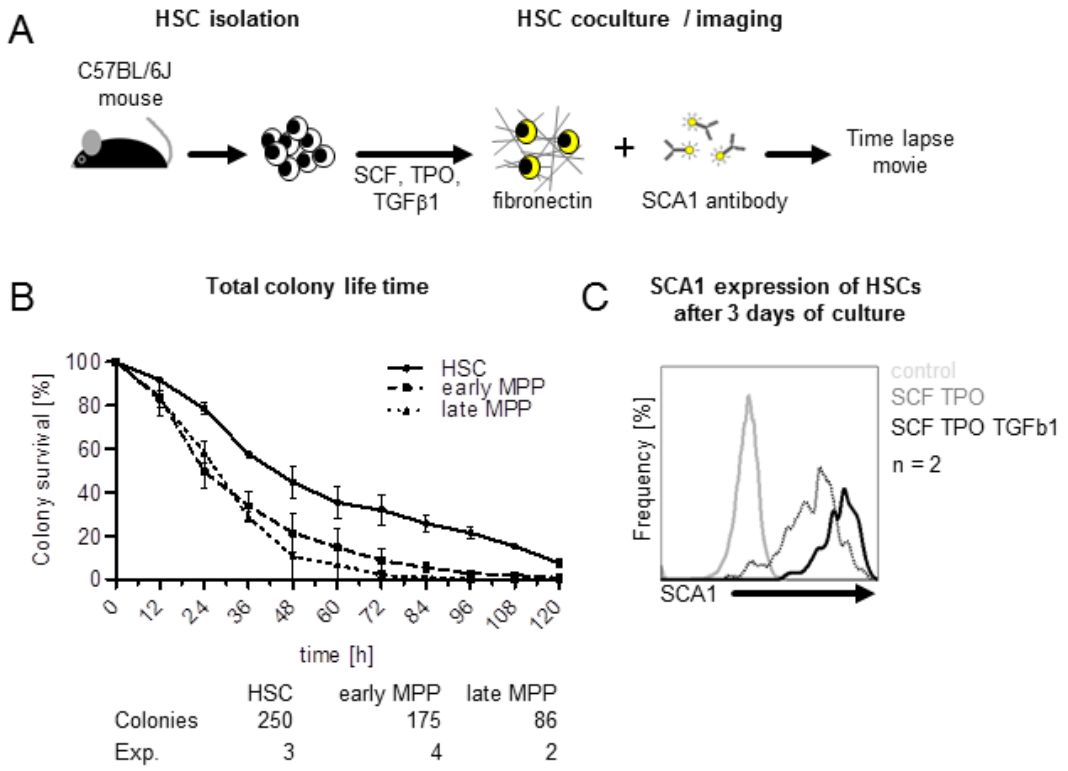

Figure 6.13: TGFb1 enriches for HSCs and increases or maintains SCA1 expression levels.

(A) To determine whether TGFβ1 selectively induces apoptosis in differentiated cells as previously published, HSCs, early and late MPPs were isolated and cultured in medium containing SCF, TPO, TGFβ1on fibronectin supplemented by fluorescently tagged SCA1 antibody to determine whether TGFβ1 selectively induces apoptosis in differentiated cells as previously published. (B) HSC derived colonies are selectively enriched when cultured in SCF, TPO, TGFβ1 and have a total colony life time (=colony survival) that is longer than early and late MPP derived colonies(B) Representative flow cytometric analysis showing that SCA1 expression levelsof HSCs are increased or maintained when cultured for 3 days with TGFβ1.

HSC divisions were defined as symmetric (59 of 128 divisions) or asymmetric (32 of 128 divisions) according to the normalized SCA1 daughter intensity ratios (Figure 5.15B). The daughters receiving more or less SCA1 derived from the as asymmetric defined divisions were pooled and the frequency of apoptosis within the same generation calculated (Figure 5.15C). Daughters receiving more SCA1 did not die more frequently than their sisters, demonstrating that the asymmetric segregation of SCA1 does not directly affect the viability of HSC daughters (Figure 5.15C). Since the overall colony life time of HSCs declines with time (Figure 5.13B) and the frequency of asymmetric apoptotic genealogies increases (Figure 5.14B), we speculated that the asymmetric segregation of SCA1 might affect the viability of the subsequent generations. In order to test this hypothesis we tracked all colonies for at least one additional generation. The cellular genealogies derived from this analysis are highly

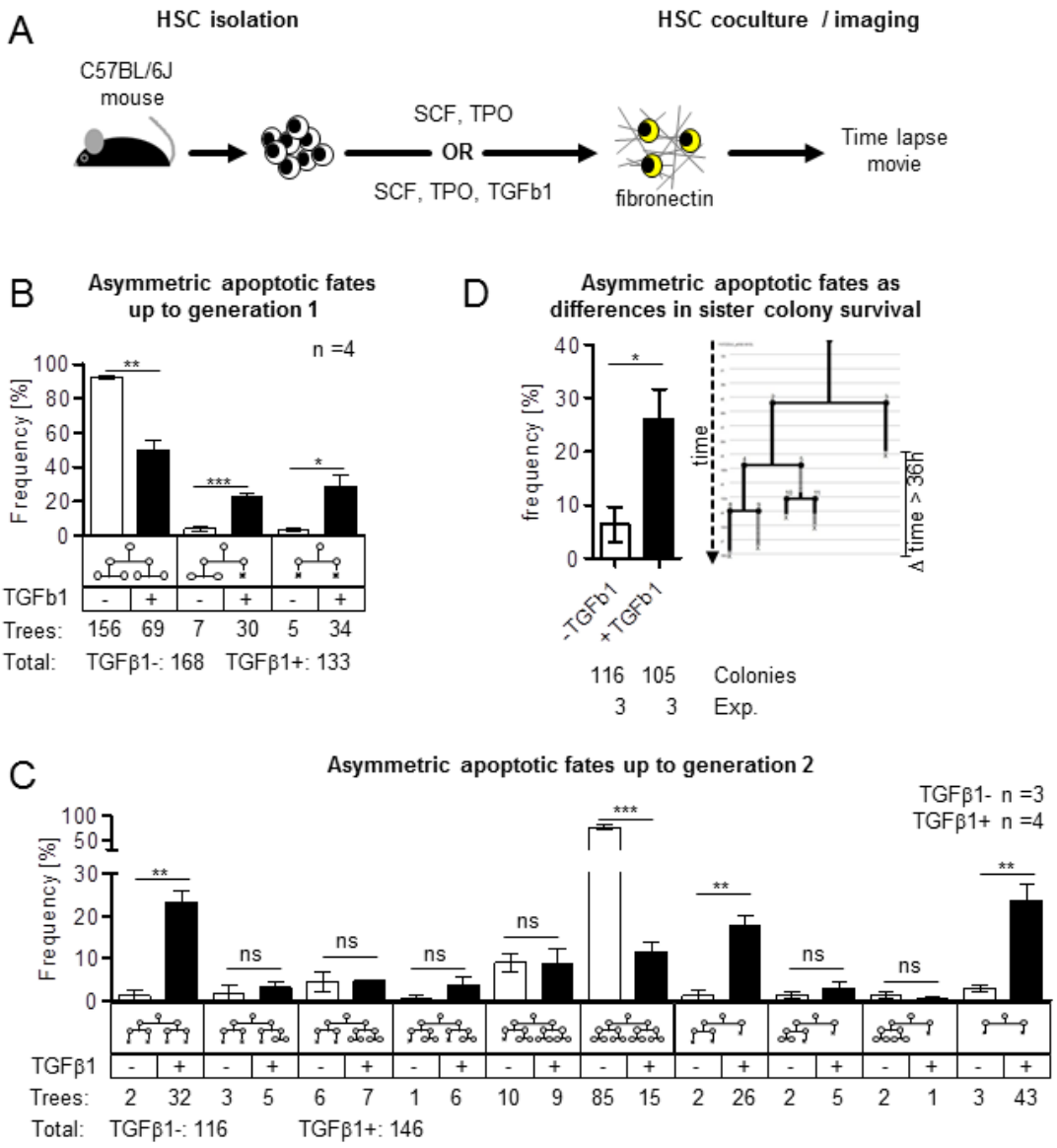

Figure 6.14: TGFβ1 induces asymmetric apoptotic daughter cell and colony fates in HSC derived cellular genealogies.

(A) To determine whether TGFβ1 induced asymmetric apoptotic fates could be detected, HSCs were isolated and cultured in medium containing SCF, TPO and TGFβ1 on fibronectin. (B) HSC derived asymmetric apoptotic genealogies are increased in the presence of TGFβ1 compared to SCF, TPO only as determined by time-lapse imaging. (C) Tracking HSC derived colonies for over 3 generations reveals a highly heterogeneous occurrence of apoptosis making the definition of asymmetric apoptotic fates difficult. (D) Differences in sister colony survival also reveal and increase occurrence of asymmetric apoptotic genealogies. Statistical results were calculated using two-tailed unpaired student´s t-test and are indicated with: * p<0.05, ** p<0.01, *** p<0.001. ns refers to not significant (p>0.05).

heterogeneous. The majority of the colonies previously regarded to contain asymmetric fates (Figure 5.14C) showed an early death of both daughters in the following generation. Colonies in which both daughters were surviving showed a

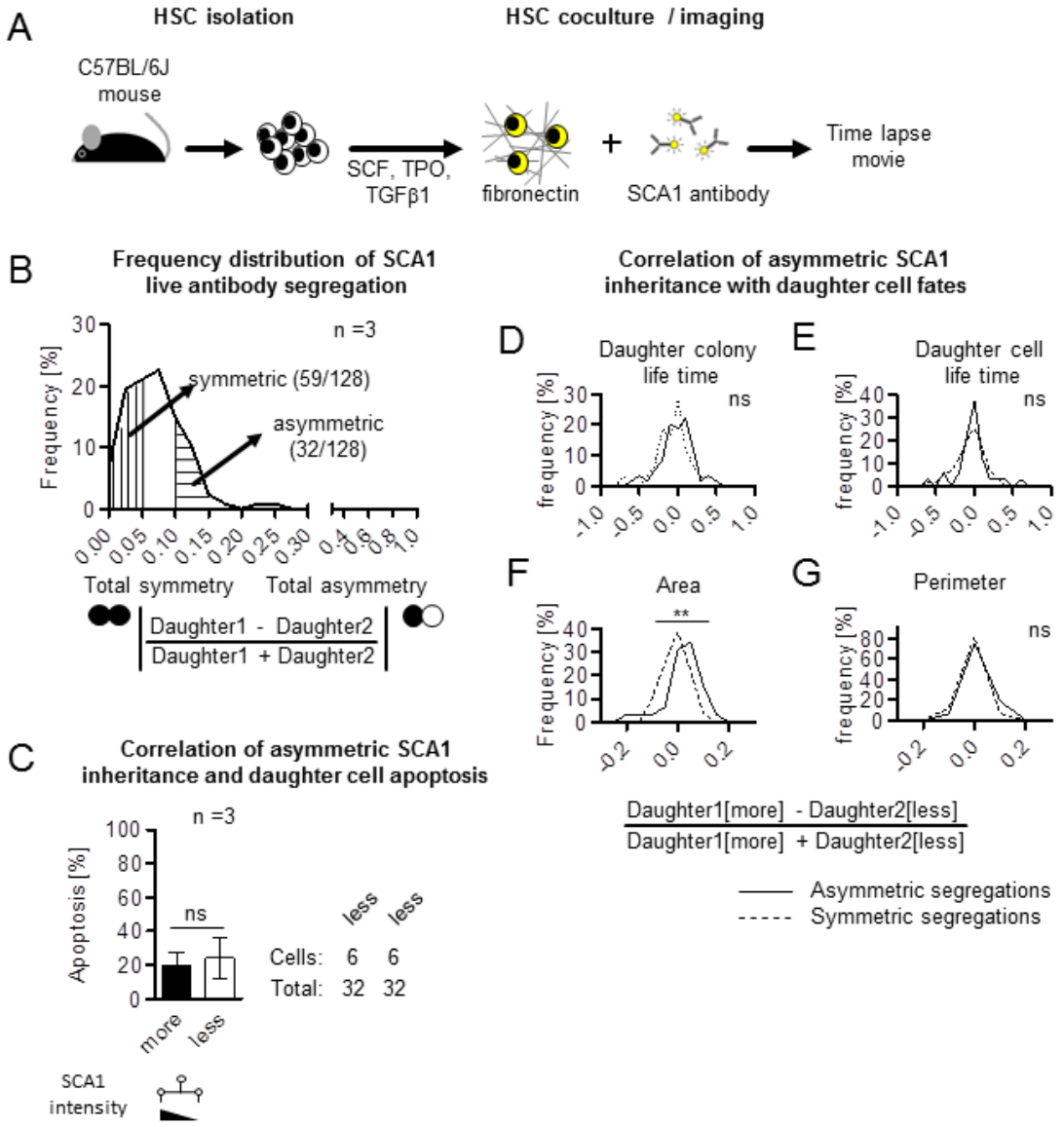

Figure 6.15: Asymmetric SCA1 inheritance does not correlate with TGFβ1 induced asymmetric apoptotic daughter cell fates

(A) To determine whether TGFβ1 induced asymmetric apoptotic cell fates correlate with the asymmetric inheritance of SCA1, HSCs were isolated and cultured in medium containing SCF, TPO and TGFβ1 on fibronectin supplemented by fluorescently tagged SCA1 antibody. (B) SCA1 inheritance during HSC divisions was quantified using the depicted formula and clustered into symmetric and asymmetric segregations based on arbitrary thresholds as indicated. (C) Asymmetric SCA1 inheritance does not influence the occurrence of apoptosis in HSC daughter cells (D-G) Asymmetric SCA1 inheritance does affect the daughter cell life or daughter colony life time and does not influence cell morphology (=perimenter), but correlates with daughter cell size or adherence (=area). Statistical results were calculated using one-tailed Mann-Whitney U test and are indicated with: * p<0.05, ** p<0.01, *** p<0.001. ns refers to not significant (p>0.05).

sudden cell death of all daughters just one generation further (Figure 5.14C). Since we do not know if the number of surviving generations or the absolute time of survival is of importance for cells, we defined asymmetric apoptotic genealogies as trees

where the absolute difference of the HSC daughter colony life time was bigger than 36h. Using this definition, HSCs cultured with TGFβ1 showed an increased frequency of asymmetric apoptotic fates (29 of 105 colonies) when compared to the control (9 of 116 colonies) (Figure 5.14D). However, neither daughter colony life time, daughter cell life time or daughter cell shape (=perimeter) correlated with the asymmetric segregation of SCA1 (Figure 5.15.D-G). Interestingly, as observed before when cultured in SCF/TPO, the SCA1 segregation positively correlates with the determined area of the daughter cells, demonstrating the cells receiving more SCA1 occupy a bigger area and might therefore either be bigger or more adherent (Figure 5.15F).

6.7 A quantitative differentiation assay as a reliable in vitro readout for lineage potential

So far we did not find a clear correlation between the asymmetric segregation of SCA1 and early differentiation events like the downregulation of SCA1 itself or the TGFβ1 induced apoptosis. Instead of being involved in controlling stemness we speculated that the asymmetric segregation might be involved in the regulation of lineage choice. Indeed, SCA1 has been suggested to be a negative regulator of erythropoiesis (Azalea-Romero et al., 2012; Chang et al., 2008). In order to test if the asymmetric segregation of SCA1 is associated with lineage choice we required culture conditions that would permit the differentiation into as many hematopoietic lineages as possible. Unfortunately, no culture condition promoting the differentiation into the entire hematopoietic system has been reported yet. However, liquid culture conditions supporting the differentiation of single HSCs into megakaryocytes, erythrocytes, granulocytes and macrophages have been described (Ema et al., 2006; Takano et al., 2004). These culture conditions have been successfully used to detect asymmetric lineage potential of HSC daughters separated via micromanipulation (Takano et al., 2004). However, the readout of this assay is based on May-Giemsa-Grünwald staining of colonies and the morphological classification of up to 1000 cells per colony by microscopy. Screening a bigger number of colonies is therefore not

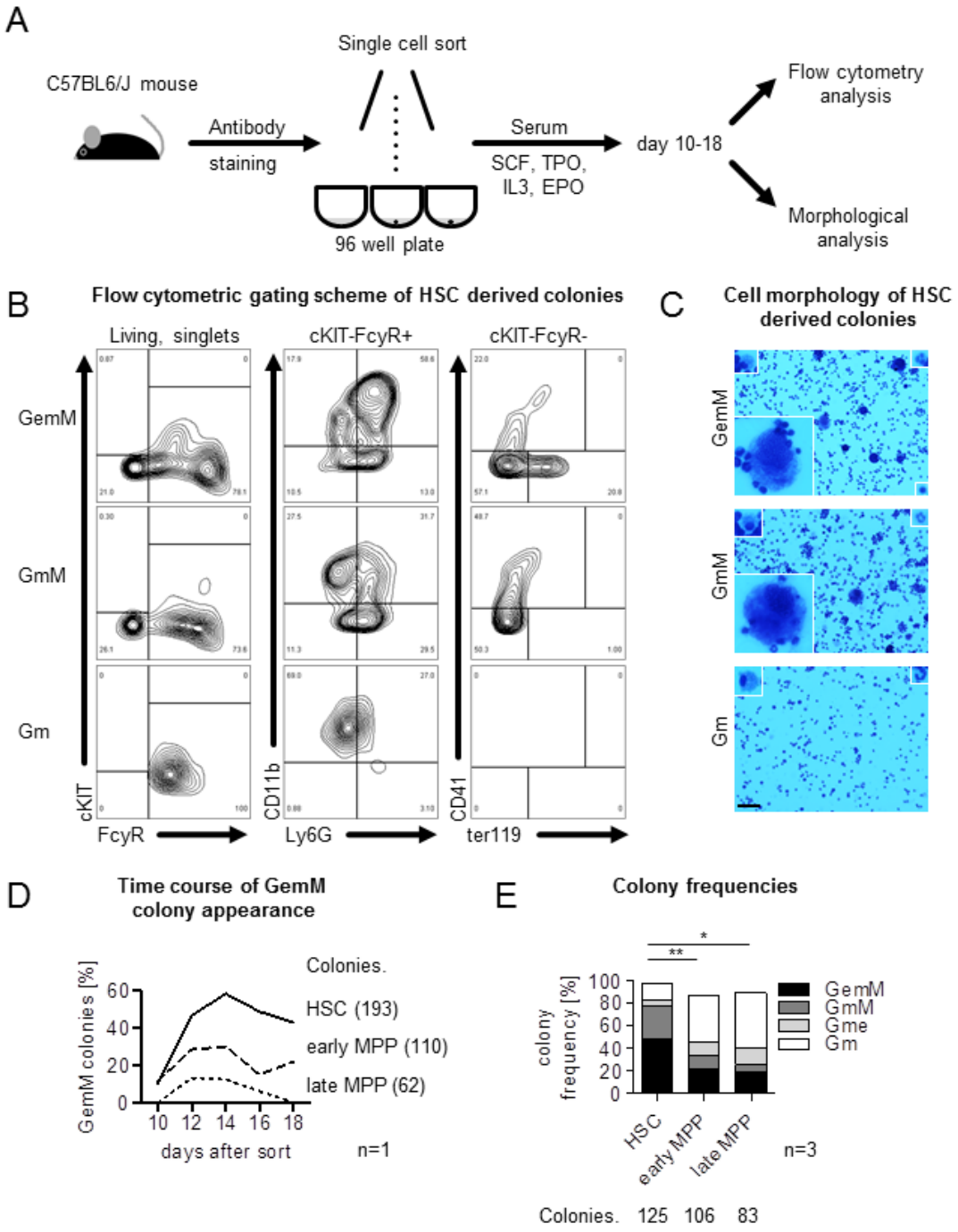

Figure 6.16: A quantitative, clonal differentiation assay to readout lineage potential

(A) HSCs were isolated, stained and sorted as single cells into 96 well plates and incubated for 10-18days in the indicated culture conditions in order to determine the lineage potential of the initially sorted cells by flow cytometry and/or morphological analysis. (B-C) Combinatorial analysis of 6 antibodies by flow cytometry (B) and morphological analysis by May-Giemsa Grünwald staining (C) of the same colonies give the same results. Scale bar: 200µm (D) Optimal time-point to readout multipotency (GemM potential) is day 14, as determined by time course and flow cytometric analysis. (E) Colony frequency generated by HSC, early and late MPPs determined by flow cytometry at day 14 resemble previously published frequencies determined by morphological analysis. Statistical results were calculated using two-tailed unpaired student´s t-test and are indicated with: * p<0.05, ** p<0.01, *** p<0.001. ns refers to not significant (p>0.05).

feasible in a reasonable amount of time. In addition to that is the morphological classification of hematopoietic cell types highly subjective and varies between individuals. Although this problem has been controlled for in the original publication by analyzing each colony by two individuals, the lineage contribution of the colonies was not analyzed quantitatively and potential lineage biases might have been missed.

We therefore needed to improve the throughput and sensitivity of this assay while simultaneously making the readout more objectively. Classical flow cytometry has been described to allow the simultaneous and quantitative measurement of up to 17 different markers and allows the analysis of thousands of cells within seconds (Perfetto et al., 2004). In order to test if we could reproduce the results of the original publication using a different readout we sorted single HSCs into 96 well plates and analyzed half of the generated colonies after 14 days by May-Giemsa-Grünwald staining and the other half with fluorescent labeled antibodies and flow cytometry (Figure 5.16A). Combinatorial analysis of 6 different antibodies by flow cytometry (Figure 5.16.B) showed a strong correlation with the morphological classification achieved by May-Giemsa-Grünwald staining (Figure 5.16C)). Based on these results we defined macrophages as $cKIT^{-}FcyR^{+}CD11b^{+}Ly6G^{-}$, granulocytes as $cKIT^{-}FcyR^{+}CD11b^{+}Ly6G^{+}$, megakaryocytes as $cKIT^{-}FcyR^{-}CD41^{+}TER119^{-}$ and erythrocytes as $cKIT^{-}FcyR^{-}CD41^{-}TER119^{+}$. Based on the presence of these 4 lineages the colonies were classified as GemM (G= Granulocytes, e= erythrocytes, m= macrophages, M= Megakaryocytes), GmM, Gm etc. However it should be mentioned that although megakaryocytes, macrophages and granulocytes were easily detectable by May-Giemsa-Grünwald staining we are not certain about the morphological classification used for erythrocytes. However, since the small cells detected in GemM colonies were not present in colonies classified as Gm and GmM we conclude that this population must represent cells of the erythroid lineage. Using this classification we determined the optimal time point for detection of GemM colonies (Figure 5.16D) and compared the different colony forming potentials between HSCs, early and late MPPs (Figure 5.17). GemM colony frequencies were comparable to what has been described in the literature (Takano et al., 2004) and the colony forming potential differed between HSCs, early and late MPPs as expected. Flow cytometric classification of colonies thus is able to reproduce the same data and

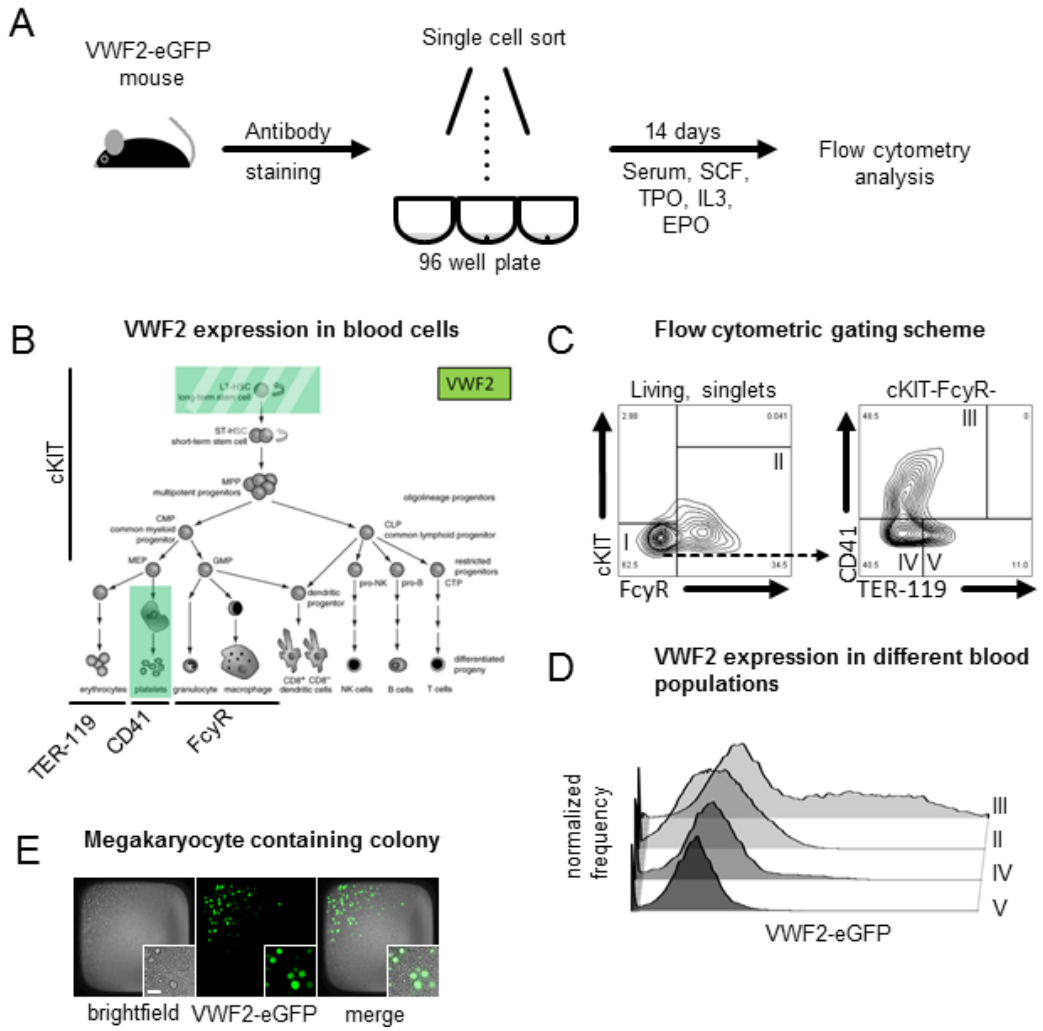

Figure 6.17: Validation of flow cytometric gating using a megakaryocyte reporter mouse.

(A) HSCs were isolated, stained and sorted as single cells into 96 well plates and incubated for 14days in the indicated culture conditions in order to determine whether the combinatorial usage of 6 antibodies recapitulates the expression pattern of a megakaryocyte reporter (VWF2-eGFP) mouse. (B) Classical hematopoietic hierarchy illustrating the expression of lineage marker used: VWF2-eGFP, cKIT, FcyR, CD41, TER-119. (C) Flow cytometric gating scheme used to identify megakaryocytes (D) VWF2-eGFP is expressed in putative megakaryocytes identified by combinatorial gating scheme, but absent in all other populations, demonstrating that Megakaryocytes can be detected reliably. (E) Representative fluorescence image of a single HSC derived megakaryocyte containing colony isolated from VWF2-eGFP mice. Megakaryocytes are recognizable by morphology and VWF2-eGFP expression.

can be used as a surrogate assay. In order to further validate that we can detect different hematopoietic lineages reliably, we repeated the analysis with sorted single HSCs derived from VWF-eGFP (Figure 5.17) and *Pu.1Yfp*/*Gata1mCherry* mice (Figure 5.18). Von Willebrand factor is a marker of the megakaryocytic lineage and should therefore be expressed in megakaryocytes (Figure 5.17B) identified by morphology as well immunophenotype

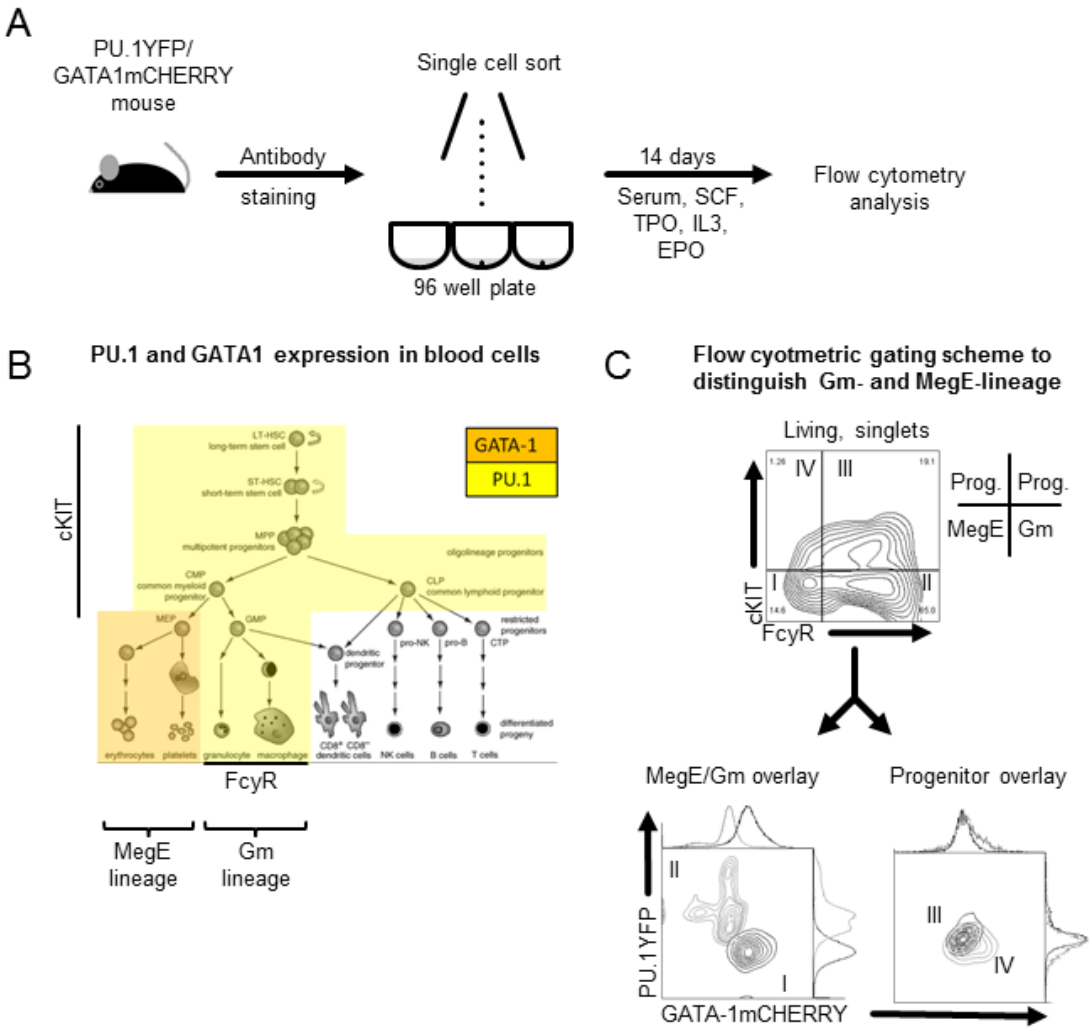

Figure 6.18: Validation of flow cytometric gating scheme using a Gm- and MegE-lineage reporter mouse.

(A) HSCs were isolated, stained and sorted as single cells into 96 well plates and incubated for 14days in the indicated culture conditions in order to determine whether the combinatorial usage of 6 antibodies recapitulates the expression pattern of a Gm- and MegE-lineage reporter (PU.1YFP/GATA1mCHERRY) mouse. (B) Classical hematopoietic hierarchy illustrating the expression of lineage marker used: PU.1, GATA1, FcyR, cKIT. (C) Putative Gm- and MegE-lineages (population I and II) are PU.1YFP^{+}/GATA1mCHERRY^{-} and PU.1YFP^{-}/GATA1mCHERRY^{+} respectively demonstrating that both lineages are detected reliably.

(Sanjuan-Pla et al., 2013). As expected, VWF-eGFP is expressed in cells of the cKIT^{-} FcyR^{-}CD41^{+}TER119^{-} population (Figure 5.17CIII and DIII), but not in erythrocytes (Figure 5.17CV and V) or cells of the granulocytic, macrophage lineage (Figure 5.17EII and DII). Also, morphologically recognizable megakaryocytes were VWF-eGFP positive (Figure 7E lower panel). However, it should be noted that only about 50% of all cKIT^{-}FcyR^{-}CD41^{+}TER119^{-} cells showed detectable levels of VWF-eGFP indicating that this marker combination is not sufficient to detect megakaryocytes with

100% purity.

PU.1 is a transcription factor expressed in B-cells as well as in cells of the granulocytic/macrophage lineage. GATA1 on the contrary is expressed on cells of the megakaryocytic/erythroid lineage (Figure 5.18B). All cells of the granulocytic/macrophage lineage are therefore $PU.1^{+}GATA1^{-}$ and cells of the megakaryocytic/erythroid lineage $PU.1^{-}GATA1^{+}$. Another hallmark of the granulocytic/macrophage lineage is the expression of the Fcγ receptor (FcγR). Megakaryocytes and erythrocytes on the other side are negative for this marker. If our gating scheme would reliably distinguish between the granulocytic/macrophage and the megakaryocyte/erythroid lineage, $cKIT^{-}Fc\gamma R^{+}CD11b^{+}Ly6G^{-}$ macrophages and $cKIT^{-}Fc\gamma R^{+}CD11b^{+}Ly6G^{+}$granulocytes would expected to be $PU.1^{+}GATA1^{-}$. Furthermore would we expect that $cKIT^{-}FcyR^{-}CD41^{+}TER119^{-}$ megakaryocytes and $cKIT^{-}FcyR^{-}CD41^{-}TER119^{+}$ erythrocytes are $PU.1^{-}GATA1^{+}$. Indeed, $Fc\gamma R^{+}$cKIT- cells are low or negative for GATA1mCHERRY (Figure 7F II and III) while PU.1YFP is expressed at intermediate or high levels (Figure 5.18C). $Fc\gamma R^{-}cKIT^{-}$ cells also express GATA1mCHERRY as expected, but are negative for PU.1YFP (Figure 5.18C). Cells positive for $cKIT^{+}$ are considered to be immature progenitors and are low or negative for PU.1 and GATA1. In summary, flow cytometric analysis of single cell derived colonies allows the reliable identification of myeloid blood lineages.

6.8 The asymmetric segregation of CTxB does not correlate with in vitro lineage potential

After the in vitro readout for lineage potential had been established we wanted to determine if HSCs would give rise to daughters with different lineage potential and if so, if we could correlate this with asymmetric segregations. Due to technical reasons we were using CTxB instead of SCA1 as an asymmetric segregation marker. As demonstrated before, SCA1 and CTxB colocalize strongly and cosegregate during symmetric and asymmetric segregations in vitro (Figure 5.8A-C). Instead of using micromanipulation we were separating the daughters by transferring manually half of the medium into two adjacent wells of a 1536 multi well plate, and visually confirming

the presence of only one sister, respectively. A total of 9216 putative HSC daughter cells were separated, quantified and analyzed by flow cytometry for the lineage potential in 7 independent experiments (Figure 5.19C). The theoretical maximum of successful separation of two daughter cells is ~33%. The divisional kinetics however dictate a narrow time window (36-50h after isolation) where the daughter separation can take place efficiently. At 36h after isolation, around 50% of the HSCs had already divided while the remaining ones would divide to a later time point and were therefore not available for successful daughter separation. This decreases the theoretical efficiency to successfully separate HSC daughters to ~16%. The time window for daughter separations is the limiting factor of this assay. Earlier separations will decrease the available HSC daughter pairs while later separations increase the likelihood for additional cell divisions of at least one of the separated daughters before the amount of CTxB in both daughters can be quantified. The latter as well as an expected cloning efficiency of 90% in these culture conditions further decrease the number of the theoretical successful separations. After the HSC daughters have been successfully separated the amount of CTxB was determined in 3 technical replicates (Figure 5.19B) and all data points with inconsistent quantification results were excluded from the analysis. Comparing the quantification results of two cells in two different wells is not trivial because a number of factors like, fluctuation of the fluorescence light source, differences in the illumination pattern etc. can influence the quantification result. However, comparing the distribution calculated for the daughter separation assay with the previously calculated distributions determined in time-lapse experiment suggests that our image correction minimizes these effects (compare Figure 5.19C with 5.15B and 5.12C). In order to determine if the asymmetric segregations of CTxB influences the differentiation potential of the HSC daughters, asymmetric (97 of 272) and symmetric (101 of 272) segregations were defined as described above (Figure 5.19C). The lineage contributions of a HSC daughter colony pairs were normalized using the depicted formula and pooled for asymmetrically and symmetrically segregating HSC. Since the values of symmetrically segregating HSCs are entered in a random fashion into the formula one would expect a gaussian distribution centered around 0. The values of asymmetrically segregating HSCs are

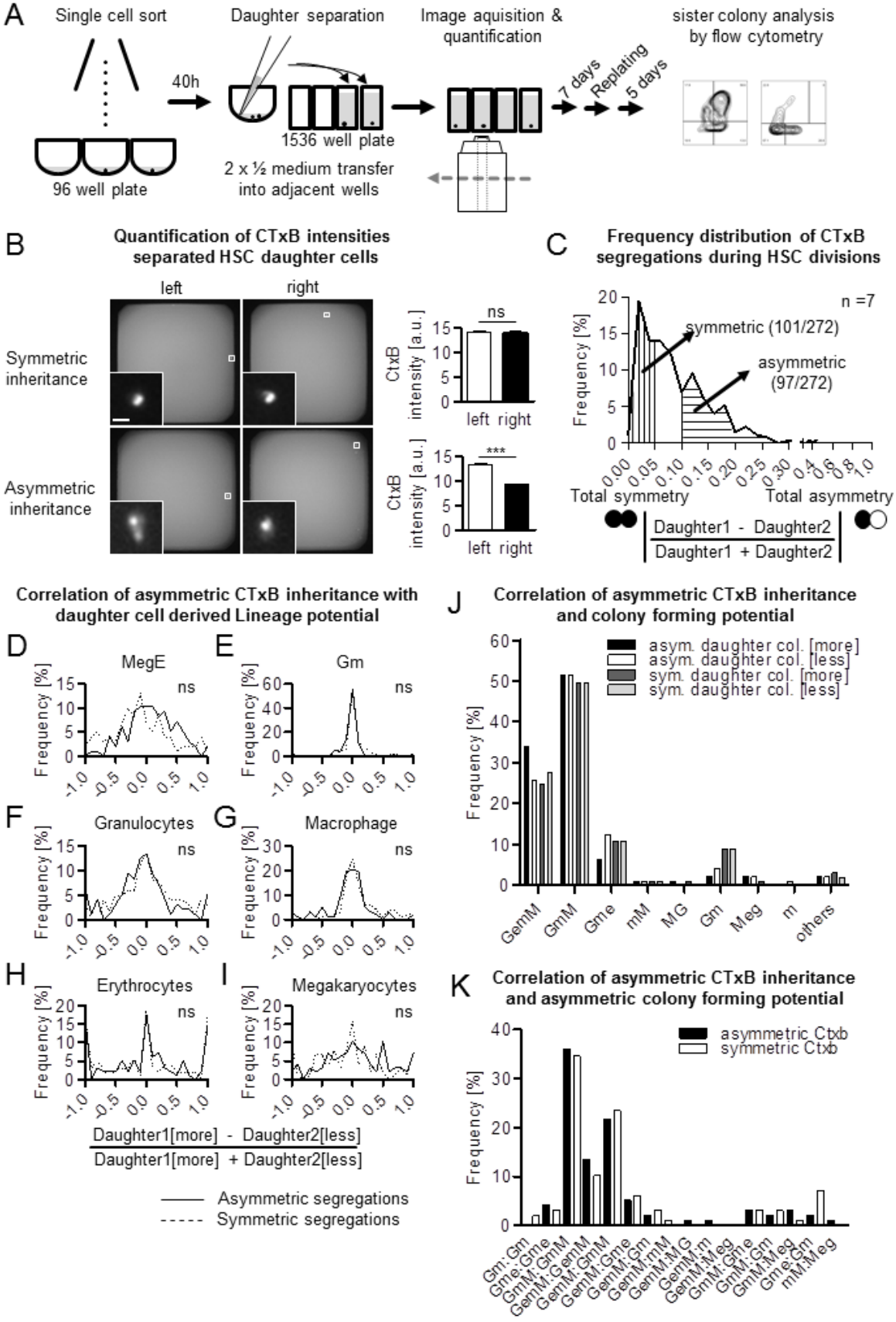

Figure 6.19: The asymmetric segregation of CTxB does not correlate with in vitro lineage potential.

(A) HSC daughters were manually separated, fluorescence images acquired, quantified and lineage

potential of sister colonies determined by flow cytometry. (B) Representative images and quantification of successfully separated HSC daughters were classified according to the calculated normalized sister intensity ratio as symmetric (top; int. 14.6 vs. 14) and asymmetric (bottom; CtxB int.13.8 vs. 9.4) segregation. Scale bar: 10µm. Two-tailed unpaired student´s t-test. (C) Frequency distributions of normalized sister CTxB intensity ratio were calculated using the depicted formula. (D-E) Asymmetric CTxB inheritance does not affect the lineage output of HSC daughter cells as determined by flow cytometric analysis. (J) The absolute colony forming potential is not affected by asymmetric inheritance of CTxB. (K) The number of asymmetric colony forming potential is not affected by CTxB inheritance. Statistical results were calculated using one-tailed Mann-Whitney U test and are indicated with: * $p<0.05$, ** $p<0.01$, *** $p<0.001$. ns refers to not significant ($p>0.05$).

entered into an ordered way according to the CTxB intensity of the colony and should deviate from the frequency distribution of the symmetric segregation if the lineage potential is influenced by the amount of CTxB inherited by the daughters. Neither the frequencies of granulocytes, macrophages, erythrocytes or megakaryocytes nor the overall frequencies of the megakaryocytic/erythrocytic (MegE) or granulocytic/macrophage (Gm) lineage of the HSC daughters are influenced by the asymmetric segregation of CTxB (Figure 5.19 D-I). This is also reflected in the overall frequencies of daughter colony types (Figure 5.19K) and the absolute colony frequencies generated by daughters receiving more or less CTxB (Figure 5.18J).

7 Discussion

7.1 The asymmetric segregation of proteins in highly purified, living HSCs can be observed and quantified in vitro

Hematopoietic stem cells are capable of maintaining their numbers while simultaneously giving rise to all cell types of the hematopoietic system lifelong. Based on findings in other model organisms it has been suggested that this is accomplished by a mechanism referred to as asymmetric cell division. According to the hypothesis, cell fate determinants are asymmetrically inherited by the HSC daughters and exert different cellular programs to induce asymmetric fates such as self-renewal or differentiation. The simplicity and elegance of this hypothesis has led to its general acceptance in the field. However, neither the asymmetric segregation of proteins nor their functional relevance has ever been demonstrated directly in living HSCs. In other words, the experimental evidence required to support this hypothesis has not been demonstrated.

In order to test this hypothesis we screened the behavior of a number of putative cell fate determinants during in vitro divisions of living HSCs using a novel quantitative bio imaging approach. We investigated if the first prerequisite of the asymmetric cell division hypothesis, the asymmetric inheritance of proteins, could be confirmed. In 4 out of 17 analyzed candidates we were able to detect evidence for asymmetric segregations as determined by fluorescence quantification and visual examination of time-lapse experiments (Figure 2C and D). One of these candidates, CD63 had previously been suggested to segregate asymmetrically during in vitro divisions of human umbilical cord blood derived $CD34^{+}CD133^{+}$ cells as determined by immunofluorescence analysis of fixed cells (Beckmann et al., 2007). However, since the HSC purity of this population is smaller than 1% (Drake et al., 2011), it is unclear if and to what extend this segregation actually occurs in human HSCs. The other asymmetrically segregating proteins, namely SCA1, VANGL2 and LAMP1 have recently been described also by others to be highly polarized themselves or to be part of highly polarized complexes in hematopoietic cells, but their segregation during

HSC divisions has never been analyzed before (Sugimura et al., 2012; Thaunat et al., 2012; Vannini et al., 2012a). Since the screen to identify asymmetrically segregating proteins was based on lentiviral delivery of fluorescence reporter fusion proteins, the observed effects could be the result of overexpression. Although we cannot entirely exclude this possibility for CD63, VANGL2 and LAMP1 the occurrence of an overexpression artifact is unlikely given that we were able to reproduce the observed asymmetric segregations of SCA1VENUS when endogenous SCA1 was labeled by live antibody staining (Figure 3C, E, F and 5G). Although live antibody staining of the other asymmetrically segregating candidates did not work, we conclude from the observations made using SCA1 antibodies that the overexpression of fluorescence reporters does not necessarily induce artifacts resembling asymmetric segregations. This is further supported by the observation that 8 out of 17 overexpressed candidates did not show any signs of asymmetric segregation (Figure 2C).

We therefore demonstrate, to our knowledge for the first time, that CD63, VANGL2, SCA1 and LAMP1 are asymmetrically segregating during in vitro divisions of highly purified, living HSCs. Besides that, this is the first report analyzing HSC divisions quantitatively over time, allowing us to use objective criteria rather than the previously applied qualitative assessments to classify asymmetric and symmetric segregations.

Although we did not see convincing evidence for the asymmetric segregation of the remaining candidates we cannot exclude the possibility of their asymmetric inheritance when expressed at endogenous protein levels or in different microenvironments. It is possible that the cellular sorting machinery has been overloaded by the overexpression of the fusion proteins and that putative asymmetries were masked. Indeed, TGFβRI, CD53, Msi2, Prominin1 and Numb fusion proteins demonstrated, based on the quantification of HSC daughter fluorescence intensities, a slight but significant tendency to be inherited more unequally when compared to the control (Figure 2C). However, since these results could not be confirmed by the visual examination of the cell divisions we did not consider them to be asymmetric. It is anyways interesting to note that CD53, Prominin1 and Numb have previously been suggested to segregate asymmetrically (Beckmann et al., 2007; Lathia et al., 2011; Wu et al., 2007a). Especially whether NUMB, a widely accepted cell fate determinant in other model organisms, is

asymmetrically segregating in HSCs, is still highly controversial. Our results confirm a recently conducted study that did not see a clear asymmetric segregation of NUMB when overexpressed as a mCHERRY fusion (Ting et al., 2012). However, an older study suggested its asymmetric segregation by analyzing fixed cells via immunofluorescence microscopy (Wu et al., 2007b). It is therefore possible, as mentioned above, that the actual overexpression of proteins is masking potential asymmetric segregations by overloading the cell. Alternatively, the use of the microtubli depolymerization agent nocodazole in the latter study might have introduced artifacts as well. Indeed, nocodazole has recently been shown to be inappropriate to study the asymmetric segregation of proteins due to its effects on the positioning of centrosomes and its overall cytotoxicity (Nteliopoulos and Gordon, 2012). Regardless, given that the future daughter fates of fixed cells cannot be analyzed, it is not possible to demonstrate the functional relevance of any putative asymmetric segregation directly by using this technique. It is therefore likely that this issue will not be solved until a fluorescently tagged NUMB knock-in mouse line is available for analysis.

7.2 Asymmetric segregation of candidate proteins is regulated by secreted growth factors and not influenced by the microenvironment

It has previously been suggested that the asymmetric segregation of proteins during HSC divisions is influenced by the microenvironment (Ting et al., 2012; Wu et al., 2007b). However, we did not find evidence that this is true for CD63, SCA1, LAMP1 or VANGL2 (Figure 3A). No detectable changes in asymmetric segregation frequencies could be observed for HSCs cultured on OP9 stromal cells, on the extra cellular matrix protein fibronectin or on glass. The comparison with early and late MPPs, populations committed to differentiation, demonstrated that the asymmetric segregations are not restricted to the HSC compartment. This suggests that the underlying mechanism is a common feature of hematopoietic cells and is not based on a specialized interaction between HSCs and the niche. The observation that different cytokine cocktails alter the asymmetric segregation frequencies of

endogenous SCA1 (Figure 4F) demonstrates, that secreted growth factors, rather than cell-cell or cell-matrix mediated signals are responsible for the observed asymmetric segregations. We therefore conclude that the observed asymmetric segregations are controlled extrinsically.

Although we do not see evidence for a cell-cell contact mediated control of the asymmetric segregations of CD63, SCA1, LAMP1 or VANGL2 we cannot exclude this possibility when different culture conditions are used. That VENUS expressing HSCs show a higher degree of unequal inheritance during HSC divisions when cultured on OP9 stromal cells compared to fibronectin or glass might be indicative of a potential influence mediated by cell-cell contacts (Figure 3A). However, this effect does not seem to influence the asymmetric segregation of CD63, SCA1, LAMP1 and VANGL2 and its implications are unclear.

7.3 Lysosomal like compartments are asymmetrically segregating and are equivalent to CTxB labeled lipid raft cluster

That different cytokines can either induce or decrease the polarity of HSCs has recently been demonstrated by measuring the formation of lipid raft clusters by staining of living hematopoietic cells with fluorescently labeled Cholera Toxin B (Vannini et al., 2012b). Although this study did not determine the behavior of lipid raft clusters during the in vitro divisions of HSCs, it demonstrated that SCA1 is able to form similar clusters upon cytokine stimulation, implying that the asymmetric segregation of SCA1 detected by us and the formation of lipid raft clusters might be associated. SCA1, as well as CD63, VANGL2 and LAMP1 colocalize with the lipid raft marker CTxB and are present in clusters in cytokine stimulated, living HSCs (Figure 4A and C), suggesting a common localization and mechanism for the asymmetric segregation of these proteins. Although the colocalization of SCA1 and CTxB was expected, the localization of CD63, LAMP1 and VANGL2 in lipid rafts had not been reported before. Since CD63 and LAMP1 are known to be enriched in the lysosomal membrane we tested their colocalization with a commonly used marker for

acidified organelles, LysoTracker Red, demonstrating that not only CD63 and LAMP1, but also SCA1 and VANGL2 are located in lysosomes. Taken together the presented data suggests that CD63, VANGL2, SCA1 and LAMP1 accumulate and colocalize in lysosomes (Figure 4D) which are asymmetrically segregating during HSC divisions (Figure 2D and 4E). Furthermore we demonstrated that Cholera Toxin B, a commonly used marker for lipid rafts is accumulating in lysosomes of activated HSCs, and that so called lipid raft clusters might actually reflect its transport to this compartment upon internalization. The internalization of Cholera Toxin B and its delivery to lysosomes has been reported before (Ewers and Helenius, 2011; te Vruchte et al., 2010) but the exact nature of these clusters has never been investigated in hematopoietic stem and progenitor cells. The concept of lipid raft cluster formation is based on studies of T-cell receptor signaling and the formation of the immunological synapse (Miceli et al., 2001; Yamazaki et al., 2006) and has been applied to the activation of quiescent HSC given that similar clusters have been observed (Yamazaki et al., 2006). However, the colocalization with lysosomal markers strongly suggests that the observed CTxB clusters in activated HSPCs are in fact lysosomes. A thorough reanalysis and reinterpretation of the published literature of lipid raft cluster formation in HSCs will therefore be required.

7.4 Lysosomes - more than the cellular trash bin

Lysosomes are classically considered to be the terminal degradative compartments for molecules derived from the extracellular space via endocytosis or from intracellular sources via autophagy (Kornfeld and Mellman, 1989). However, an accumulating body of evidence suggests that lysosomes are more than the cellular “trash bin”.

Lysosomes have been described to be a major regulator of apoptosis. The lysosomal pathway of apoptosis can be activated by death receptors, lipid mediators and photo damage. Upon its activation, the lysosomal membrane is permeabilized and proteases are released into the cytoplasm to contribute to the apoptotic cascade upstream of mitochondria (Guicciardi et al., 2004). Interestingly, lysosomal accumulation of cholesterol has recently been described to stabilize the lysosomal

membrane in neurons to protect the cells from oxidative stress induced apoptosis (Appelqvist et al., 2012). In addition, autophagy, another closely related branch of the degradative pathways, has recently been shown to be required for the survival of HSCs under metabolic stress (Warr et al., 2013).

Beside their role in regulating apoptosis, lysosomes were recently shown to be involved in signal transduction. In the presence of nutrients the Transcription Factor EB (TFEB) colocalizes with the master growth regulator mTOR complex 1 (mTORC1) on the lysosomal membrane. Upon starvation and lysosomal disruption TFEB is activated and translocates to the nucleus to induce the transcription of genes involved in autophagy, lysosomal biogenesis and starvation response (Settembre et al., 2012). Another study reported that a C-terminal lysosomal sorting motif is required for proper NOTCH activation in HeLa cells (Zheng et al., 2013). And that the lysosomal inhibitors bafilomycin (Baf) and glycyl-L-phenylalanine-β-naphthylamide (GPN) are able to block the FasL-induced formation of lipid raft clusters has been shown in coronary artery endothelial cells (CAEC) cells (Jin et al., 2007).

It is surprising how little is known about the role of lysosomes in HSPCs. Although studies demonstrating that lysosomes exceed their previously recognized function as the terminal degradative compartment have not been conducted in HSPCs yet, it is possible that similar mechanisms participate in the regulation of hematopoietic cells as well. The discovery that HSCs exert a pro-autophagy gene program demonstrates that the degradative compartment is critical for the regulation of HSCs (Warr et al., 2013).

7.5 The functional relevance of asymmetrically segregating lysosomes remains unclear.

Although the asymmetric segregation of proteins is indicative of an underlying mechanism used by HSCs, it is not sufficient to demonstrate asymmetric cell division as long as its functional implications (correlating asymmetric daughter cell fates) have not been demonstrated (Horvitz and Herskowitz, 1992; Morrison and Spradling, 2008). Several studies have reported either directly or indirectly the occurrence of

asymmetric HSC daughter cell fates (Ema et al., 2000a; Noda et al., 2008; Takano et al., 2004; Yamazaki et al., 2009). Based on these reports, three different in vitro readouts were established and adapted in ways that allowed us to use them in quantitative time-lapse microscopy (Figure 5-8). Two of these readouts were based on early detectable differentiation events as measured by the loss of the stem cell marker SCA1 or the TGFβ1 mediated apoptosis of differentiated cells. The third readout was supposed to detect putative influences on the lineage choice during long-term differentiation in permissive culture conditions. Although we were able to successfully detect the expected asymmetric fates in all three readouts (Figure 5F, 6F-G and 8K) we were not able to find a clear correlation with the observed asymmetric segregations of SCA1 or CTxB (Figure 5, 6 and 8). Neither the lineage choice, the TGFβ1 induced apoptosis nor the SCA1 offset were influenced by the asymmetric segregation. Since we demonstrated that SCA1 and CTxB accumulate in the degradative compartment over time (see section 7.3) they are used as surrogate markers and their asymmetric inheritance can be interpreted as the asymmetric segregation of lysosomes. We therefore conclude that lysosomes are not directly associated with the regulation of differentiation and lineage choice in the culture conditions used in this study. However, we cannot exclude the possibility that the asymmetric segregation of lysosomes has functional relevance in other culture conditions. That different cytokine cocktails alter the frequency of the observed asymmetric segregations suggests that the lysosomal inheritance is an actively controlled process instead of a random event. It is interesting to note that the combination of cytokines with opposing functions seems to increase the frequency of asymmetric segregation. While TGFβ1 is considered to be an inhibitory cytokine promoting the quiescence of HSCs, IL3 has been known for its ability to induce proliferation (Takano et al., 2004; Vannini et al., 2012b; Yamazaki et al., 2009). Although we can currently not generalize this observation it will be interesting to see if this is true for other cytokines as well.

7.6 Conclusions, critical points and future perspective

HSCs are able to give rise to daughters with equal (symmetric) or unequal (asymmetric) cell fates. If these cell fate decision are made during cell divisions or by post mitotic events is not well understood. We conducted this study to clarify this issue by testing for the first prerequisite of the asymmetric cell division hypothesis, the asymmetric inheritance of cell fate determinants.

As predicted by the hypothesis we were able to identify several asymmetrically segregating proteins. Although this had been suggested before (Beckmann et al., 2007; Ting et al., 2012; Wu et al., 2007a), we are providing for the first time quantitative evidence that this is happening in highly purified, living HSCs at endogenous protein levels. Furthermore could we demonstrate that asymmetric inheritance of these proteins is based on their accumulation in lysosomes. We also demonstrated that our approach, in contrast to previous studies, can be used to directly test the correlation of asymmetric protein segregations to future asymmetric daughter cell fates.

However, the asymmetric segregations detected in this study do not seem to be involved in the regulation of HSC differentiation or lineage choice. We are therefore currently not able to provide the experimental evidence required to demonstrate that HSCs utilize asymmetric cell divisions to regulate cell fate decisions. However, the possibility that HSC fate decisions are controlled by asymmetric cell divisions also cannot be excluded. Besides the possibility that there is simply no correlation between the asymmetric segregation of lysosomes and the investigated asymmetric daughter cell fates the elusive functional correlation might be related to a variety of either technical or biological reasons which are discussed below.

(1) Instead of being involved in the regulation of differentiation and lineage choice, the asymmetric segregation of lysosomes might affect alternative cell fate decisions that have not been addressed in this study. Although a variety of alternative cell fate decisions can be analyzed, the recently reported importance of autophagy for the HSC survival under starvation conditions might provide hints for the functional

relevance of asymmetrically inherited lysosomes (Warr et al., 2013). Based on the assumption that the degradative compartment exerts pro survival effects, its asymmetric segregation during division might provide the daughter receiving the lysosome an advantage when external sources of nutrients are limited. Alternatively, the asymmetric segregation of cellular trash contained within lysosomes might lead to the rejuvenation of one daughter while “toxic” proteins are accumulating in the other. A similar mechanism has been reported for the aggresome, an aggregate of misfolded proteins (Lerit et al., 2013). If the asymmetric inheritance of the lysosome would reduce the “fitness” of one daughter one would expect an increased apoptosis rate in daughters receiving the lysosome over several rounds of asymmetric segregation.

(2) Although other asymmetric fates might reveal the functional relevance of the asymmetric segregation the absence of correlation might also be explained by the lack of polarized cues from the microenvironment. It is possible that the asymmetric segregation of lysosomes alone, although necessary, is not sufficient to establish stable asymmetric fates by itself. The daughter cells would therefore be merely primed to acquire asymmetric fates, but the acquisition of these fates manifested by different environmental cues. Since the in vitro environment in our culture conditions does not provide different environmental cues, initially different daughter cells are exposed to the same microenvironment and might therefore be prone to acquire the same fate. The asymmetric fates observed in our cultures would in this model be explained by stochastic fluctuations. Similar systems have been described before and involve the regulated spindle orientation upon stem cell divisions (Lerit et al., 2013; Morrison and Spradling, 2008). GSC in Drosophila´s testis are attached to the hub, specialized niche cells ensuring the maintenance of stem cells by localized unpaired signaling. Upon division the regulated spindle orientation at the hub/GSC ensures that one daughter is displaced from the niche and ends up in a different signaling environment, determining its fate. Based on the observation that the mother centrosome is associated with the GSC-hub cortex interface and is retained by the stem cell we speculate that if similar mechanisms are utilized by HSCs one would expect that the asymmetric segregation of lysosomes should correlate with the segregation of mother or daughter centrosome. Furthermore would we expect that the introduction of localized signals (i.e. cytokine or antibody labeled beads) should lead to a directed segregation of lysosomes (i.e. into the cell touching the bead) if

HSC utilize mechanisms dependent on the controlled displacement of daughter cells by the regulated spindle orientation during divisions.

(3) A third explanation is based on the observations that lysosomes are involved in antigen processing and presentation to cells of the immune system (Hsing and Rudensky, 2005). Indeed, asymmetric segregation of antigens during B-Cell division has recently been reported and functionally linked to their capacity to activate T-cells (Thaunat et al., 2012). Interestingly, the antigens in this study colocalized with compartments positive for the lysosomal marker LAMP1 as well as the major histocompatibility complex 2 (MHC-II). It is therefore possible that effects mediated by the asymmetric segregation of lysosomes in HSCs do not affect the HSCs or their progeny but act by modulating the activity of cells of the immune system. If this would be true one would expect that lysosomes receiving daughters are able to induce the proliferation of immune cells more efficiently than their sisters. However, HSCs have not been reported to function as antigen presenting cells and the expression of MHC-II has not been demonstrated. It is anyways interesting to note that MHC-I has been shown to be involved in the engraftment of HSCs after transplantation (Huang et al., 2004).

In order to clarify the functional implications of the asymmetric inheritance of lysosomes we are planning to address the above mentioned alternative explanations in future experiments. Continuous, quantitative imaging of dividing HSPCs under starvation conditions, in culture with antibody or cytokine labeled beads or in coculture with naive T-cells should allow us to determine whether these processes are related to lysosome segregation or not. The combination of quantitative time-lapse imaging and classical single snap shot analysis after fixation might also provide valuable insights. Using antibodies specific for phosphorylation events might reveal changes in the activation status of certain signaling cascades and its relation to lysosome segregation. Analyzing whether lysosomes cosegregate with either the mother or daughter centrosomes is also of interest. Furthermore do we want to test what happens to the lysosome associated transcription factor TFEB during the asymmetric inheritance of lysosomes. In addition to that do we want to test if additional functional assays to determine HSC potential such as the LTC-IC or single daughter cells transplantations correlate with the observed asymmetric segregations.

8 References

Adolfsson, J., Borge, O.J., Bryder, D., Theilgaard-Mönch, K., Astrand-Grundström, I., Sitnicka, E., Sasaki, Y., and Jacobsen, S.E. (2001). Upregulation of Flt3 expression within the bone marrow Lin(-)Sca1(+)c-kit(+) stem cell compartment is accompanied by loss of self-renewal capacity. Immunity *15*, 659–669.

Akashi, K. (2009). Lymphoid lineage fate decision of hematopoietic stem cells. Annals Of The New York Academy Of Sciences *1176*, 18–25.

Akashi, K., Traver, D., Miyamoto, T., and Weissman, I.L. (2000). A clonogenic common myeloid progenitor that gives rise to all myeloid lineages. Nature *404*, 193–197.

Akashi, K., He, X., Chen, J., Iwasaki, H., Niu, C., Steenhard, B., Zhang, J., Haug, J., and Li, L. (2003). Transcriptional accessibility for genes of multiple tissues and hematopoietic lineages is hierarchically controlled during early hematopoiesis. Blood *101*, 383–389.

Alexander, W.S., Roberts, a W., Nicola, N. a, Li, R., and Metcalf, D. (1996). Deficiencies in progenitor cells of multiple hematopoietic lineages and defective megakaryocytopoiesis in mice lacking the thrombopoietic receptor c-Mpl. Blood *87*, 2162–2170.

Appelqvist, H., Sandin, L., Björnström, K., Saftig, P., Garner, B., Ollinger, K., and Kågedal, K. (2012). Sensitivity to lysosome-dependent cell death is directly regulated by lysosomal cholesterol content. PloS One *7*, e50262.

Arai, F., Hirao, A., Ohmura, M., Sato, H., Matsuoka, S., Takubo, K., Ito, K., Koh, G.Y., and Suda, T. (2004). Tie2/angiopoietin-1 signaling regulates hematopoietic stem cell quiescence in the bone marrow niche. Cell *118*, 149–161.

Avecilla, S.T., Hattori, K., Heissig, B., Tejada, R., Liao, F., Shido, K., Jin, D.K., Dias, S., Zhang, F., Hartman, T.E., et al. (2004). Chemokine-mediated interaction of hematopoietic progenitors with the bone marrow vascular niche is required for

thrombopoiesis. Nature Medicine *10*, 64–71.

Azalea-Romero, M., González-Mendoza, M., Cáceres-Pérez, A.A., Lara-Padilla, E., and Cáceres-Cortés, J.R. (2012). Low expression of stem cell antigen-1 on mouse haematopoietic precursors is associated with erythroid differentiation. Cellular Immunology *279*, 187–195.

Bakstad, D., Adamson, A., Spiller, D.G., and White, M.R.H. (2012). Quantitative measurement of single cell dynamics. Current Opinion in Biotechnology *23*, 103–109.

Beckmann, J., Scheitza, S., Wernet, P., Fischer, J.C., and Giebel, B. (2007). Asymmetric cell division within the human hematopoietic stem and progenitor cell compartment: identification of asymmetrically segregating proteins. Blood *109*, 5494–5501.

Benveniste, P., Frelin, C., Janmohamed, S., Barbara, M., Herrington, R., Hyam, D., and Iscove, N.N. (2010). Intermediate-term hematopoietic stem cells with extended but time-limited reconstitution potential. Cell Stem Cell *6*, 48–58.

Berdnik, D., Török, T., González-Gaitán, M., and Knoblich, J. a (2002). The endocytic protein alpha-Adaptin is required for numb-mediated asymmetric cell division in Drosophila. Developmental Cell *3*, 221–231.

Bergeland, T., Widerberg, J., Bakke, O., and Nordeng, T.W. (2001). Mitotic partitioning of endosomes and lysosomes. Current Biology : CB *11*, 644–651.

Blackett, N.M., Necas, E., and Frindel, E. (1986). Diversity of haematopoietic stem cell growth from a uniform population of cells. Nature *322*, 289–290.

Boussif, O., Lezoualc'h, F., Zanta, M.A., Mergny, M.D., Scherman, D., Demeneix, B., and Behr, J.P. (1995). A versatile vector for gene and oligonucleotide transfer into cells in culture and in vivo: polyethylenimine. Proceedings of the National Academy of Sciences of the United States of America *92*, 7297–7301.

Bradfute, S.B., Graubert, T. a, and Goodell, M. a (2005). Roles of Sca-1 in hematopoietic stem/progenitor cell function. Experimental Hematology *33*, 836–843.

Bryder, D., Rossi, D.J., and Weissman, I.L. (2006). Hematopoietic stem cells: the paradigmatic tissue-specific stem cell. The American Journal of Pathology *169*, 338–346.

Calvi, L.M., Adams, G.B., Weibrecht, K.W., Weber, J.M., Olson, D.P., Knight, M.C., Martin, R.P., Schipani, E., Divieti, P., Bringhurst, F.R., et al. (2003). Osteoblastic cells regulate the haematopoietic stem cell niche. Nature *425*, 841–846.

Camargo, F.D., Chambers, S.M., Drew, E., McNagny, K.M., and Goodell, M. a (2006). Hematopoietic stem cells do not engraft with absolute efficiencies. Blood *107*, 501–507.

Carmena, a, Murugasu-Oei, B., Menon, D., Jiménez, F., and Chia, W. (1998). Inscuteable and numb mediate asymmetric muscle progenitor cell divisions during Drosophila myogenesis. Genes & Development *12*, 304–315.

Carver-Moore, K., Broxmeyer, H.E., Luoh, S.M., Cooper, S., Peng, J., Burstein, S. a, Moore, M.W., and de Sauvage, F.J. (1996). Low levels of erythroid and myeloid progenitors in thrombopoietin-and c-mpl-deficient mice. Blood *88*, 803–808.

Lo Celso, C., Fleming, H.E., Wu, J.W., Zhao, C.X., Miake-Lye, S., Fujisaki, J., Côté, D., Rowe, D.W., Lin, C.P., and Scadden, D.T. (2009). Live-animal tracking of individual haematopoietic stem/progenitor cells in their niche. Nature *457*, 92–96.

Challen, G. a, Boles, N.C., Chambers, S.M., and Goodell, M. a (2010). Distinct hematopoietic stem cell subtypes are differentially regulated by TGF-beta1. Cell Stem Cell *6*, 265–278.

Chambers, I., Silva, J., Colby, D., Nichols, J., Nijmeijer, B., Robertson, M., Vrana, J., Jones, K., Grotewold, L., and Smith, A. (2007). Nanog safeguards pluripotency and mediates germline development. *450*, 3–8.

Chang, H.H., Hemberg, M., Barahona, M., Ingber, D.E., and Huang, S. (2008a). Transcriptome-wide noise controls lineage choice in mammalian progenitor cells. Nature *453*, 544–547.

Chang, H.H., Hemberg, M., Barahona, M., Ingber, D.E., and Huang, S. (2008b).

Transcriptome-wide noise controls lineage choice in mammalian progenitor cells. Nature *453*, 544–547.

Chang, J.T., Palanivel, V.R., Kinjyo, I., Schambach, F., Intlekofer, A.M., Banerjee, A., Longworth, S. a, Vinup, K.E., Mrass, P., Oliaro, J., et al. (2007). Asymmetric T lymphocyte division in the initiation of adaptive immune responses. Science (New York, N.Y.) *315*, 1687–1691.

Chang, J.T., Ciocca, M.L., Kinjyo, I., Palanivel, V.R., McClurkin, C.E., Dejong, C.S., Mooney, E.C., Kim, J.S., Steinel, N.C., Oliaro, J., et al. (2011). Asymmetric proteasome segregation as a mechanism for unequal partitioning of the transcription factor T-bet during T lymphocyte division. Immunity *34*, 492–504.

Cho, R.H., and Müller-Sieburg, C.E. (2000). High frequency of long-term culture-initiating cells retain in vivo repopulation and self-renewal capacity. Experimental Hematology *28*, 1080–1086.

Chow, A., Lucas, D., Hidalgo, A., Méndez-Ferrer, S., Hashimoto, D., Scheiermann, C., Battista, M., Leboeuf, M., Prophete, C., van Rooijen, N., et al. (2011). Bone marrow CD169+ macrophages promote the retention of hematopoietic stem and progenitor cells in the mesenchymal stem cell niche. The Journal of Experimental Medicine *208*, 261–271.

Conklin, E. (1905). The Organization and Cell-Lineage of the Ascidian Egg. J Acad Nat Sci Phila 1–119.

Coumailleau, F., Fürthauer, M., Knoblich, J. a, and González-Gaitán, M. (2009). Directional Delta and Notch trafficking in Sara endosomes during asymmetric cell division. Nature *458*, 1051–1055.

Couturier, L., Vodovar, N., and Schweisguth, F. (2012). Endocytosis by Numb breaks Notch symmetry at cytokinesis. Nature Cell Biology *14*, 131–139.

Cowan, C.R., and Hyman, A. a (2004). Asymmetric cell division in C. elegans: cortical polarity and spindle positioning. Annual Review of Cell and Developmental Biology *20*, 427–453.

Deneault, E., Cellot, S., Faubert, A., Laverdure, J.-P., Fréchette, M., Chagraoui, J., Mayotte, N., Sauvageau, M., Ting, S.B., and Sauvageau, G. (2009). A functional screen to identify novel effectors of hematopoietic stem cell activity. Cell *137*, 369–379.

Ding, L., Saunders, T.L., Enikolopov, G., and Morrison, S.J. (2012). Endothelial and perivascular cells maintain haematopoietic stem cells. Nature *481*, 457–462.

Dittrich W., G.W. (1971). FLOW-THROUGH CHAMBER FOR PHOTOMETERS TO MEASURE AND COUNT PARTICLES IN A DISPERSION MEDIUM (Dittrich W., Goehde W.).

Drake, A.C., Khoury, M., Leskov, I., Iliopoulou, B.P., Fragoso, M., Lodish, H., and Chen, J. (2011). Human CD34+ CD133+ hematopoietic stem cells cultured with growth factors including Angptl5 efficiently engraft adult NOD-SCID Il2rγ-/- (NSG) mice. PloS One *6*, e18382.

Duncan, A.W., Rattis, F.M., DiMascio, L.N., Congdon, K.L., Pazianos, G., Zhao, C., Yoon, K., Cook, J.M., Willert, K., Gaiano, N., et al. (2005). Integration of Notch and Wnt signaling in hematopoietic stem cell maintenance. Nature Immunology *6*, 314–322.

Dykstra, B., Ramunas, J., Kent, D., McCaffrey, L., Szumsky, E., Kelly, L., Farn, K., Blaylock, A., Eaves, C., and Jervis, E. (2006). High-resolution video monitoring of hematopoietic stem cells cultured in single-cell arrays identifies new features of self-renewal. Proceedings of the National Academy of Sciences of the United States of America *103*, 8185–8190.

Dykstra, B., Kent, D., Bowie, M., McCaffrey, L., Hamilton, M., Lyons, K., Lee, S.-J., Brinkman, R., and Eaves, C. (2007a). Long-term propagation of distinct hematopoietic differentiation programs in vivo. Cell Stem Cell *1*, 218–229.

Dykstra, B., Kent, D., Bowie, M., McCaffrey, L., Hamilton, M., Lyons, K., Lee, S.-J., Brinkman, R., and Eaves, C. (2007b). Long-term propagation of distinct hematopoietic differentiation programs in vivo. Cell Stem Cell *1*, 218–229.

Ema, H., Takano, H., Sudo, K., and Nakauchi, H. (2000a). In vitro self-renewal division of hematopoietic stem cells. The Journal of Experimental Medicine *192*, 1281–1288.

Ema, H., Takano, H., Sudo, K., and Nakauchi, H. (2000b). In vitro self-renewal division of hematopoietic stem cells. The Journal of Experimental Medicine *192*, 1281–1288.

Ema, H., Morita, Y., Yamazaki, S., Matsubara, A., Seita, J., Tadokoro, Y., Kondo, H., Takano, H., and Nakauchi, H. (2006). Adult mouse hematopoietic stem cells: purification and single-cell assays. Nature Protocols *1*, 2979–2987.

Emery, G., Hutterer, A., Berdnik, D., Mayer, B., Wirtz-Peitz, F., Gaitan, M.G., and Knoblich, J. a (2005). Asymmetric Rab 11 endosomes regulate delta recycling and specify cell fate in the Drosophila nervous system. Cell *122*, 763–773.

Engering, a, and Pieters, J. (2001). Association of distinct tetraspanins with MHC class II molecules at different subcellular locations in human immature dendritic cells. International Immunology *13*, 127–134.

Escola, J.-M. (1998). Selective Enrichment of Tetraspan Proteins on the Internal Vesicles of Multivesicular Endosomes and on Exosomes Secreted by Human B-lymphocytes. Journal of Biological Chemistry *273*, 20121–20127.

Essers, M. a G., Offner, S., Blanco-Bose, W.E., Waibler, Z., Kalinke, U., Duchosal, M. a, and Trumpp, A. (2009). IFNalpha activates dormant haematopoietic stem cells in vivo. Nature *458*, 904–908.

Ewers, H., and Helenius, A. (2011). Lipid-mediated endocytosis. Cold Spring Harbor Perspectives in Biology *3*, a004721.

Forsberg, E.C., Prohaska, S.S., Katzman, S., Heffner, G.C., Stuart, J.M., and Weissman, I.L. (2005). Differential expression of novel potential regulators in hematopoietic stem cells. PLoS Genetics *1*, e28.

Gekas, C., and Graf, T. (2013). CD41 expression marks myeloid biased adult

hematopoietic stem cells and increases with age. Blood.

Giebel, B., and Beckmann, J. (2007). Asymmetric cell divisions of human hematopoietic stem and progenitor cells meet endosomes. Cell Cycle (Georgetown, Tex.) *6*, 2201–2204.

Giebel, B., and Wodarz, A. (2012). Notch signaling: numb makes the difference. Current Biology : CB *22*, R133–5.

Glickman, J.N., Morton, P. a, Slot, J.W., Kornfeld, S., and Geuze, H.J. (1996). The biogenesis of the MHC class II compartment in human I-cell disease B lymphoblasts. The Journal of Cell Biology *132*, 769–785.

Goodell, M.A., Brose, K., Paradis, G., Conner, A.S., and Mulligan, R.C. (1996). Isolation and functional properties of murine hematopoietic stem cells that are replicating in vivo. The Journal of Experimental Medicine *183*, 1797–1806.

Graham, F.L., and van der Eb, A.J. (1973). A new technique for the assay of infectivity of human adenovirus 5 DNA. Virology *52*, 456–467.

Gratwohl, A., Baldomero, H., Aljurf, M., Pasquini, M.C., Bouzas, L.F., Yoshimi, A., Szer, J., Lipton, J., Schwendener, A., Gratwohl, M., et al. (2010). Hematopoietic stem cell transplantation: a global perspective. JAMA : the Journal of the American Medical Association *303*, 1617–1624.

Gromley, A., Yeaman, C., Rosa, J., Redick, S., Chen, C.-T., Mirabelle, S., Guha, M., Sillibourne, J., and Doxsey, S.J. (2005). Centriolin anchoring of exocyst and SNARE complexes at the midbody is required for secretory-vesicle-mediated abscission. Cell *123*, 75–87.

Guicciardi, M.E., Leist, M., and Gores, G.J. (2004). Lysosomes in cell death. Oncogene *23*, 2881–2890.

Guo, M., Jan, L.Y., and Jan, Y.N. (1996). Control of daughter cell fates during asymmetric division: interaction of Numb and Notch. Neuron *17*, 27–41.

Hemler, M.E. (2005). Tetraspanin functions and associated microdomains. Nature

Reviews. Molecular Cell Biology *6*, 801–811.

Holmes, C., and Stanford, W.L. (2007). Concise review: stem cell antigen-1: expression, function, and enigma. Stem Cells (Dayton, Ohio) *25*, 1339–1347.

Hope, K.J., Cellot, S., Ting, S.B., MacRae, T., Mayotte, N., Iscove, N.N., and Sauvageau, G. (2010). An RNAi screen identifies Msi2 and Prox1 as having opposite roles in the regulation of hematopoietic stem cell activity. Cell Stem Cell *7*, 101–113.

Horejsí, V., Drbal, K., Cebecauer, M., Cerný, J., Brdicka, T., Angelisová, P., and Stockinger, H. (1999). GPI-microdomains: a role in signalling via immunoreceptors. Immunology Today *20*, 356–361.

Horvitz, H.R., and Herskowitz, I. (1992). Mechanisms of asymmetric cell division: two Bs or not two Bs, that is the question. Cell *68*, 237–255.

Howlader, N. (2012). SEER Cancer Statistics Review 1975-2010.

Hsing, L.C., and Rudensky, A.Y. (2005). The lysosomal cysteine proteases in MHC class II antigen presentation. Immunological Reviews *207*, 229–241.

Huang, Y., Rezzoug, F., Chilton, P.M., Grimes, H.L., Cramer, D.E., and Ildstad, S.T. (2004). Matching at the MHC class I K locus is essential for long-term engraftment of purified hematopoietic stem cells: a role for host NK cells in regulating HSC engraftment. Blood *104*, 873–880.

Ito, C.Y., Li, C.Y.J., Bernstein, A., Dick, J.E., and Stanford, W.L. (2003). Hematopoietic stem cell and progenitor defects in Sca-1/Ly-6A-null mice. Blood *101*, 517–523.

Jenq, R.R., and van den Brink, M.R.M. (2010). Allogeneic haematopoietic stem cell transplantation: individualized stem cell and immune therapy of cancer. Nature Reviews. Cancer *10*, 213–221.

Jin, S., Yi, F., and Li, P.-L. (2007). Contribution of lysosomal vesicles to the formation of lipid raft redox signaling platforms in endothelial cells. Antioxidants & Redox

Signaling *9*, 1417–1426.

Keller, J.R., Mantel, C., Sing, G.K., Ellingsworth, L.R., Ruscetti, S.K., and Ruscetti, F.W. (1988). Transforming growth factor beta 1 selectively regulates early murine hematopoietic progenitors and inhibits the growth of IL-3-dependent myeloid leukemia cell lines. The Journal of Experimental Medicine *168*, 737–750.

Kent, D., Copley, M., Benz, C., Dykstra, B., Bowie, M., and Eaves, C. (2008a). Regulation of hematopoietic stem cells by the steel factor/KIT signaling pathway. Clinical Cancer Research : an Official Journal of the American Association for Cancer Research *14*, 1926–1930.

Kent, D.G., Dykstra, B.J., Cheyne, J., Ma, E., and Eaves, C.J. (2008b). Steel factor coordinately regulates the molecular signature and biologic function of hematopoietic stem cells. Blood *112*, 560–567.

Kent, D.G., Copley, M.R., Benz, C., Wöhrer, S., Dykstra, B.J., Ma, E., Cheyne, J., Zhao, Y., Bowie, M.B., Zhao, Y., et al. (2009). Prospective isolation and molecular characterization of hematopoietic stem cells with durable self-renewal potential. Blood *113*, 6342–6350.

Kiel, M.J., and Morrison, S.J. (2008). Uncertainty in the niches that maintain haematopoietic stem cells. Nature Reviews. Immunology *8*, 290–301.

Kiel, M.J., Yilmaz, O.H., Iwashita, T., Yilmaz, O.H., Terhorst, C., and Morrison, S.J. (2005a). SLAM family receptors distinguish hematopoietic stem and progenitor cells and reveal endothelial niches for stem cells. Cell *121*, 1109–1121.

Kiel, M.J., Yilmaz, O.H., Iwashita, T., Yilmaz, O.H., Terhorst, C., and Morrison, S.J. (2005b). SLAM family receptors distinguish hematopoietic stem and progenitor cells and reveal endothelial niches for stem cells. Cell *121*, 1109–1121.

Kiger, a a, Jones, D.L., Schulz, C., Rogers, M.B., and Fuller, M.T. (2001). Stem cell self-renewal specified by JAK-STAT activation in response to a support cell cue. Science (New York, N.Y.) *294*, 2542–2545.

Köhler, G., and Milstein, C. (1975). Continuous cultures of fused cells secreting

antibody of predefined specificity. Nature *256*, 495–497.

Kollet, O., Dar, A., Shivtiel, S., Kalinkovich, A., Lapid, K., Sztainberg, Y., Tesio, M., Samstein, R.M., Goichberg, P., Spiegel, A., et al. (2006). Osteoclasts degrade endosteal components and promote mobilization of hematopoietic progenitor cells. Nature Medicine *12*, 657–664.

Korn, A.P., Henkelman, R.M., Ottensmeyer, F.P., and Till, J.E. (1973). Investigations of a stochastic model of haemopoiesis. Experimental Hematology *1*, 362–375.

Kornfeld, S., and Mellman, I. (1989). The biogenesis of lysosomes. Annual Review of Cell Biology *5*, 483–525.

Lathia, J.D., Hitomi, M., Gallagher, J., Gadani, S.P., Adkins, J., Vasanji, a, Liu, L., Eyler, C.E., Heddleston, J.M., Wu, Q., et al. (2011). Distribution of CD133 reveals glioma stem cells self-renew through symmetric and asymmetric cell divisions. Cell Death & Disease *2*, e200.

Leary, a G., Strauss, L.C., Civin, C.I., and Ogawa, M. (1985). Disparate differentiation in hemopoietic colonies derived from human paired progenitors. Blood *66*, 327–332.

Lee, C.-Y., Robinson, K.J., and Doe, C.Q. (2006). Lgl, Pins and aPKC regulate neuroblast self-renewal versus differentiation. Nature *439*, 594–598.

Lerit, D. a, Smyth, J.T., and Rusan, N.M. (2013). Organelle asymmetry for proper fitness, function, and fate. Chromosome Research : an International Journal on the Molecular, Supramolecular and Evolutionary Aspects of Chromosome Biology *21*, 271–286.

Li, J.-Y., Adams, J., Calvi, L.M., Lane, T.F., DiPaolo, R., Weitzmann, M.N., and Pacifici, R. (2012). PTH expands short-term murine hemopoietic stem cells through T cells. Blood *120*, 4352–4362.

Li, W., Johnson, S.A., Shelley, W.C., and Yoder, M.C. (2004). Hematopoietic stem cell repopulating ability can be maintained in vitro by some primary endothelial cells. Experimental Hematology *32*, 1226–1237.

Luc, S., Buza-Vidas, N., and Jacobsen, S.E.W. (2007). Biological and molecular evidence for existence of lymphoid-primed multipotent progenitors. Annals of the New York Academy of Sciences *1106*, 89–94.

Maillard, I., Koch, U., Dumortier, A., Shestova, O., Xu, L., Sai, H., Pross, S.E., Aster, J.C., Bhandoola, A., Radtke, F., et al. (2008). Canonical notch signaling is dispensable for the maintenance of adult hematopoietic stem cells. Cell Stem Cell *2*, 356–366.

Mancini, S.J.C., Mantei, N., Dumortier, A., Suter, U., MacDonald, H.R., and Radtke, F. (2005). Jagged1-dependent Notch signaling is dispensable for hematopoietic stem cell self-renewal and differentiation. Blood *105*, 2340–2342.

Mansour, A., Abou-Ezzi, G., Sitnicka, E., Jacobsen, S.E.W., Wakkach, A., and Blin-Wakkach, C. (2012). Osteoclasts promote the formation of hematopoietic stem cell niches in the bone marrow. The Journal of Experimental Medicine *209*, 537–549.

Mantegazza, A.R., Barrio, M.M., Moutel, S., Bover, L., Weck, M., Brossart, P., Teillaud, J.-L., and Mordoh, J. (2004). CD63 tetraspanin slows down cell migration and translocates to the endosomal-lysosomal-MIICs route after extracellular stimuli in human immature dendritic cells. Blood *104*, 1183–1190.

Matsuzaki, Y., Kinjo, K., Mulligan, R.C., and Okano, H. (2004). Unexpectedly efficient homing capacity of purified murine hematopoietic stem cells. Immunity *20*, 87–93.

McCarthy, K.F., Ledney, G.D., and Mitchell, R. (1977). A deficiency of hematopoietic stem cells in steel mice. Cell and Tissue Kinetics *10*, 121–126.

Méndez-Ferrer, S., Michurina, T. V, Ferraro, F., Mazloom, A.R., Macarthur, B.D., Lira, S. a, Scadden, D.T., Ma'ayan, A., Enikolopov, G.N., and Frenette, P.S. (2010). Mesenchymal and haematopoietic stem cells form a unique bone marrow niche. Nature *466*, 829–834.

Metzelaar, M.J., Wijngaard, P.L., Peters, P.J., Sixma, J.J., Nieuwenhuis, H.K., and Clevers, H.C. (1991). CD63 antigen. A novel lysosomal membrane glycoprotein, cloned by a screening procedure for intracellular antigens in eukaryotic cells. The

Journal of Biological Chemistry *266*, 3239–3245.

Miceli, M.C., Moran, M., Chung, C.D., Patel, V.P., Low, T., and Zinnanti, W. (2001). Co-stimulation and counter-stimulation: lipid raft clustering controls TCR signaling and functional outcomes. Seminars in Immunology *13*, 115–128.

Morita, Y., Ema, H., and Nakauchi, H. (2010). Heterogeneity and hierarchy within the most primitive hematopoietic stem cell compartment. The Journal of Experimental Medicine *207*, 1173–1182.

Morrison, S.J., and Spradling, A.C. (2008). Stem cells and niches: mechanisms that promote stem cell maintenance throughout life. Cell *132*, 598–611.

Muller-Sieburg, C.E., Whitlock, C. a, and Weissman, I.L. (1986). Isolation of two early B lymphocyte progenitors from mouse marrow: a committed pre-pre-B cell and a clonogenic Thy-1-lo hematopoietic stem cell. Cell *44*, 653–662.

Muller-Sieburg, C.E., Cho, R.H., Karlsson, L., Huang, J.-F., and Sieburg, H.B. (2004). Myeloid-biased hematopoietic stem cells have extensive self-renewal capacity but generate diminished lymphoid progeny with impaired IL-7 responsiveness. Blood *103*, 4111–4118.

Muller-Sieburg, C.E., Sieburg, H.B., Bernitz, J.M., and Cattarossi, G. (2012). Stem cell heterogeneity: implications for aging and regenerative medicine. Blood *119*, 3900–3907.

Müller-Sieburg, C.E., Cho, R.H., Thoman, M., Adkins, B., and Sieburg, H.B. (2002). Deterministic regulation of hematopoietic stem cell self-renewal and differentiation. Blood *100*, 1302–1309.

Mullis, K., Faloona, F., Scharf, S., Saiki, R., Horn, G., and Erlich, H. (1986). Specific enzymatic amplification of DNA in vitro: the polymerase chain reaction. Cold Spring Harbor Symposia on Quantitative Biology *51 Pt 1*, 263–273.

Nakamura-Ishizu, A., and Suda, T. (2013). Hematopoietic stem cell niche: an interplay among a repertoire of multiple functional niches. Biochimica et Biophysica

Acta *1830*, 2404–2409.

Neumüller, R. a, and Knoblich, J. a (2009). Dividing cellular asymmetry: asymmetric cell division and its implications for stem cells and cancer. Genes & Development *23*, 2675–2699.

Noda, S., Horiguchi, K., Ichikawa, H., and Miyoshi, H. (2008). Repopulating activity of ex vivo-expanded murine hematopoietic stem cells resides in the CD48-c-Kit+Sca-1+lineage marker- cell population. Stem Cells *26*, 646–655.

Nteliopoulos, G., and Gordon, M.Y. (2012). Protein segregation between dividing hematopoietic progenitor cells in the determination of the symmetry/asymmetry of cell division. Stem Cells and Development *21*, 2565–2580.

Ogawa, M., Porter, P.N., and Nakahata, T. (1983). Renewal and commitment to differentiation of hemopoietic stem cells (an interpretive review). Blood *61*, 823–829.

Oguro, H., Ding, L., and Morrison, S.J. (2013). SLAM Family Markers Resolve Functionally Distinct Subpopulations of Hematopoietic Stem Cells and Multipotent Progenitors. Cell Stem Cell *13*, 102–116.

Ohlstein, B., and Spradling, A. (2007). Multipotent Drosophila intestinal stem cells specify daughter cell fates by differential notch signaling. Science (New York, N.Y.) *315*, 988–992.

Ohneda, O., Fennie, C., Zheng, Z., Donahue, C., La, H., Villacorta, R., Cairns, B., and Lasky, L. a (1998). Hematopoietic stem cell maintenance and differentiation are supported by embryonic aorta-gonad-mesonephros region-derived endothelium. Blood *92*, 908–919.

Oliaro, J., Van Ham, V., Sacirbegovic, F., Pasam, A., Bomzon, Z., Pham, K., Ludford-Menting, M.J., Waterhouse, N.J., Bots, M., Hawkins, E.D., et al. (2010). Asymmetric cell division of T cells upon antigen presentation uses multiple conserved mechanisms. Journal of Immunology (Baltimore, Md. : 1950) *185*, 367–375.

Osawa, M., Hanada, K., Hamada, H., and Nakauchi, H. (1996). Long-term lymphohematopoietic reconstitution by a single CD34-low/negative hematopoietic

stem cell. Science (New York, N.Y.) *273*, 242–245.

Perfetto, S.P., Chattopadhyay, P.K., and Roederer, M. (2004). Seventeen-colour flow cytometry: unravelling the immune system. Nature Reviews. Immunology *4*, 648–655.

Peters, P.J., Neefjes, J.J., Oorschot, V., Ploegh, H.L., and Geuze, H.J. (1991). Segregation of MHC class II molecules from MHC class I molecules in the Golgi complex for transport to lysosomal compartments. Nature *349*, 669–676.

Petit, I., Szyper-Kravitz, M., Nagler, A., Lahav, M., Peled, A., Habler, L., Ponomaryov, T., Taichman, R.S., Arenzana-Seisdedos, F., Fujii, N., et al. (2002). G-CSF induces stem cell mobilization by decreasing bone marrow SDF-1 and up-regulating CXCR4. Nature Immunology *3*, 687–694.

Pols, M.S., and Klumperman, J. (2009). Trafficking and function of the tetraspanin CD63. Experimental Cell Research *315*, 1584–1592.

Pronk, C.J.H., Rossi, D.J., Månsson, R., Attema, J.L., Norddahl, G.L., Chan, C.K.F., Sigvardsson, M., Weissman, I.L., and Bryder, D. (2007). Elucidation of the phenotypic, functional, and molecular topography of a myeloerythroid progenitor cell hierarchy. Cell Stem Cell *1*, 428–442.

Qian, H., Buza-Vidas, N., Hyland, C.D., Jensen, C.T., Antonchuk, J., Månsson, R., Thoren, L. a, Ekblom, M., Alexander, W.S., and Jacobsen, S.E.W. (2007). Critical role of thrombopoietin in maintaining adult quiescent hematopoietic stem cells. Cell Stem Cell *1*, 671–684.

Rando, T. a (2007). The immortal strand hypothesis: segregation and reconstruction. Cell *129*, 1239–1243.

Rhyu, M.S., Jan, L.Y., and Jan, Y.N. (1994). Asymmetric distribution of numb protein during division of the sensory organ precursor cell confers distinct fates to daughter cells. Cell *76*, 477–491.

Sacchetti, B., Funari, A., Michienzi, S., Di Cesare, S., Piersanti, S., Saggio, I., Tagliafico, E., Ferrari, S., Robey, P.G., Riminucci, M., et al. (2007). Self-renewing

osteoprogenitors in bone marrow sinusoids can organize a hematopoietic microenvironment. Cell *131*, 324–336.

Sanjuan-Pla, A., Macaulay, I.C., Jensen, C.T., Woll, P.S., Luis, T.C., Mead, A., Moore, S., Carella, C., Matsuoka, S., Jones, T.B., et al. (2013). Platelet-biased stem cells reside at the apex of the haematopoietic stem-cell hierarchy. Nature.

Santolini, E., Puri, C., Salcini, a E., Gagliani, M.C., Pelicci, P.G., Tacchetti, C., and Di Fiore, P.P. (2000). Numb is an endocytic protein. The Journal of Cell Biology *151*, 1345–1352.

Schambach, A., Galla, M., Modlich, U., Will, E., Chandra, S., Reeves, L., Colbert, M., Williams, D. a, von Kalle, C., and Baum, C. (2006). Lentiviral vectors pseudotyped with murine ecotropic envelope: increased biosafety and convenience in preclinical research. Experimental Hematology *34*, 588–592.

Schink, K.O., and Stenmark, H. (2011). Cell differentiation: midbody remnants - junk or fate factors? Current Biology : CB *21*, R958–60.

Schofield, R. (1978). The relationship between the spleen colony-forming cell and the haemopoietic stem cell. Blood Cells *4*, 7–25.

Seifert, J.R.K., and Mlodzik, M. (2007). Frizzled/PCP signalling: a conserved mechanism regulating cell polarity and directed motility. Nature Reviews. Genetics *8*, 126–138.

Seita, J., Sahoo, D., Rossi, D.J., Bhattacharya, D., Serwold, T., Inlay, M. a, Ehrlich, L.I.R., Fathman, J.W., Dill, D.L., and Weissman, I.L. (2012). Gene Expression Commons: an open platform for absolute gene expression profiling. PloS One *7*, e40321.

Sekulovic, S., Gasparetto, M., Lecault, V., Hoesli, C. a, Kent, D.G., Rosten, P., Wan, A., Brookes, C., Hansen, C.L., Piret, J.M., et al. (2011). Ontogeny stage-independent and high-level clonal expansion in vitro of mouse hematopoietic stem cells stimulated by an engineered NUP98-HOX fusion transcription factor. Blood *118*, 4366–4376.

Settembre, C., Zoncu, R., Medina, D.L., Vetrini, F., Erdin, S., Erdin, S., Huynh, T.,

Ferron, M., Karsenty, G., Vellard, M.C., et al. (2012). A lysosome-to-nucleus signalling mechanism senses and regulates the lysosome via mTOR and TFEB. The EMBO Journal *31*, 1095–1108.

Shimazu, T., Iida, R., Zhang, Q., Welner, R.S., Medina, K.L., Alberola-Lla, J., and Kincade, P.W. (2012). CD86 is expressed on murine hematopoietic stem cells and denotes lymphopoietic potential. Blood *119*, 4889–4897.

Sieburg, H.B., Cho, R.H., Dykstra, B., Uchida, N., Eaves, C.J., and Muller-Sieburg, C.E. (2006). The hematopoietic stem compartment consists of a limited number of discrete stem cell subsets. Blood *107*, 2311–2316.

Sieburg, H.B., Rezner, B.D., and Muller-sieburg, C.E. (2011). Predicting clonal self-renewal and extinction of hematopoietic stem cells.

Sitnicka, E., Ruscetti, F.W., Priestley, G. V, Wolf, N.S., and Bartelmez, S.H. (1996). Transforming growth factor beta 1 directly and reversibly inhibits the initial cell divisions of long-term repopulating hematopoietic stem cells. Blood *88*, 82–88.

Spana, E.P., Kopczynski, C., Goodman, C.S., and Doe, C.Q. (1995). Asymmetric localization of numb autonomously determines sibling neuron identity in the Drosophila CNS. Development (Cambridge, England) *121*, 3489–3494.

Spangrude, G.J., Heimfeld, S., and Weissman, I.L. (1988). Purification and characterization of mouse hematopoietic stem cells. Science (New York, N.Y.) *241*, 58–62.

Stier, S., Cheng, T., Dombkowski, D., Carlesso, N., and Scadden, D.T. (2002). Notch1 activation increases hematopoietic stem cell self-renewal in vivo and favors lymphoid over myeloid lineage outcome. Blood *99*, 2369–2378.

Suda, J., Suda, T., and Ogawa, M. (1984a). Analysis of differentiation of mouse hemopoietic stem cells in culture by sequential replating of paired progenitors. Blood *64*, 393–399.

Suda, T., Suda, J., and Ogawa, M. (1984b). Disparate differentiation in mouse hemopoietic colonies derived from paired progenitors. Proceedings of the National

Academy of Sciences of the United States of America *81*, 2520–2524.

Sugimura, R., He, X.C., Venkatraman, A., Arai, F., Box, A., Semerad, C., Haug, J.S., Peng, L., Zhong, X.-B., Suda, T., et al. (2012). Noncanonical Wnt signaling maintains hematopoietic stem cells in the niche. Cell *150*, 351–365.

Sugiyama, T., Kohara, H., Noda, M., and Nagasawa, T. (2006). Maintenance of the hematopoietic stem cell pool by CXCL12-CXCR4 chemokine signaling in bone marrow stromal cell niches. Immunity *25*, 977–988.

Taichman, R.S., and Emerson, S.G. (1994). Human osteoblasts support hematopoiesis through the production of granulocyte colony-stimulating factor. The Journal of Experimental Medicine *179*, 1677–1682.

Takano, H., Ema, H., Sudo, K., and Nakauchi, H. (2004). Asymmetric division and lineage commitment at the level of hematopoietic stem cells: inference from differentiation in daughter cell and granddaughter cell pairs. The Journal of Experimental Medicine *199*, 295–302.

Tarrant, J.M., Robb, L., van Spriel, A.B., and Wright, M.D. (2003). Tetraspanins: molecular organisers of the leukocyte surface. Trends in Immunology *24*, 610–617.

Thaunat, O., Granja, A.G., Barral, P., Filby, A., Montaner, B., Collinson, L., Martinez-Martin, N., Harwood, N.E., Bruckbauer, A., and Batista, F.D. (2012). Asymmetric segregation of polarized antigen on B cell division shapes presentation capacity. Science (New York, N.Y.) *335*, 475–479.

Thomas, E.D., and Blume, K.G. (1999). Historical markers in the development of allogeneic hematopoietic cell transplantation. Biology of Blood and Marrow Transplantation : Journal of the American Society for Blood and Marrow Transplantation *5*, 341–346.

Thomas, E.D., Lochte, H.L., Cannon, J.H., Sahler, O.D., and Ferrebee, J.W. (1959). Supralethal whole body irradiation and isologous marrow transplantation in man. The Journal of Clinical Investigation *38*, 1709–1716.

TILL, J.E., MCCULLOCH, E.A., and SIMINOVITCH, L. (1964). A STOCHASTIC

MODEL OF STEM CELL PROLIFERATION, BASED ON THE GROWTH OF SPLEEN COLONY-FORMING CELLS. Proceedings of the National Academy of Sciences of the United States of America *51*, 29–36.

Ting, S.B., Deneault, E., Hope, K., Cellot, S., Chagraoui, J., Mayotte, N., Dorn, J.F., Laverdure, J.-P., Harvey, M., Hawkins, E.D., et al. (2012). Asymmetric segregation and self-renewal of hematopoietic stem and progenitor cells with endocytic Ap2a2. Blood *119*, 2510–2522.

Trentin, J.J. (1971). Determination of bone marrow stem cell differentiation by stromal hemopoietic inductive microenvironments (HIM). The American Journal of Pathology *65*, 621–628.

Tse, W., and Laughlin, M.J. (2005). Hematopoietic Stem Cell Transplantation Umbilical Cord Blood Transplantation : A New Alternative Option. 377–383.

Uchida, N., Dykstra, B., Lyons, K.J., Leung, F.Y.K., and Eaves, C.J. (2003). Different in vivo repopulating activities of purified hematopoietic stem cells before and after being stimulated to divide in vitro with the same kinetics. Experimental Hematology *31*, 1338–1347.

Ueno, H., Sakita-Ishikawa, M., Morikawa, Y., Nakano, T., Kitamura, T., and Saito, M. (2003). A stromal cell-derived membrane protein that supports hematopoietic stem cells. Nature Immunology *4*, 457–463.

Upadhyay, G., Yin, Y., Yuan, H., Li, X., Derynck, R., and Glazer, R.I. (2011). Stem cell antigen-1 enhances tumorigenicity by disruption of growth differentiation factor-10 (GDF10)-dependent TGF-beta signaling. Proceedings of the National Academy of Sciences of the United States of America *108*, 7820–7825.

Vannini, N., Roch, A., Naveiras, O., Griffa, A., Kobel, S., and Lutolf, M.P. (2012a). Identification of in vitro HSC fate regulators by differential lipid raft clustering. Cell Cycle (Georgetown, Tex.) *11*, 1535–1543.

Vannini, N., Roch, A., Naveiras, O., Griffa, A., Kobel, S., and Lutolf, M.P. (2012b). Identification of in vitro HSC fate regulators by differential lipid raft clustering. Cell

Cycle (Georgetown, Tex.) *11*, 1535–1543.

Visnjic, D., Kalajzic, Z., Rowe, D.W., Katavic, V., Lorenzo, J., and Aguila, H.L. (2004). Hematopoiesis is severely altered in mice with an induced osteoblast deficiency. Blood *103*, 3258–3264.

Te Vruchte, D., Jeans, A., Platt, F.M., and Sillence, D.J. (2010). Glycosphingolipid storage leads to the enhanced degradation of the B cell receptor in Sandhoff disease mice. Journal of Inherited Metabolic Disease *33*, 261–270.

Wagers, A.J., Sherwood, R.I., Christensen, J.L., and Weissman, I.L. (2002). Little evidence for developmental plasticity of adult hematopoietic stem cells. Science (New York, N.Y.) *297*, 2256–2259.

Warr, M.R., Binnewies, M., Flach, J., Reynaud, D., Garg, T., Malhotra, R., Debnath, J., and Passegué, E. (2013). FOXO3A directs a protective autophagy program in haematopoietic stem cells. Nature *494*, 323–327.

Whitman, C. (1878). The embryology of Clepsine. Q J Microsc Sci 215–315.

Williams, M. a, and Fukuda, M. (1990). Accumulation of membrane glycoproteins in lysosomes requires a tyrosine residue at a particular position in the cytoplasmic tail. The Journal of Cell Biology *111*, 955–966.

Wilson, A., Ardiet, D., Saner, C., Vilain, N., Beermann, F., Aguet, M., Macdonald, H.R., and Zilian, O. (2007). Normal hemopoiesis and lymphopoiesis in the combined absence of numb and numblike. Journal of Immunology (Baltimore, Md. : 1950) *178*, 6746–6751.

Wilson, A., Laurenti, E., Oser, G., Van Der Wath, R.C., Blanco-Bose, W., Jaworski, M., Offner, S., Dunant, C.F., Eshkind, L., Bockamp, E., et al. (2008). Hematopoietic stem cells reversibly switch from dormancy to self-renewal during homeostasis and repair. Cell *135*, 1118–1129.

Winkler, I.G., Sims, N. a, Pettit, A.R., Barbier, V., Nowlan, B., Helwani, F., Poulton, I.J., van Rooijen, N., Alexander, K. a, Raggatt, L.J., et al. (2010). Bone marrow macrophages maintain hematopoietic stem cell (HSC) niches and their depletion

mobilizes HSCs. Blood *116*, 4815–4828.

Wu, M., Kwon, H.Y., Rattis, F., Blum, J., Zhao, C., Ashkenazi, R., Jackson, T.L., Gaiano, N., Oliver, T., and Reya, T. (2007a). Imaging hematopoietic precursor division in real time. Cell Stem Cell *1*, 541–554.

Wu, M., Kwon, H.Y., Rattis, F., Blum, J., Zhao, C., Ashkenazi, R., Jackson, T.L., Gaiano, N., Oliver, T., and Reya, T. (2007b). Imaging hematopoietic precursor division in real time. Cell Stem Cell *1*, 541–554.

Yamashita, Y.M., and Fuller, M.T. (2008). Asymmetric centrosome behavior and the mechanisms of stem cell division. The Journal of Cell Biology *180*, 261–266.

Yamashita, Y.M., Jones, D.L., and Fuller, M.T. (2003). Orientation of asymmetric stem cell division by the APC tumor suppressor and centrosome. Science (New York, N.Y.) *301*, 1547–1550.

Yamazaki, S., and Nakauchi, H. (2009). Insights into signaling and function of hematopoietic stem cells at the single-cell level. Current Opinion in Hematology *16*, 255–258.

Yamazaki, S., Iwama, A., Takayanagi, S., Morita, Y., Eto, K., Ema, H., and Nakauchi, H. (2006). Cytokine signals modulated via lipid rafts mimic niche signals and induce hibernation in hematopoietic stem cells. The The European Molecular Biology Organization Journal *25*, 3515–3523.

Yamazaki, S., Iwama, A., Morita, Y., Eto, K., Ema, H., and Nakauchi, H. (2007). Cytokine signaling, lipid raft clustering, and HSC hibernation. Annals Of The New York Academy Of Sciences *1106*, 54–63.

Yamazaki, S., Iwama, A., Takayanagi, S., Eto, K., Ema, H., and Nakauchi, H. (2009). TGF-beta as a candidate bone marrow niche signal to induce hematopoietic stem cell hibernation. Blood *113*, 1250–1256.

Yamazaki, S., Ema, H., Karlsson, G., Yamaguchi, T., Miyoshi, H., Shioda, S., Taketo, M.M., Karlsson, S., Iwama, A., and Nakauchi, H. (2011). Nonmyelinating Schwann Cells Maintain Hematopoietic Stem Cell Hibernation in the Bone Marrow Niche. Cell

147, 1146–1158.

Yoshida, T., Kawano, Y., Sato, K., Ando, Y., Aoki, J., Miura, Y., Komano, J., Tanaka, Y., and Koyanagi, Y. (2008). A CD63 Mutant Inhibits T-cell Tropic Human Immunodeficiency Virus Type 1 Entry by Disrupting CXCR4 Trafficking to the Plasma Membrane. Traffic *9*, 540–558.

Yoshihara, H., Arai, F., Hosokawa, K., Hagiwara, T., Takubo, K., Nakamura, Y., Gomei, Y., Iwasaki, H., Matsuoka, S., Miyamoto, K., et al. (2007). Thrombopoietin/MPL signaling regulates hematopoietic stem cell quiescence and interaction with the osteoblastic niche. Cell Stem Cell *1*, 685–697.

Zhang, C.C., and Lodish, H.F. (2005). Murine hematopoietic stem cells change their surface phenotype during ex vivo expansion. Blood *105*, 4314–4320.

Zhang, J., Niu, C., Ye, L., Huang, H., He, X., Tong, W.-G., Ross, J., Haug, J., Johnson, T., Feng, J.Q., et al. (2003). Identification of the haematopoietic stem cell niche and control of the niche size. Nature *425*, 836–841.

Zheng, L., Saunders, C.A., Sorensen, E.B., Waxmonsky, N.C., and Conner, S.D. (2013). Notch signaling from the endosome requires a conserved dileucine motif. Molecular Biology of the Cell *24*, 297–307.

9 Supplementary information

9.1 Supplementary Movie 5.2A-R

Time-lapse movies corresponding to figure 5.2C showing the symmetric segregation of indicated candidate genes in virally transduced HSCs cocultured on OP9 stromal cell line 3-4 days after infection. Magnification: 20x/1xTVadaptar; Time scale: days - hours:minutes:seconds.

9.2 Supplementary Movie 5.2S-V

Time-lapse movies corresponding to figure 5.2D showing the asymmetric segregation of indicated candidate genes in virally transduced HSCs cocultured on OP9 stromal cell line 3-4 days after infection. Magnification: 20x/1xTVadaptar; Time scale: days - hours:minutes:seconds.

10 Abbreviations

Abbreviation	Meaning
%	Percent
°C	Degree Celsius
µL	microliter
µm	mircometer
µM	Micromolar
2-me	β-Mercapto Ethanol
A	Adenosine
A488	Alexa488
A555	Alexa555
A647	Alexa647
a-MEM	Alpha-Minimel Essential Medium
AP-2	adaptor-protein 2
AP2A2	AP-2 complex subunit alpha-2
APC	allophycocyanin
APC-eFluor780	Allophycocyanin-eFluor780
Ang1	Angiopoietin 1
aPKC	Atypical Protein Kinase C
Baf	Bafilomycin (lysosomal inhibitor)
Bidest.	Bidestillated
BM	Bone Marrow
bp	Basepair
BS	Beam Splitter
c	concentration
C	Cytosine
C.elegans	Caenorhabditis elegans
CXCL12	CXC-Motif ligand 12 (=SDF-1)
CAEC	coronary artery endothelial cells
$CaPO_4$	CalciumPhosphate
CCD	Charged Coupled Device
CD	Cluster of Differentiation
CD11b	Itgam
CD150	Slamf1
CD34	Sialomucin CD34
CD48	Cluster of differentiation 48
CD62L	L-selectin
CD71	Transferin receptor
Celsr2	Cadherin EGF LAG Seven-Pass G-Type Receptor 2
CFSE	Carboxyfluorescein succinimidyl ester
c-KIT	CD117
CLP	Common Lymphoid Progenitor
cm^2	Square centimeter
CMP	Common Myeloid Progenitor
c-mpl	Myeloproliferative leukemia virus oncogene
CO2	Carbondioxide
Conc.	concentration
CTxB	Cholera toxin B
D.melanogaster	Drosophila melanogaster
DAPI	2-(4-amidinophenyl)-1H -indole-6-carboxamidine

ddH2O	Double-distilled water
Dlg	Disc large
DMEM	Dulbeco´s Modified Eagle Medium
DMSO	dimethylsulfoxide
DNA	Desoxyribonucleinacid
dNTP	Desoxyribonucleotides
DTT	Dithiothreitol
EDTA	EthyleneDiamineTetraAcetic acid
eGFP	Enhanced GFP
EML	Erythroid Myeloid Lymphoid
EPO	Erythropoietin
EtOH	Ethanol
FACS	Fluorescence Activated Cell Sorting
FBS	Fetal Bovine Serum
FCS	Fetal calf serum
FcγR	Fcy-receptor
FITC	fluoresceinisothiocyanat
Flk2	Fetal liver kinase-2
Fmi	Flamingo
Fz8	Frizzled8
G	Guanosine
Gata-1	GATA-binding factor 1
GFP	Green Fluorescence Protein
Gm	Granulocytic megakaryotic
GM1	monosialotetrahexosylganglioside
GMP	Granulocyte Macrophage Progenitor
GPI	Glycosil -PhosphatidylInositol
GPN	glycyl-L-phenylalanine-β-naphthylamide
GSC	germ line stem cells
h	Hours
H2B-GFP	Histone 2B Green Fluorescence Protein
H_2O	water
Hd	Homeodomain
HE	High efficiency
HEK293T	Human Embryonic Kidney 293 T
HeLa	HenriettaLacks
HEPES	2-(4-(2-Hydroxyethyl)- 1-piperazinyl)-ethansulfonacid
HLPC	High Performance Liquid Chromatography
HoxA10	HomeoboxA10
HSC	Hematopoietic Stem Cell
HSPC	Hematopoietic Stem and Progenitor Cells
IFNy	Interferon y
IFNyR	Interferon y Receptor
IL-3	Interleukin-3
IL-6	Interleukin-6
IL7Rα	Interleukin-7 Receptor alpha
ISC	Intestinal stem cell
Jak	Janus Kinase
Kb	Kilobase
KSL	c-KIT+sca1+Lineage-
Lamp	Lysosomal associated membrane protein
Laser	Light Amplification by Stimulated Emission of Radiation
LB	Lysogenic broth

LCCA	Liquid culture colony assay
LED	Light Emitting Diode
Lepr	Leptin receptor
L-Gln	L-Glutamine
LMPP	Lymphoid Biased Multipotent Progenitor
LP	Long Path
LTC-IC	Long Term Culture – Initiating Cell
LT-HSC	Long Term-Hematopoietic Stem Cells
mCherry	Monomeric Cherry
MDKC	Madin-Darby Caninie Kindney cells
MegE	Megakaryocytic erythrocytic
MEP	Megakaryocyte Erythrocyte Progenitor
$MgCl_2$	Magnesiumcloride
MHCI	Major histocompatibility complex I
MHCII	Major histocompatibility complex II
min	minute
Mito	mitochondria
mL	Milliliter
mm	Millimeter
mM	Millimolar
MOI	Multiplicity of infection
MPP	MultiPotent progenitor
MPP9	Matrix Metallo Proteases 9
mTORC1	master growth regulator mTOR complex 1
N_2	Nitrogen
NaCl	Sodiumchloride
NaN_3	Sodium azide
N-Cad	N-Cadherin
NFAT	Nuclear Factor of Activated T-cells
ng	Nanogramm
NIH3T3	Nationla Institute of Health 3T3
nm	nanometer
NMuMG	Mus Musculus Mammary Gland
Nup98	Nucleoporin98
O2	Oxygen
OD	Optical density
OP9	OsteoProgenitor 9
P/S	Penicillin / Streptomycin
Par-2	partitioning defective 2
Par-3	partitioning defective 3
Par-6	partitioning defective 6
PBS	Phosphate buffered saline
PBST	Phosphate Buffered Saline Tween20
PCP	Planar Cell Polarity
PCP-Cy5.5	Peridinin-chlorophyll-protein complex-Cyanin5.5
PCR	Polymerase chain reaction
PE	phycorerythrin
PE-Cy7	Phycoerythrine-Cyanin7
PEI	PolyEthylenImine
PFA	Para-FormAldehyde
Pins	Parter of inscuteable
PKB	Protein Kinase B
PMT	Photo Multiplier Tube

png	Portable network graphics
Pol	Polymerase
Prkci	Protein kinase C iota (or lambda)
Prkcz	Protein kinase C zeta
QTFy	Quantify
QTFy single	Quantify single
Rcf	Relative centrifugal force
RNA	RiboNucleinAcid
Rpm	Round per minute
RT	Room temperature
s	Second
Sca-1	Stem cell antigen-1
SCF	Stem cell factor
Scl	Stem Cell Leukemia
SC-LCCA	Single Cell-Liquid Culture Colony Assay
SFEM	Serum free essential medium
SI	SCF/IL3
SIT	SCF/IL3/TGFb1
SOP	Sensory Organ Precursor
ST	SCF/TPO
STAT	Signal Transducer and Activator of Transcription
ST-HSC	Short Term-Hematopoietic Stem Cells
STT	SCF/TPO/TGFb1
T	Thymindine
TAE	Tris-Acetate-EDTA
Taq	Thermus aquaticus
TAT	Timm´s acquisition tool
TB	Terrabyte
TEM	Tetraspanin Enriched Microdomains
TFEB	Transcription Factor EB
TGFβ1	Transforming growth factor beta 1
TGFβRI	Transforming growth factor beta receptor 1
TGFβRII	Transforming growth factor beta receptor 2
TPO	Thrombopoietin
tTa	tetracycline-regulated transactivator
TTT	Timm´s tracking tool
U	Units
UV	Ultraviolet
V	Voltage
v/v	Volume/volume
VBA	Visual Basic Application
VSVG	Vesicular stomatidis virus glycoprotein
w/v	Weight/volume
YFP	Yellow fluorescent protein
αMEM	α-Minimal Essential Medium
λ	Lambda
Rag	Recombination activating gene

11 Eidesstattliche Erklärung

Ich versichere hiermit an Eides statt, dass die vorgelegte Dissertation von mir selbständig und ohne unerlaubte Hilfe angefertigt ist.

München, den …… …….

Dirk Löffler

Erklärung

Hiermit erkläre ich, *

☐ dass die Dissertation nicht ganz oder in wesentlichen Teilen einer anderen Prüfungskommission vorgelegt worden ist.

☐ dass ich mich anderweitig einer Doktorprüfung ohne Erfolg **nicht** unterzogen habe.

☐ dass ich mich mit Erfolg der Doktorprüfung im Hauptfach ……..……
und in den Nebenfächern……..…….
bei der Fakultät für ……. der ...…….....……..…..
(Hochschule/Universität)
unterzogen habe.

☐ dass ich ohne Erfolg versucht habe, eine Disseration einzureichen oder mich der Doktorprüfung zu unterziehen.

München, den……..... ……

Dirk Löffler

*) Nichtzutreffendes streichen